CRANFIELD UNIVERSITY

Nithya Subramanian

DEVELOPMENT OF TAIL ROTOR POWER ANALYSIS MODEL WITH FEASIBILITY STUDY OF ELECTRICAL TAIL ROTOR

SCHOOL OF AEROSPACE, TRANSPORT AND MANUFACTURING

MSc (Research Full time)

Academic Year 2015 - 2016

Supervisor: Dr Craig Lawson
September 2016

CRANFIELD UNIVERSITY

SCHOOL OF AEROSPACE, TRANSPORT AND MANUFACTURING

MSc (Research Full time)

Academic Year 2015 - 2016

Nithya Subramanian

DEVELOPMENT OF TAIL ROTOR POWER ANALYSIS MODEL WITH FEASIBILITY STUDY OF ELECTRICAL TAIL ROTOR

Supervisor: Dr Craig Lawson
September 2016

This thesis is submitted in partial fulfilment of the requirements for the degree of MSc (Research)

(NB. This section can be removed if the award of the degree is based solely on examination of the thesis)

ABSTRACT

In recent years, there has been significant work undertaken by the aviation industry to increase the overall rotorcraft performance, and eventually, eliminate leak prone hydraulic fluids and to reduce CO_2 emissions. Even though a mechanical-gearbox-driven tail rotor has been extensively used in several applications, it comes at the expense of high life cost of the gearbox and shaft gear mechanism. This thesis concentrates on the developing a model to analyse the power requirement for the tail rotor drive and feasibility investigation of an electrical tail rotor to substitute the shaft geared system and the conventional tail rotor power transmission gearbox.

A case study is conducted on the Sikosky UH-60A rotorcraft to assess the conventional tail rotor power requirement and Electrical systems. A mathematical model based on Rankine Froude's momentum theory is created to analyse the power required to drive the anti-torque system, which could be adapted to any conventional drive train (with the main rotor and a tail rotor) rotorcraft. A mission profile and trajectory are created and implemented into Excel based mathematical model. The challenges in implementing electrical drivetrain (electrical generation, energy conversion and electric transmission) are briefly discussed in this thesis.

Electrical load analysis database is generated to find the electrical load of the generator for the entire flight phases and utilised to up-scaled the generator to compensate the new load from Electrical tail rotor. The electrical powertrain system is designed with a Brushless DC motor attached to the tail rotor and the generator and the battery for redundancy purposes.

The research thesis develops an understanding of current electric motor and battery technology to create a novel design of electric tail drive that increases the reliability of the helicopter system.

Keywords:

Electrically powered tail rotor, Power required to drive Tail rotor, Electrical load analysis, Electric tail drive, ‘More-electric’ rotorcraft, Sikorsky UH-60A, Electrical System.

ACKNOWLEDGEMENTS

First of all, I would like to thank my supervisors, Dr Craig Lawson and Dr Adrian Clarke for the constant support and dedication throughout my thesis.

I am forever indebted to my parents for all their love, understanding and encouragement towards overcoming boundaries in pursue of self-development. The magnitude of their contribution to the status of my life has been truly immeasurable and I will forever be grateful. Hasani Azamar, thank you for supporting me every day, for all the advices and cheering me up when I am stressed. I would also like to say a very big thank you to three very special people in my life: Aurora, Lalita and Constantina for all your encouragement.

I also want to thank my colleagues Farah and Hernan for all your help with the Clean Sky projects.

TABLE OF CONTENTS

LIST OF FIGURES

LIST OF TABLES

LIST OF ABBREVIATIONS

AC	Alternating Current
AH	Ampere per Hour
APU	Auxiliary Power Unit
AS	Actuation System
ATAG	Air Transport Action Group
ATRU	Auto-Transformer Rectifier Unit
ATU	Auto-Transformer Unit
BLDC	Brushless DC motor
CG	Centre of gravity
CO_2	Carbon dioxide
CS	Clean Sky
DC	Direct Current
EAV	Electric Automotive Vehicles
ECS	Environmental Control System
ELA	Electrical Load Analysis
ES	Electrical System
ETR	Electrical Tail Rotor
EU	European Union
FAA	Federal Aviation Administration
FS	Fuel System
GRC	Green Rotor-Craft
HECTOR	HEliCopTer Omni-disciplinary Research
HVDC	High Voltage Direct Current
IGB	Intermediate gearbox
IPS	Ice Protection System
JTI	Joint Technology Initiative
Li	Lithium
MEA	More Electric Aircraft
MTOW	Maximum Take-Off Weight
NOTAR	No Tail Rotor
PhoeniX	Platform Hosting Operational and Environmental Investigations for Rotorcraft
PM	Permanent Magnet
RMEM	Rotorcraft Mission Energy Management
RPM	Rotation per minute
SFC	Specific Fuel Consumption
SPS	Secondary Power System
TE	Technology Evaluator

TEM	Twin Engine Medium
TRGB	Tail rotor gearbox
TRU	Transformer Rectifier Unit
VAC	Volts - Alternating Current
VDC	Volts - Direct Current
VRP	Visual reference point

LIST OF SYMBOLS

$\Delta\gamma$	Total change in flow velocity
A	Area of disc
Ah	Ampere hour
B	No. Of blades
Cd	Cadmium
C_{d0}	Tail rotor co-efficient
Cl	Lift coefficient
CP	Pressure coefficient
CT	Thrust coefficient
ft	feet
GTR	Gear ratio between main rotor and tail rotor
hp	horse power
Hz	Hertz
I	Current
kg	kilogram
kVA	Kilo volt amps
kW	kilo-watt
lb	pound
Li	Lithium
l_{tr}	Length of the tail rotor
m	metre
$\dot{m}$	Density
$\dot{m}$	Mass flow per second through the wake
$\dot{m}$	Mass flux
Ni	Nickel
η_{IN}	integrated efficiencies of the intermediate gear and 90 deg. gearboxes
P_{Climb}	Power at climb phase
P_{Hover}	Power at hover phase
P_i	Induced power
QDS	intermediate drive shafts torque
Qtr	Tail rotor torque
R	Radius of the blades
R	Resistance
R_{IN}	the ratio between the intermediate gear and the tail rotor gear
s	second
SHPacc	accessory power required for the normal aircraft electrical systems
SHP_{MR}	main rotor power
SHP_{TR}	tail rotor power
T	Thrust

T_{tr}	Tail rotor thrust
V	Voltage
W	Weight of the rotorcraft
W	watt
γ	Induced velocity
γ_f	the velocity of the flight
γ_{tr}	the velocity of tail rotor
η	Efficiency
μ	Advance Ratio
ν	vertical velocity
ρ	Air Density
σ	Solidity
Ω	Angular velocity
Ω	RPM
ω	Wake induced velocity

LIST OF EQUATIONS

1 Introduction

The demand for more comfortable, reliable and cost effective way of inter-city commuting has spurred the aviation industry to find better air transport solutions. Due to the manoeuvrability and the potential of rotorcrafts, its usage in both civil and military transport has increased [1].

In recent years, there has been significant work undertaken by the aviation industry to increase the performance of the helicopter, and eventually, eliminate the leak-prone hydraulic fluids and to reduce Carbon dioxide (CO_2) emissions [2]. In order to attain these goals, the aviation industry is concentrating more towards electrical propulsion and improving electrical power generation.

The rotorcraft transportation is mainly concentrated on civil conveyance, fire suppression, emergency expulsion, search and rescue, offshore transportation and, patrolling. On an average 24,130 helicopter movements are accounted just in London Heathrow between the years 2007-2016[3].

1.1 Research Motivation

For last decade, the aviation industry is working towards more efficient and fewer pollutant products. The main social motivation for developing such aviation products is to preserve the environment for the forthcoming generations. According to the Air Transport Action Group (ATAG), the aviation industry is accountable for 12% of CO_2 emissions from all transport sources that compares with 74% from road transport out of the 2% of all humanly-generated CO_2 emissions[4].

The major challenge faced by air transport is to encounter the forecasted increase in 4-5% air travel demand per year, in a way ensuring the environment preservation[5]. Preserving the atmosphere and reversing the menacing climate change distresses the whole world and necessitates a worldwide action to attain a global outcome[6].

The financial demand on the restricted fossil fuel reserves and the unpredicted alteration in the resources price encourage the growth of technologies that depends on less on oil or gas and its by-products. The subsequent technologies will be concentrated on more electrical systems which will be more effective and less contaminating. These inspirations are supported at a political level by governments in most of the countries around the world. For instance, the Clean Sky (aeronautical research programme) which is a European Union (EU) project has set 20-20-20 objectives (20% upsurge in energy effectiveness, 20% decrease in CO_2 pollution, and 20% increase in renewable energy by 2020) [7].

The Clean Sky project concentrates on increasing the environmental performances of aircraft and air transportation, subsequently reducing the noise and more fuel effective aeroplanes, henceforth contributing to achieving the European Sky conservational goals. The Technology Evaluator (TE) analyses the helicopter Secondary Power System (SPS) to find the environmental impact and advantages of the Clean Sky project. The results obtained by Clean Sky JTI (Joint

Technology Initiative) project, a part of Green Rotor-Craft (GRC7) states that reduction in the weight of the rotorcraft and energy conception is possibly attained by the electrical systems alternatives[8].

The main advantages of More Electric Aircraft (MEA) are their weight reduction and the performance increment in relation to Secondary Power System (SPS). The conventional helicopter contains numerous rotating parts in the powertrain system which motivate the study of the electrical tail rotor. The aviation industry is concentrating on alternating the heavy rotating parts to light weighted and more efficient electrical systems[9]. The Twin Engine Helicopter (in particularly Sikorsky UH-60A) is concentrated on this thesis as a part of Clean Sky project.

This thesis concentrates on 'Feasibility of Electrical tail rotor' replacing the turbine - gearbox system in the conventional tail rotor drive train. On the other hand, electrical systems are lighter and hence, a higher efficiency, decreasing the fuel consumption while increasing the system reliability.

A case study was carried out, on the Sikorsky UH-60A helicopter, which is the baseline helicopter for this thesis. The data for conceptual tail rotor power analysis and the Electrical Load Analysis (ELA) is obtained from the Sikorsky Flight Manual [10] and the data to analyse conception of tail rotor power at different flight phases (start, take off, cruise, decent and land) are obtained from Clean Sky project report for Twin-engine medium helicopter[11].

1.1 Project Objectives

The main aim of this study is to concentrate on the feasibility analysis on the electrical tail rotor in Twin Engine Medium (TEM) Helicopter. In order to achieve the objective of the thesis, the following individual goals are applicable:

- Understanding the working of tail rotor and TEM helicopter through literature review and case study.
- Creating a mathematical model of the tail rotor to calculate the power required for different phases of flight.
- To conduct Electrical load analysis to find the current electrical usage of the generator for the entire flight phases to analyse the power increase with Electrical tail rotor design.
- As the course of this research to design schematics of electrical tail rotor to produce enough counter torque.
- Analysing the Electrical Tail rotor design and conducting a reliability study for the design.

1.2 THESIS STRUCTURE

Chapter 1: Introduction - Overview of the purpose of study of Electrical Tail Rotor.

Chapter 2: Literature Review - Starts with the review on the evolution of the rotorcrafts and its types and, classifications. Followed by a brief description of the Systems and the conventional power train.

Chapter 3: Methodology - Describes the methods carried out to calculate the power required to drive the anti-torque system. The knowledge obtained in this section will be implemented on the Sikorsky UH-60A.

Chapter 4: Creating and simulating the power required to drive the tail rotor model and Electrical load analysis for Sikorsky UH-60A.

Chapter 5: Results and Discussion on the results obtained from the power required to drive the tail rotor model and the Electrical load analysis model.

Chapter 6 – Conclusion **-** Draws a conclusion on the whole work carried out and a brief description of further development

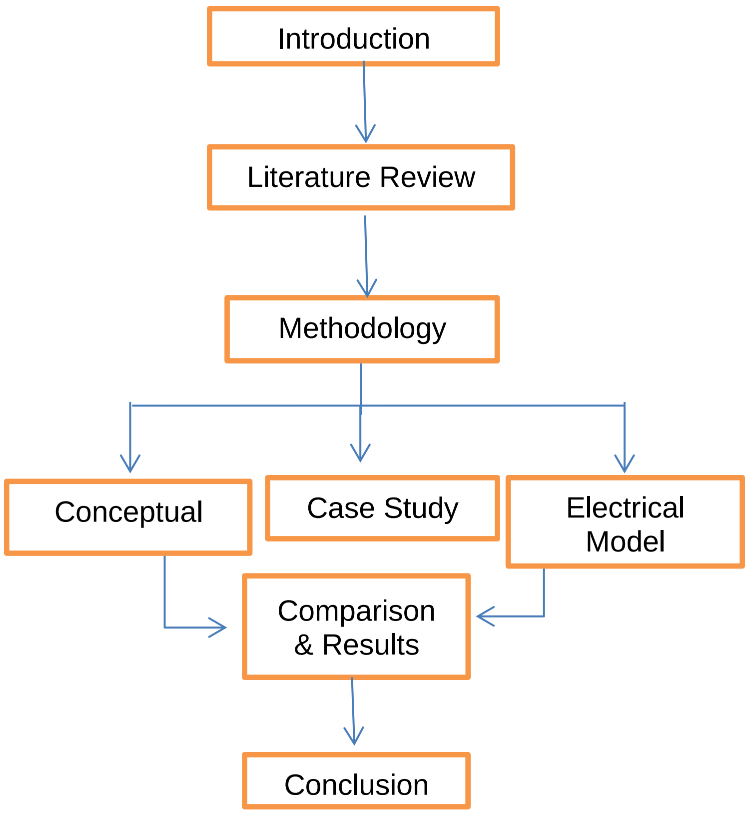

Figure 1 Thesis Structure

2 Literature Review

A rotary wing aircraft is a versatile machine that vertically take-off and land, hover over a constant position or change direction in the air[12]. The working principles of rotorcrafts are far more complex compared to the fixed-wing aircraft, due to their rotational parts, aerodynamics and the intervention within the framework. There are further stability, control, vibration and noise issues, and a range of flight conditions unique to helicopters[13].

Figure 2- VS-300 Rotorcraft[14]

In aviation history, the early 19th century is noted as the era of man's relentless search for practical flying machines [15]. In 1861 a French pioneer, Gustave de Ponton d' Amécourt conceived the word 'Helicopter'. The pioneers of helicopter developed many extraordinary designs, but they lacked two essentials: (1) adequate engine power (2) understanding the nature of lift. In November 1907, Paul Cornu builds a twin-rotor helicopter and vertically lifted the vehicle for few seconds [16].

In 1939, Igor Sikorsky piloted the first practical helicopter. The VS-300 was designed with a single main rotor with the torque-compensating tail rotor, becoming the standard configuration for most of the helicopters constructed since 1941[17]. The invention of the helicopter was achieved in the early 1950s, in the following years the designing aspects of the helicopter have reached successful production records, and some very large helicopters were also constructed.

The development of the helicopter is considered lagging as they require higher engine power density compared to the fixed wing aircraft for the stable hover flights. A significant improvement of rotary wing models was noted during the 19th century due to the availability of fuel-efficient high-performance lightweight turboshaft engines[18].

2.1 Mechanism - Rotor System

The parts of a conventional helicopter’s rotor system are the main rotor and the anti-torque system. The main rotor system controls the lift of the helicopter, thrust and lateral control in four directions: forward, aft, right and left. Tail rotor or the anti-torque control designed with variable pitch also balances the torque[19], if else would turn the fuselage of the helicopter. The tail rotor is otherwise used for directional control of the rotorcraft which is attained by altering the pitch of the tail rotor blades[20].

A significant amount of power is transmitted from the engine to the tail rotor which is attached to the tail boom, through the main transmission. The main rotor and the tail rotor are connected by a tail drive shaft, the tail rotor rpm is controlled through the main gear box. The main rotor gearbox drives the tail rotor in case of engine failure and aids to land the helicopter safely[21].

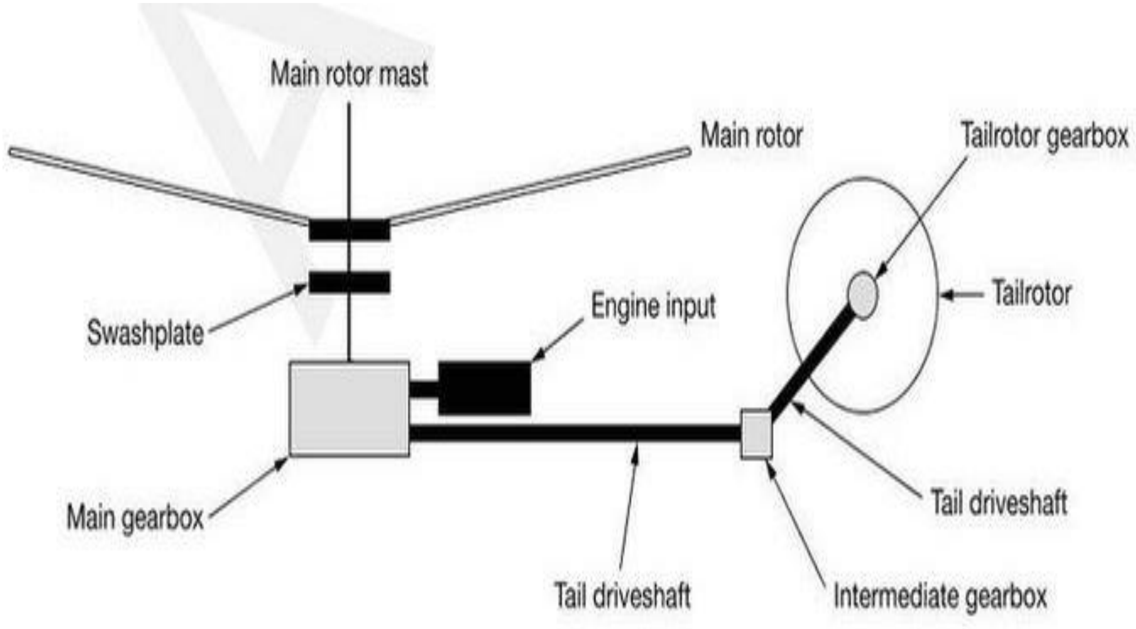

Figure 3 Transmission overview[20]

In Sikorsky UH-60 Series helicopters the main transmission has five (a main module, two engine input modules and two accessory modules individual, interchangeable modules (Figure 4). The powertrain has two spiral bevel gear meshes (17.3:1 reduction and a spur gear planetary system with five pinions (4.67:1 reduction). Three additional spiral bevel meshes provide power take-off for the accessory modules and tail rotor while four spur gear meshes drive the accessories and lubrication pumps. This drive-train configuration provides an overall reduction ratio of 80:1 and reduces the input speed from 20,900 to 258 rpm at the main rotor[22].

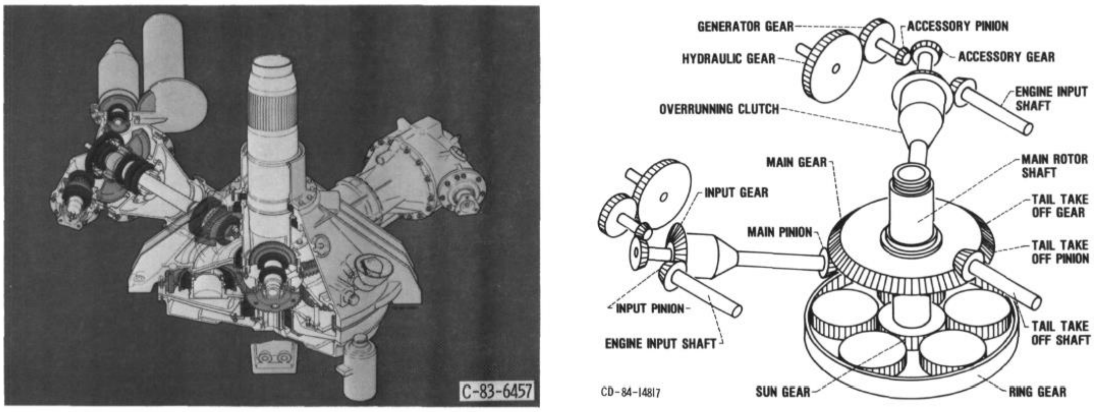

(a) Detail. (b) Schematic.

Figure 4 UH-60 Series Main Transmission[22]

2.2 Helicopter Configuration

Rotary wing aircraft are mainly differentiated on the parameters of gross weight, type of rotors and performance operations (civil, commercial and military) [7]. The configuration of the helicopter has an influence on the control and stability characteristics.

The difference in types helicopter on the rotor drive category is mainly based on the number and the positioning of the main rotors and the type of anti-torque system used in the rotorcraft[12].

The classification of helicopters made under the weight cateogory is based on Clean Sky project A lightweight helicopter has a maximum take-off weight (MTOW) less than 5450kg; medium helicopters weigh up to 10,000 kg, but this category still includes many heavy helicopters or heavy-lift helicopters above this MTOW[13].

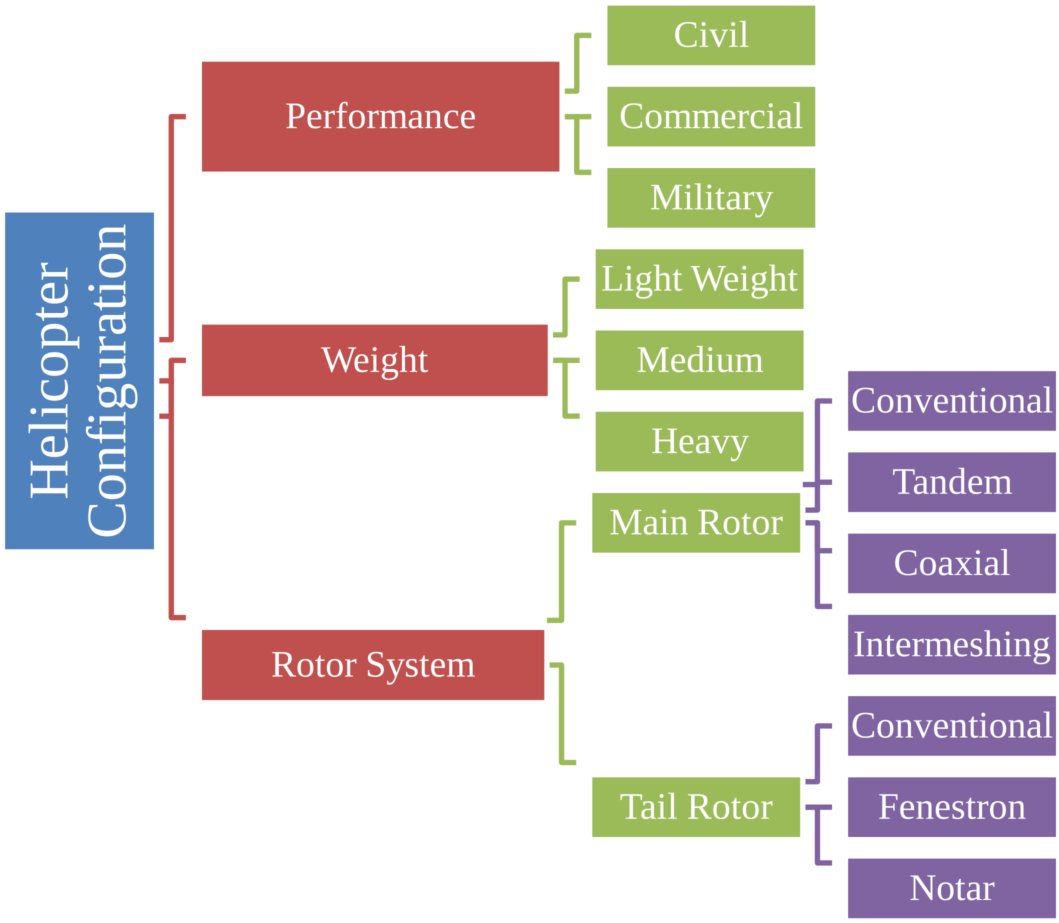

Figure 5 Helicopter Configuration

2.2.1 Anti-torque System

According to Newton's 3rd law of motion "For every action, there is equal and opposite reaction"; the rotating motion created by the main rotor has to be counterbalanced to avoid the impact on the fuselage, forcing it to turn in the opposite direction.

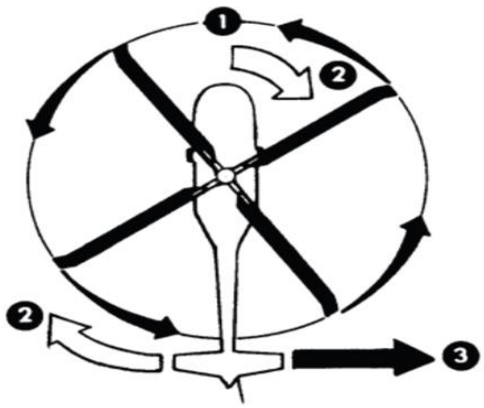

1 Rotation direction of engine driven main rotor

2 Torque effect rotates fuselage in direction opposite to main rotor

3 Tail rotor counteracts torque effect and provides positive fuselage heading control

Figure 6 Torque reaction[19]

2.2.2 Anti-torque configurations

There are different types of Anti-torque system

1. Conventional
2. NOTAR
3. Fenestron
4. Contra-rotating Main rotor
5. Coaxial main rotor
6. Transverse rotor

Conventional Helicopter

The conventional helicopter configuration consists of a single main rotor and an anti-torque system (Tail rotor). The tail rotor which is mounted on the tail boom (vertically) produces anti-torque and acts as a yaw controller. Generally, the moment arm of the tail rotor thrust acting on the main rotor shaft is higher than the radius of the main rotor blades.

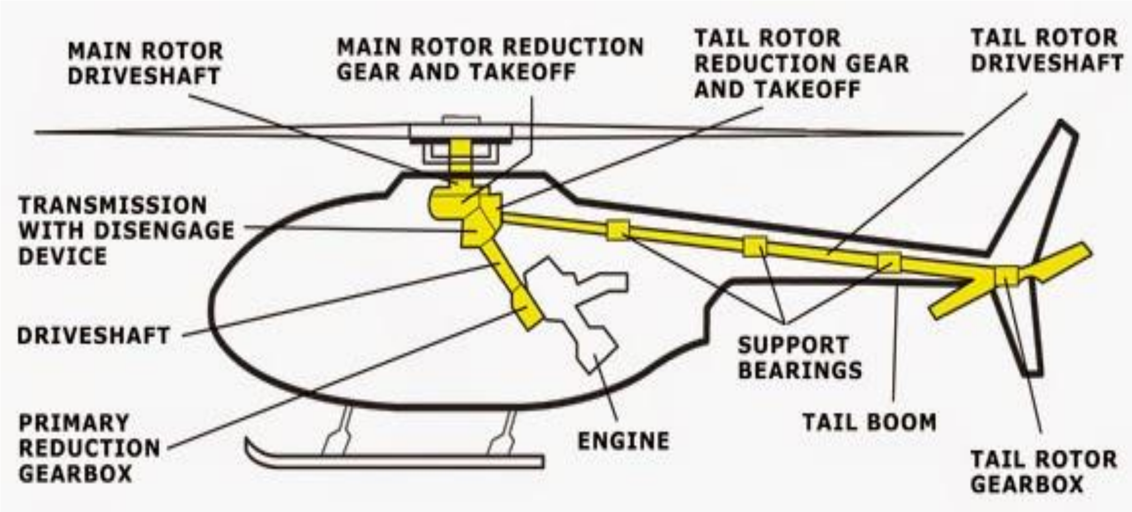

Figure 7 Conventional Helicopter[23]

The tail rotor system is either two bladed teetering assemblies or advanced design with four no bearing or no hinge design. The common working of any of these designs is that it has only collective pitch and no cyclic pitch (as there is no requirement of control on disk orientation)[24]. However, the tail rotor has the flapping movement to react to the modification in aerodynamic conditions.

In order to reduce the mechanical intricacies and weight, the lead-lag hinges are avoided. But numerous pitch-flap couplings are used to provide the cyclic pitch which reduces the flapping created to balance the aerodynamic load in the tail rotor design. Further, an advantage weight is generally added to the high cambered aerofoil tail rotor pitch horns to reduce the moments getting transmitted to the pitch control[24].

Figure 8 Tail Rotor[25]

The pitch and roll movements in a helicopter are attained by altering the angle of the main rotor employing the cyclic pitch; altitude is altered by a collective pitch and by altering the tail rotor’s thrust magnitude using collective pitch the yaw control is attained[12].

The typical single rotor helicopter configuration has a single main rotor coupled with a tail rotor. The tail rotor acts an anti-torque, balances yawing moment and provides stability to the overall helicopter lift. The tail rotor restores moment by reducing and increasing the thrust when the helicopter climb or descent attained by yawing nose-left or nose-right.

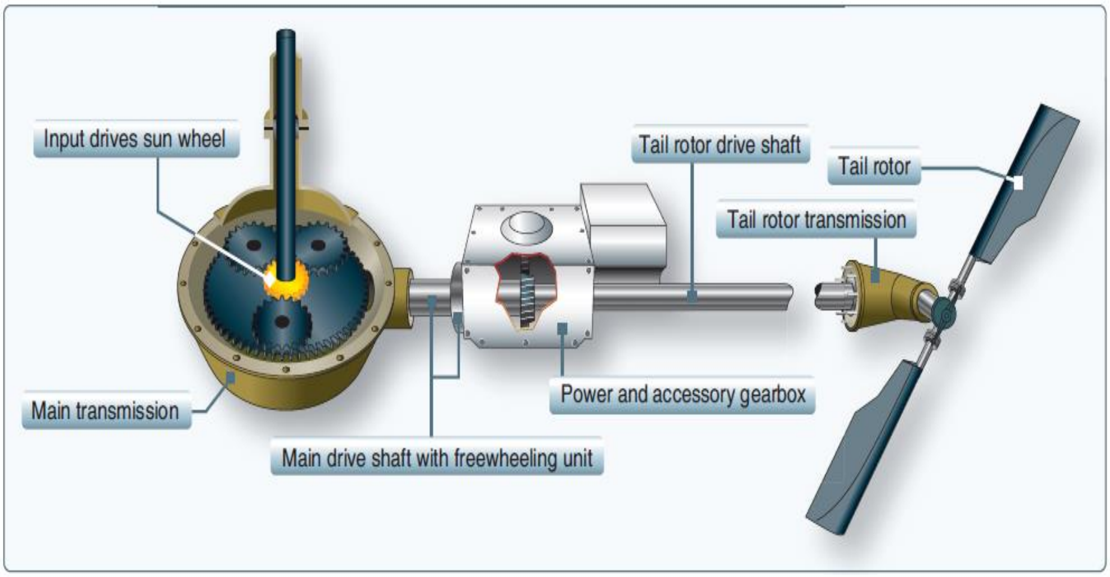

Figure 9 The Tail rotor Driveshaft[18]

The conventional tail rotor assembly is complex and requires frequent maintenance due to the requirement of the long and angular shaft to transfer the power from the main gearbox.

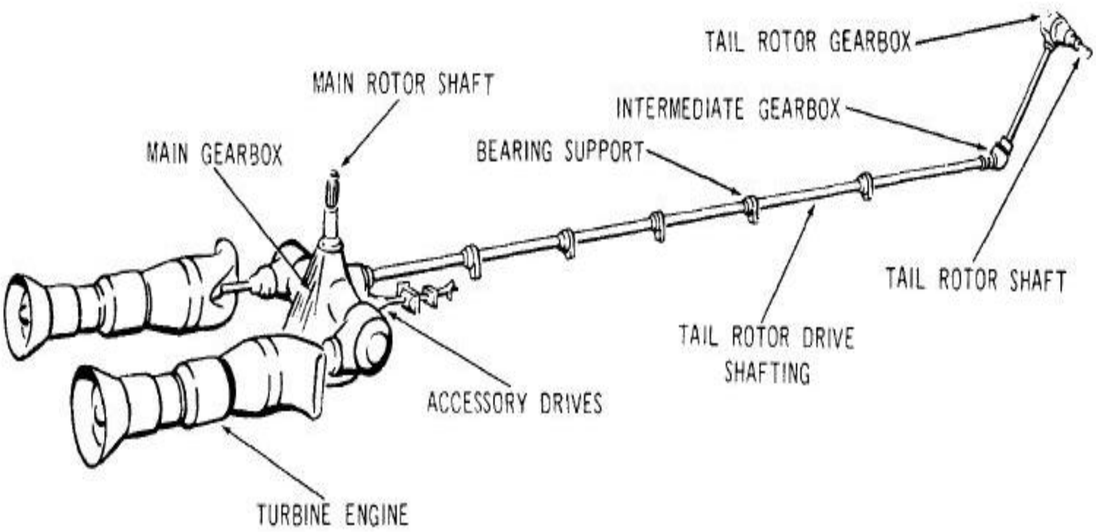

Figure 10 Typical Transmission system in Single-rotor Helicopter[26]

In contrast to the main rotor, the tail rotor operates in a complex aerodynamic condition; the tail rotor is subjected to same turbulent weather conditions as the main rotor and also the wake interface and the turbulent flow caused by the fuselage and the main rotor hub. Additionally, the tail rotor undergoes the effect of sideward winds and relative flow from any direction during yawing moments and possible encounter of vortex ring state. The interaction with the vertical fin and other assemblies also has a minor impact on the tail rotor[15]. Because of these aerodynamic disturbances causes the dynamic stress on the blades which reduces the blade longevity and high maintenance of the components.

NOTAR

The anti-torque in No Tail Rotor (NOTAR) is produced by blowing jet air at one side and creating pressure suction on the other side of the tail rotor. The NOTAR anti-torque system eliminates some of the mechanical disadvantages of a tail rotor, including long drive shafts, hanger bearings, intermediate gearboxes and 90° gearboxes[27].

As there is no mechanical system involved the helicopter tail rotor drive train, NOTAR are presumed to be the quietest among the other tail rotors. It also eliminates the vulnerability of accidents by blade striking. But the drawback for this type of anti-torque system is that it requires more power from the centrifugal compressor, making it suitable only for smaller helicopters[24].

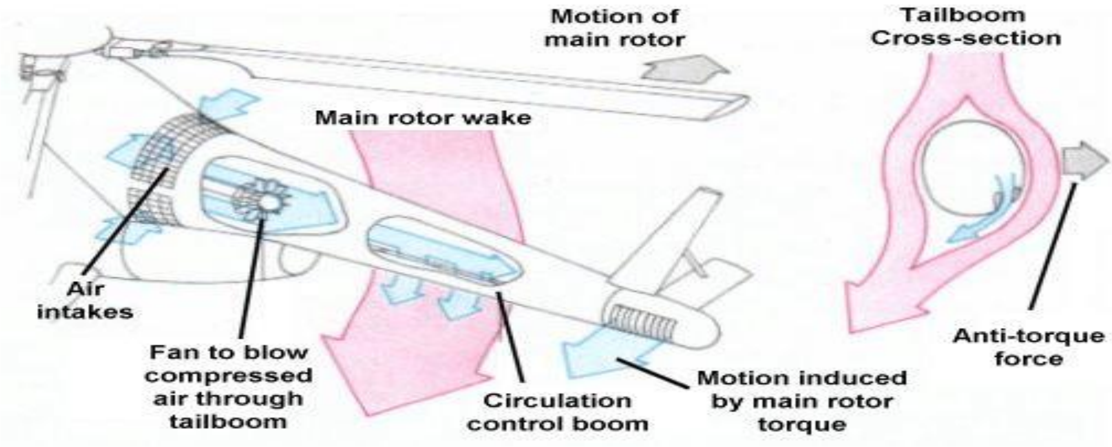

Figure 11 NOTAR[25]

Fenestron

Many researches are carried out to replace the conventional tail rotor; so far, the most effective alternative in terms of stability, power, weight, and auto rotating capability is the Fenestron. The level noise and vibration produced are main disadvantages of the tail rotor. The Fenestron model reduces these issues and also avoids the personal hazard or accidents created by the conventional tail rotor[28].

Figure 12 Fenestron[29]

Contra-rotating Main rotor

The anti-torque is balanced by two or more contra-rotating main rotors requiring less power eliminating the necessity of the tail rotor. Therefore, the aerodynamic losses between the fuselage and the rotors are high, in turn reducing the overall efficiency of the helicopter. The mechanical complexity of this type of helicopter is high due to the requirement of two control systems almost mirroring each other and the difficulty in the distribution of increased weight.

Pitch and roll	Main rotor Cyclic pitch
Altitude	Collective pitch
Yaw	achieved by differential torque control of the main rotors

Table 1Helicopter Controls for Contra-Rotating Main rotor

Coaxial main rotor

Coaxial rotorcrafts are compact and have two contra-rotating main rotors with smaller diameters. The Main rotors are separated by different concentric shafts which reduce the mechanical effort. In coaxial Rotor class rotorcrafts, the rotor assembly is placed one on top of the other. The rotor assembly controlled by a complex mechanical rotor hub with two swashplates independently rotates on the same axis and same speed but in opposite directions. The Coaxial model doesn’t have a tail rotor as both the rotor cancels each other’s torque[30].

Figure 13 Coaxial rotorcraft[31]

Tandem Rotorcraft

In tandem rotorcraft, the anti-torque is balanced by two contra-rotating main rotors which overlap each other 30-50% longitudinally. To reduce the aerodynamic losses in the rotor, the rear rotor is elevated 0.3 to 0.5 R over the front rotor. The length of the fuselage is more compared to other typical rotorcrafts this is due to the large longitudinal centre of gravity. Usually, the tandem rotors are used in a heavier helicopter because of their structural weight penalty.

Longitudinal Control	The main rotor thrust magnitude
Altitude	Collective pitch of the main rotor
Yaw	Cyclic pitch of the main rotor
Roll	Lateral thrust tilts with cyclic pitch

Table 2 Helicopter Controls for Tandem Rotorcraft

Figure 14 Tandem Rotor[32]

Side by Side Rotor

The side by side or transverse rotor is similar to the contra-rotating rotor; the main difference is that the main rotor is separated laterally. Generally, in this type of rotorcrafts, the main rotor doesn't overlap as it is being separated by 2R.

Roll	Collective pitch
Altitude	Longitudinal cyclic pitch

Table 3 Helicopter Controls Side by side rotor

Figure 15 Transverse rotor[33]

2.3 ELECTRICAL POWER SYSTEM

The Electrical system in an aircraft contains a power source(generator), power distributors and power consumers[34]. The aircraft power system technology has developed parallel to the evolution of aircraft itself. Depending on the type of avionics and other electrical systems are powered by either Alternating Current (AC) or Direct current (DC) [35,36]. The Generators for in-service aircraft are generally 115 VAC at 400 Hz.

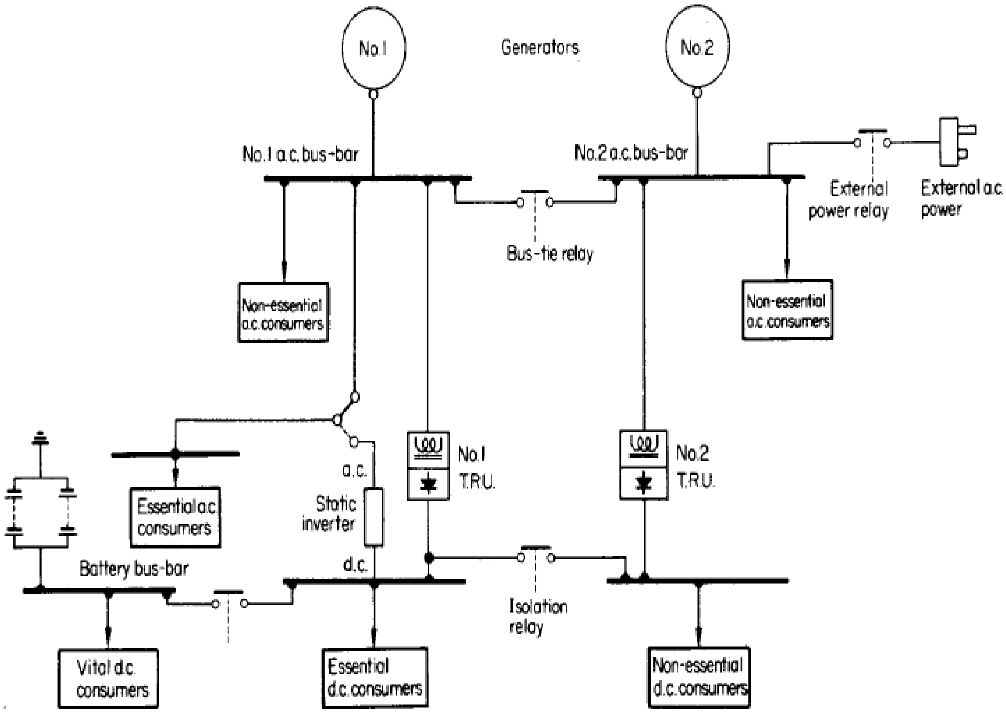

Figure 16 Typical Aircraft Power Distribution[37]

In case of Boeing 787, categorised as More Electric Aircraft (MEA) is built with 230 VAC generator to provide enough power to satisfy the required electrical load of the aircraft[38].

The spur in the improvement of power generation increases with the evolution of the avionics equipment, as it increases the demand for higher voltage, less power loss and, reduction in weight[39]. The new present generation of aircraft is produced with solid state switches, microelectronics and high power controls for power distribution management and safety requirements[36].

2.3.1 Power generation

Aircraft Electrical System energy production depends on AC or DC generators which are coupled to the main engines, Auxiliary Power Unit (APU) and the batteries. The electrical power for most of the electrical equipment in the aircraft relies on the generators [23]. The Required voltage is induced by AC and/or DC generators, they are distinguished by the way the electrical power is collected and transferred to the generator connected externally through circuits[35].

AC Power Generation

The Alternating Current (AC) generator produces voltage in a constant sine wave frequency. The AC generator design is less complex compared to the DC design as it doesn’t require commutator. In the initial AC, generators design the current transmitted to the rotor windings through slip rings, which were corroded and dented mainly in high electricity flow at higher altitude[40].

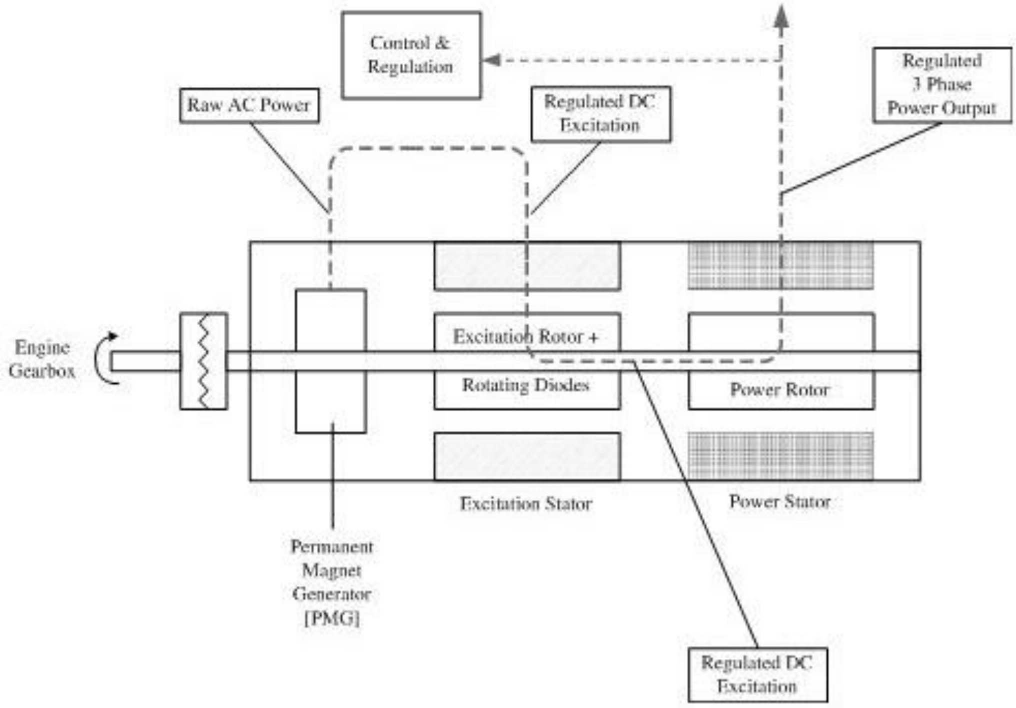

Figure 17 Principle of AC generator[40]

The recent technology AC generators working is shown in Figure 18 illustrates the parts of a typical AC generator. The electrical energy flows from the generator to the rotor and rotating diodes, at this stage the DC current is modulated and controlled and then power is passed through the power rotor, where it is regulated as 3 phase output. The AC power is produced by power rotor by creating a rotating field.

A 3-phase AC current is used in most of the aircraft, which are linked in a star pattern with a terminal of each of the phases linked to a neutral point as illustrated in Figure 18. This figure explains the two primary methods of electrical energy production used on aircraft for years - the phase voltage of a normal aircraft system is 115 VAC, however, the line voltage measured among lines is 200 VAC with typical 400 Hz frequency.

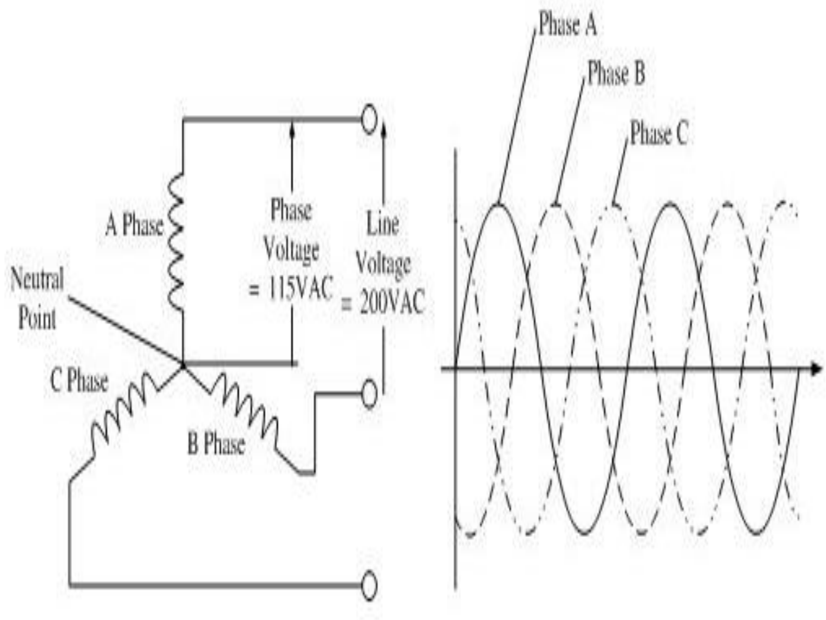

Figure 18 Star Linked 3 phase AC generator[40]

The main benefit of AC current is that they work at a high voltage as much as 115 VAC but the DC works usually at 28VDC. As the voltage is high the current flowing will be low which in turn has low voltage drops or power losses. The drawback of higher voltage is that they require a good standard of insulation. As the weight of the conductors is usually high, the decrease the current will make it lighter; a very significant consideration in aircraft design[40].

In most large aircraft the DC is supplied from an AC alternator and passed through a transformer-rectifier unit. Brushless alternator system with integrated oil cooler is employed in modern aircrafts[41].

DC Power Generation

The DC generators are usually used generate and regulate 28 VDC to supply DC loads in the aircraft electrical system, but there are also 270VDC loads as well. DC generators are self-powered by the revolving electromagnets that produce the electrical energy. The AC is converted into DC by using commutator which allows a simple sine wave output voltage, as a corrected half-wave and flattened to attain a sturdy DC voltage. In the aircraft, the generators are usually ‘shunt-wound’ in which the high resistance field coils are linked in parallel with the armature as illustrated in Figure 20.

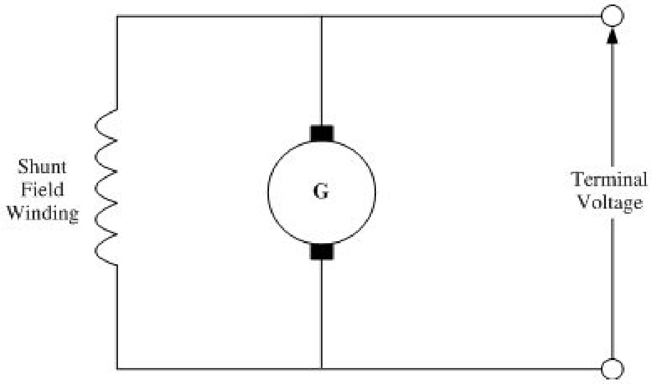

Figure 19 DC generator[40]

The DC generator is developed to adjust the voltage automatically when the current increases due to the aircraft regulator or electrical load vary the voltage is maintained by the voltage regulator coupled to the generator. The working principle of the DC voltage regulator is illustrated Figure 20.

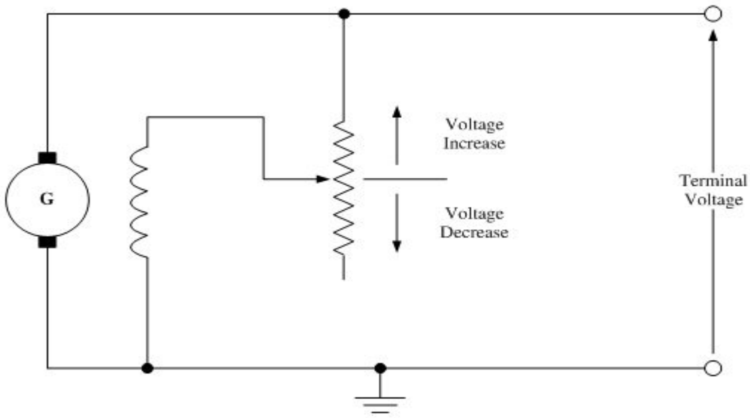

Figure 20 DC voltage regulator[40]

Most of the DC generators are designed with the similar parts - field frame, rotating armature and brush assembly. The basic design of DC generator is similar to the design of a DC motor; containing a series of coils would on a laminated soft core of iron which is rotated inside an electromagnetic field. As a result, AC is produced within the coils, which are converted into DC by the commutator. To regulate the voltage produced the field current is controlled as the function of the output voltage from the generator[41].

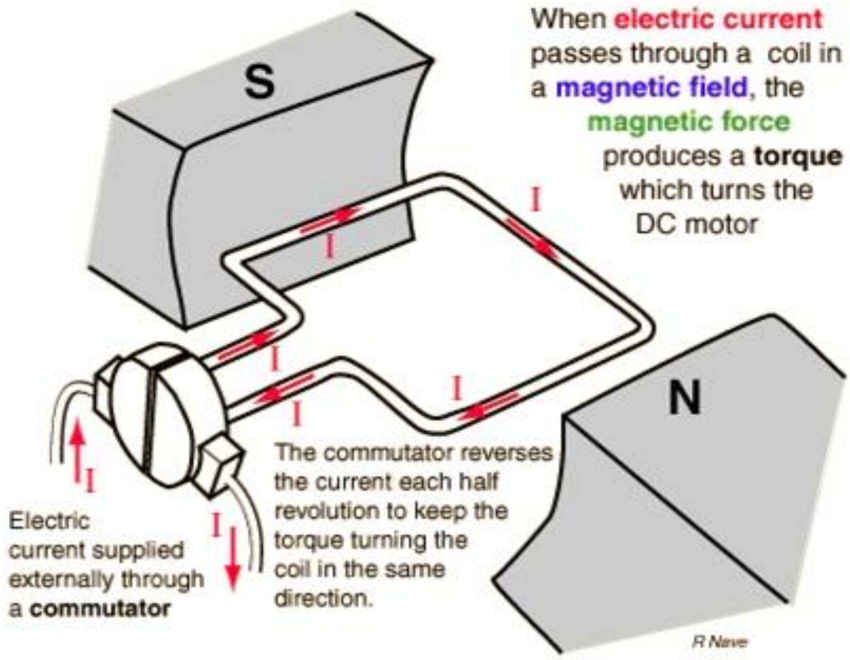

Figure 21 AC to DC converter[42]

Battery

The rechargeable battery is the oldest form of man-made supply which stores electricity in the form of chemical energy. A battery comprised of one or more electrochemical cells and each cell consists of a liquid, paste, or solid electrolyte together with a positive electrode (anode) and a negative electrode (cathode).

During discharge, an electrochemical reaction occurs at the two electrodes producing a flow of electrons through an external circuit. The reactions are reversible, allowing the battery to be recharged by applying an external voltage across the electrodes. Batteries usually have very low standby losses and can have high energy efficiency (60-95%)[43]. Batteries that are either in use and/or potentially suitable for the utility scale battery energy storage application includes lead acid, nickel cadmium, sodium sulphur, sodium nickel chloride and lithium ion[44].

Lead-acid Battery

Battery Voltage	**Plates per Cell**	**Discharge Rate**					
		5-Hour		*20-Min*		*5-Min*	
		Ah	*amps*	*Ah*	*amps*	*Ah*	*Amps*
12	9	25	5	16	48	12	140
24	9	17	3.4	10.3	31	6.7	80

Table 4 Battery discharge rate

In the case of generator failure, the lead-acid battery is used for starting the engines. During a sudden electrical load increase, the battery is stabilised the generator output. For single engine aircraft, 12V batteries are used and 24V batteries are used for larger aircraft. The voltage production is dictated by the number of cells per plate, the area and the electrolyte in the plate determine the ampere hour (Ah) capacity [41].

Nickel-Cadmium Battery

The Lead-acid battery is superseded by nickel cadmium (NiCd) batteries due to high-demand electrical systems. The main advantages of the nickel cadmium batteries are that they remain nearly charged due to their low internal resistance caused by the closed-circuit voltage, which in turn provides enough power to start the turbine engine. The disadvantage of this type of battery is that due to its low internal resistance it causes high-temperature discharge leading to “thermal runaway”. Most aircraft employing NiCd battery uses battery overcharge sensor to alter the pilot to avoid a potential thermal runaway[41].

Lithium Battery

Lithium-ion (Li-ion) batteries deliver 270V and 28V to start the engines, flight control and secondary power. Li-ion battery is used as it has high energy density and life expectancy compared to other batteries. Li-ion batteries produce current by transferring the charge between the electrodes. The electrodes are distanced by a polymer membrane to avoid short circuits internally, and the organic solvent mixture with lithium salt is included to the cell to deliver an average for ion migration[45].

The main drawback of Lithium-ion batteries is its risk of fires and explosions. There were numerous cases reported to Federal Aviation Administration (2016) regarding the battery explosions especially for the cell phones, Samsung tablets and laptops with lithium-ion battery[46].

The lithium-ion battery fire and explosion is related to the flammability of the electrolyte, the rate of charge and/or discharge, and the engineering of the battery pack [47]. Increased temperature of the Lithium ion battery can cause the battery to rupture, ignite, or explode. Therefore, many researches are being conducted to reduce its safety hazards [48].

2.3.2 Anti-torque system failure

If the tail rotor fails in the forward flight, the nose of the fuselage will roll to some degrees and yaw towards the right-hand side of the helicopter. The direction in which the helicopter roll will depend on the configuration and distribution of centre of gravity[49,50].

In the case of tail rotor failure in hover phase of the helicopter, the rolling motion will be uncontrollable due to the torque reaction created by the high power main rotor. There are 119 accidents accounted due to anti-torque failure[50], which is 38% of the total single turbine helicopter accidents occurred during the study period from 1963 to 1987. Out of 119 tail rotor accidents, 73 are caused due to the drive shaft failure and 46 due to gearbox failure.

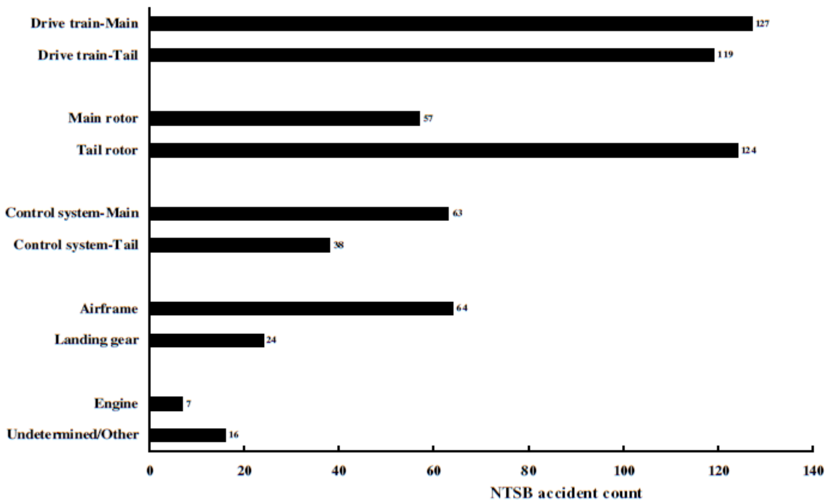

Figure 22 Airframe failure accidents by system: single- engine helicopter[50]

2.4 Conventional Power Train

The conventional aircraft power train embodied with electrical, mechanical, pneumatic and hydraulic systems. The schematic in Figure 23 describes the functions of each sub-system. In the architecture of conventional aircraft, fuel is converted into power by the help of engines[51].

The power obtained from the engine is mainly used for creating thrust to move the aircraft. The remaining power is used for running the ECS, IPS, Mechanical system and the electrical power generation system. The ECS system uses the pneumatic power of the engine to provide high pressurised air to maintain cabin pressure and temperature. The IPS uses the hot air to avoid ice formation on the aircraft.

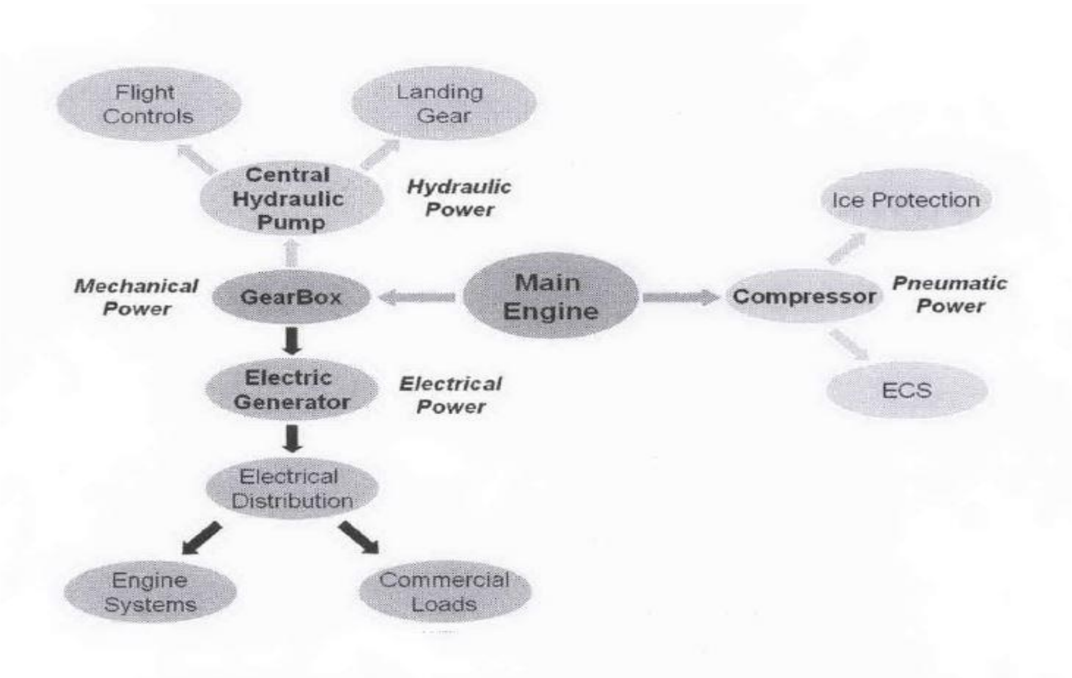

Figure 23 Conventional Power train[51]

The mechanical power is transmitted by the gear system to the central and local hydraulic pumps. The hydraulic power obtained from the pumps controls the flight control through actuation system; the hydraulic system is very robust and has very high power density, but they are heavy and the corrosive fluid used in the pipes are prone to leakage. The mechanical system also provides power to the anti-torque system and the electrical generators. The electrical power provides power to the avionics, cabin, cockpit, lighting, etc.

As the components in these systems increases, their interactions becomes complex, the efficiency of the whole aircraft reduces[51]. The schematic below represents the convention helicopter drive train, which has high power to weight ratio, but the efficiency of the turbine and the reliability of gearbox is low.

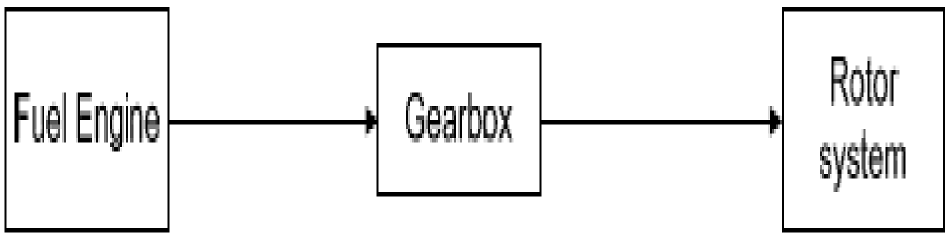

Figure 24 Conventional helicopter drivetrain[51]

2.4.1 Rotorcraft Mission Energy Management

Rotorcraft Mission Energy Management (RMEM) which is been developed at Cranfield University[52] simulates the onboard helicopter systems and determines, the shaft power and engine bleed air off-take requirement for each sub-system for designated missions and flight profiles.

The RMEM-TEM (Twin-engine medium)[11] model contains four sub-system models; each of which represents the secondary power systems onboard of the rotorcraft. These sub-systems are Actuation System (AS), Electrical System (ES), Fuel System (FS), Environmental Control System (ECS) and Ice Protection System (IPS).

A demonstrative case study for a TEM class helicopter has been carried out to assess the potential of the tool and to identify the limitations of the developed approach. RMEM has been coupled with Cranfield University's comprehensive rotorcraft code HECTOR (HEliCopTer Omni-disciplinary Research platform) [53].

The combined approach has been deployed to investigate the performance of the various subsystems on the board of a representative TEM rotorcraft. The implemented coupling strategy between HECTOR and RMEM is discussed and the adapted interfaces between the two codes are described.

General description of RMEM

RMEM is a model capable of wide range of onboard electrical and mechanical systems employed on rotorcraft. To facilitate this, RMEM comprises a series of analytical methods for the analysis of various subsystems, such as Ice Protection System (IPS), Actuation System (AS), Environmental Control System (ECS), Electrical System (ES) and Fuel System (FS). The result of the analysis includes the engine shaft power and bleed-air off-takes required to sustain the operation of the onboard systems for a given flight phase.

The system's power extracted in the form of shaft power together with the bleed-air off-takes required affects the installed powerplant operating point, Specific

Fuel Consumption (SFC), and the gaseous emissions produced. It is therefore understood that accounting for the shaft power and bleed-air off-take requirements of the on-board systems, can be critical in the context of a mission analysis where accurate estimates of the total mission fuel burn and environmental impact are required.

RMEM can be used to model conventional as well as conceptual systems at the preliminary design stage. When used in combination with a suitable mission analysis code, such as HECTOR[53], RMEM can be used in estimated the effect of the onboard subsystem on the powerplant performance. Figure 25 shows an overview of the RMEM.

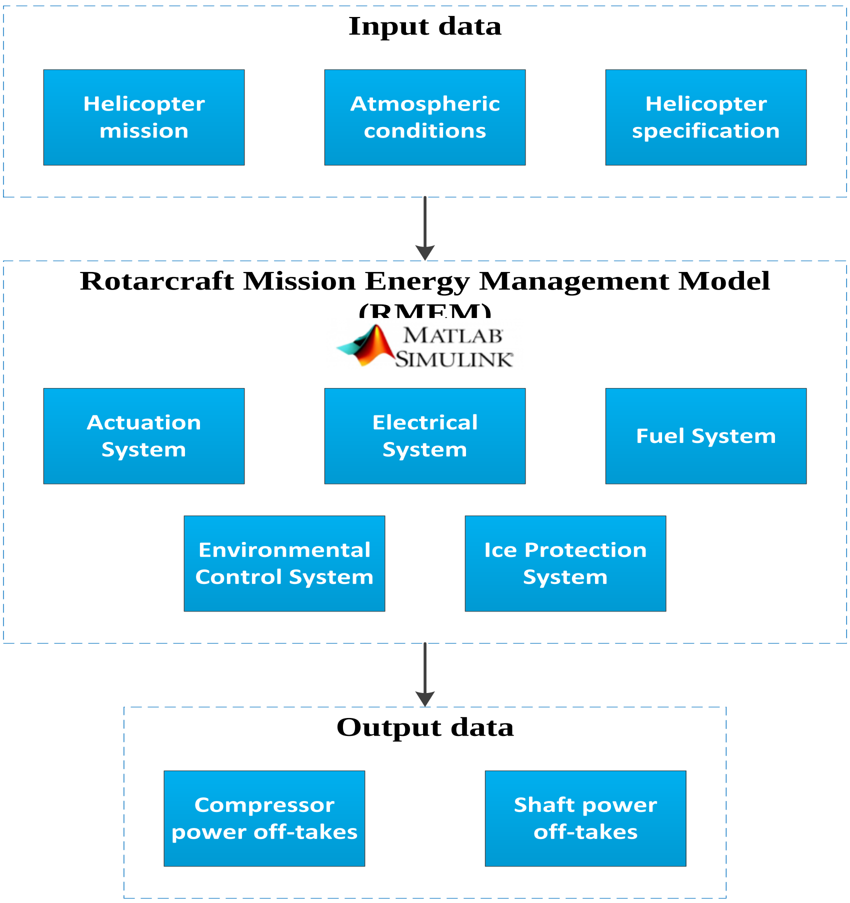

Figure 25 RMEM overview[11]

RMEM has been developed exclusively in MATLAB-Simulink® with the underlying system models is built upon physics-based methods. Furthermore, the overall framework includes an extensive user-defined database with vehicle-specific geometries and system components. The developed system architecture allows the compilation of vehicle-specific standalone models in the form of Windows executables (*.exe) or Dynamic Link Libraries (*.dll). This enables the effortless integration of RMEM with other rotorcraft performance simulation tools, such as HECTOR or the Clean Sky Project's PhoeniX platform (Platform Hosting Operational and Environmental Investigations for Rotorcraft)[54]. The data from the RMEM-TEM is utilised as the input for the power requirement calculation of the tail rotor drive in the Modelling chapter of the thesis.

2.5 More Electric Aircraft

The aviation industry is moving towards 'all-electric aeroplanes, which eliminates the requirement of hydraulic power and bleed air off-takes from the engine. The elimination of bleed air off-takes needs novel high-voltage electrical systems and innovative solutions, such as air-conditioning, wing ice protection, or electric engine start-up[51].

Elimination of the engine hydraulic pumps needs completely operational electrical power actuators and electically opereated principal flight controls. The "all-electric" aeroplane is not a new concept; the research on electric power aircraft has started during world war II[55], even though till recently the capability of electrical power production to satisfy the required load was feasible particularly for commercial and civil transportation purpose[51].

The main advantage of using electric system instead of hydraulics is that they reduce the weight of the system and the maintenance cost of the helicopter[51]. The increase in number electricity load consumers increases in MEA, which leads to upscaling of the electrical power producers. With the progression in the high-power density electrical system in recent years, it is now achievable to drive the aircraft subsystems by electrical power.

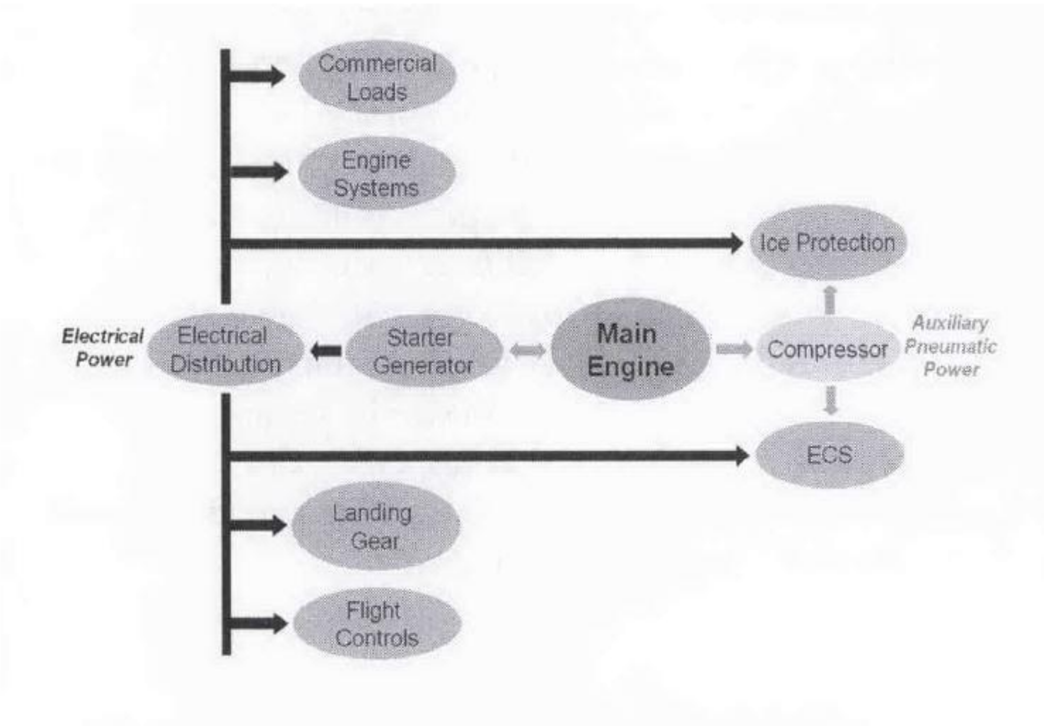

Figure 26 Electrical power train[51]

The study by Durkee and Muzetze[9] investigate the feasibility of converting Robinson R22 helicopter mechanical power train to electrical. In the conceptual More Electric Aircraft design, the electrical power is provided by AC and/or DC generators which are connected to the Main engine. The power is then transmitted to the electrical tail rotor decreasing the weight of the gearbox[9].

The recent aviation industry research is concentrated towards lighter electrical systems to decrease the weight of an aircraft and accordingly decreasing the fuel consumption and life cost expenses[56], substituting the heavy mechanical systems such as the pneumatic pipes and hot air IPS systems.

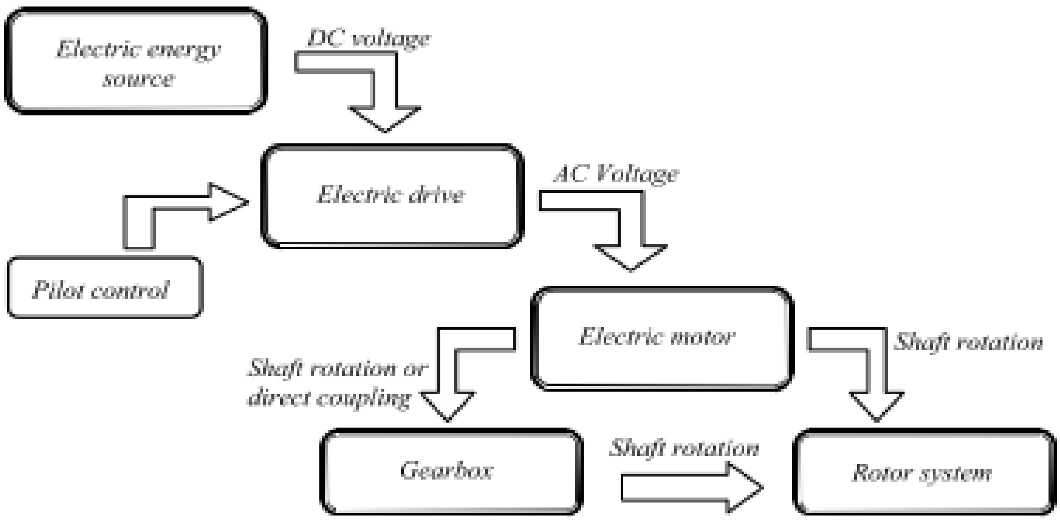

Figure 27 Electric Powertrain for helicopters[9]

Conversely, the increase in electrical load to provide these alternate electrical systems required high voltages and/or currents. An upsurge amount of current flowing through wires is not generally ideal as the voltage fluctuations and increasing in weight of alternative wiring. Due to this reason, the higher voltage in aircraft wiring is preferred.

The avionics system was operating at 14.25 VDC in 1936, increased to 28 VDC in 1946 [57] and eventually increased to 115/200 VAC 400Hz systems which are used in most of the transport aircraft. From the 1980s The military aircraft uses 270 VDC to further decrease the weight[40].

The current MEA such as Boeing 787 has two 250kVA generators mounted to both the engines. To maintain the amount to electric produced by the generators, Boeing has increased from an 115/200 VAC 400 Hz components to a combination of 230/400 VAC 360– 800 Hz (variable frequency) and a 230/400V[58]. Accompanied by the auxiliary power production, the total electric power produced will be nearly 1500 kVA [58]. The new aeroplanes such as Airbus A350 and A380 are estimated to produce 800 kVA, and also increases the voltage and frequency of aircraft electrical systems.

Figure 28 Sikorsky's Firefly[59]

Little work has been carried out by Clean Sky project in regard to the electric rotor, but other initiatives like the Sikorsky's Firefly is an example of advancement towards the more electric helicopter. The Sikorsky S-300 (Figure 28) helicopter substituted completely with electrical drivetrain[59]. In the Firefly concept, the main engine is replaced with a 142 kW Permanent Magnet (PM) motor with Li-ion batteries supply power.

The battery-driven Firefly has the efficiency of 76.3% that includes the efficiency of the batteries and electrical motor[60]. Compared to the baseline Sikorsky S-300, the efficiency of Firefly increased to 300% (not considering the power loss in battery charging process. As the moving parts in this model is reduced compared to the baseline the operating costs decreased accordingly.

Conversely, the major drawback of using only battery-driven motors is that it has limited flight range. The Firefly has a flight time of approximately 15 minutes; the baseline S-300 has more than 3 hours [61]. This is a familiar concern also for the Electric Automotive Vehicles (EAV) where fuel cars are substituted with no emission electric variants. The common resolution used in EAV's such as charging the battery or inductive charging is not appropriate for aircraft. So, to produce a fully electric concept, research towards battery technology should be concentrated. The ideology of electric rotorcraft is different from the fixed wing aircraft as they could be mounted with electric-powered propellers.

The aerodynamic advancement in fixed wing aircraft makes it more effective; compensating the additional weight of the electric motor and batteries. When it comes to more electric rotorcraft altering the aerodynamic design becomes complex. The main rotor is used for the thrust of the helicopter and also maintaining the lift, which requires more power and torque. If the weight of helicopter increases due to electrification the rotorcraft, the energy demand to lift the helicopter increases, which make the design process challenging.

The gas turbine engines are widely used in the aircraft (weight is a critical feature) as their power to weight ratio is high. However, an essential property of these engines is the low efficiency of a maximum of 45%, though this efficiency is occasionally attained in practice [62]. Due to this reason, the diesel engines are considered to be less emission alternative with a practical efficiency of more than 50% and a theoretic maximum efficiency of about 75% [63]. Combining this with electrical generators and motors of more than 90% efficiency, this drivetrain can be more efficient and flexible than the current turboshaft system.

3 Methodology

3.1 Theory

3.1.1 Helicopter Performance

The overall performance of the rotorcraft is generally assessed as the difference of the power delivered by the engine to the power required for the rotorcraft to operate in different flight phases (climb, cruise, hover and descent)[64]. In the following chapter the power required in hover, climb, cruise and descent of the tail rotor are calculated. As per Leishman[24] to get a close approximation of the power required to drive tail rotor the momentum theory and blade element theory has to be considered.

Momentum Theory

In momentum theory, the rotor performance is obtained by introducing basic fluid mechanics conversion law to the rotor. Following the principles of Newton's 3rd law of the velocity – the rotor increases obtaining the rotor wake and the thrust is created in the opposite direction[64]. The fluid (Air) is considered to be compressible and inviscid.

By conservation of mass, the mass flux is constant.

$$\dot{m} = \boldsymbol{\rho A \gamma}$$ **Equation 3-1**

$\dot{m}$ - Mass flux

ρ – Density

A – Area of disc

γ- Induced velocity

Since the upstream flow is at rest for the hovering rotor

$$\boldsymbol{T} = \dot{m}\boldsymbol{\omega}$$ **Equation 3-2**

T – Thrust of tail rotor

ω - Wake induced velocity

By energy conversion equation

$$\boldsymbol{T\gamma} = \frac{\mathbf{1}}{\mathbf{2}}\,\dot{m}\boldsymbol{\omega}^{\mathbf{2}}$$ **Equation 3-3**

$$\boldsymbol{\omega} = \mathbf{2}\boldsymbol{\gamma}$$ **Equation 3-4**

Therefore, Induced power required

$$P = T\gamma = \frac{T}{\sqrt{\frac{T}{2\rho A}}} = \frac{T^{\frac{3}{2}}}{\sqrt{2\rho A}}$$ **Equation 3-5**

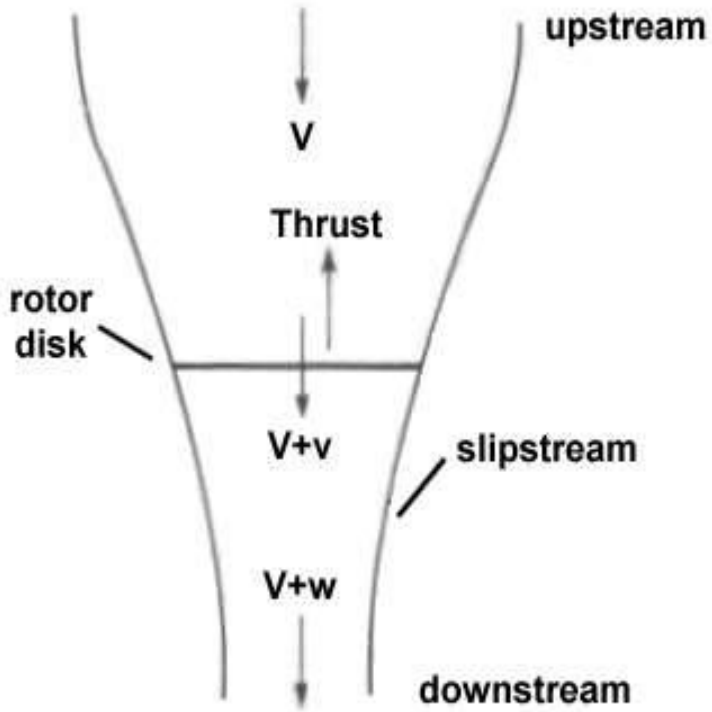

Figure 29 Air acceleration in hovering phase[64]

Blade Element Theory

Blade Element Theory is the basis of most of the aerodynamic analysis in rotorcraft as it is considered the loading of the rotor blade and the flow on the blades are explained more in detail[64].

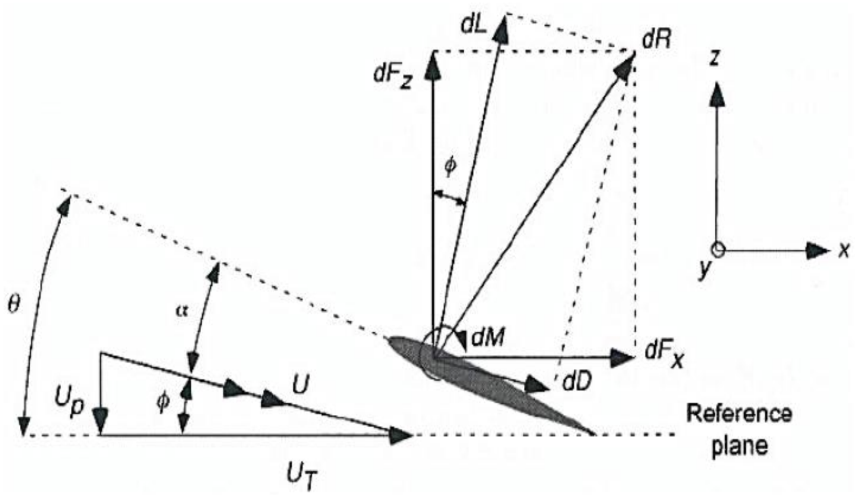

Figure 30 Aerodynamic environment at a blade element[24]

The below formula is to determine the total thrust and power

$$C_T = \frac{1}{2}\sigma C_{l_\alpha}\left[\frac{\theta_0}{3} - \frac{\lambda}{2B}\right]$$ **Equation 3-6**

$$C_P = \frac{1}{2}\sigma C_{l_\alpha} k\lambda \left[\frac{\theta_0}{3} - \frac{\lambda}{2B}\right] + \frac{\sigma C_{d_o}}{8}$$

Equation 3-7

Where

C_T – Thrust Co-efficient

C_P – Pressure Co-efficient & C_l – Lift Co-efficient

3.1.2 Helicopter Performance at hover phase

The rotorcraft performance in hover flight phase is obtained by analysing the power needed for the atmospheric condition with the power provided by the engine, which leads to an understanding of features such as increasing the ceiling condition in hover flight phase.

The rotorcrafts are mainly designed to hover efficiently, as the rotorcraft hover during most of the flight time during most of the missions. Due to this reason, rotorcraft researches are concentrated more towards achieving sufficient vertical lift and maintain the hover state. The airflow through the rotor at hover is symmetrical to the axis, of the rotor making it viable flow pattern to mathematically analyse[24].

The Rankine Froude momentum theory that is derived from ‘the equations of fluid mass momentum and energy conservation laws’, is utilised for the analysis of the rotorcraft performance[26]. Due to the increase in the air mass, from the origination of the finite velocity at the wake, a force of list is created that allows the rotorcraft to maintain the altitude as illustrated in Figure 31. The lift caused when the rotorcraft is hovering is described as[24]

$$\boldsymbol{T} = \dot{\mathrm{m}}(\Delta\boldsymbol{\gamma})$$ **Equation 3-8**

$\dot{\mathrm{m}}$ −Mass flow per second through the wake

$\Delta\gamma$ - Total change in flow velocity

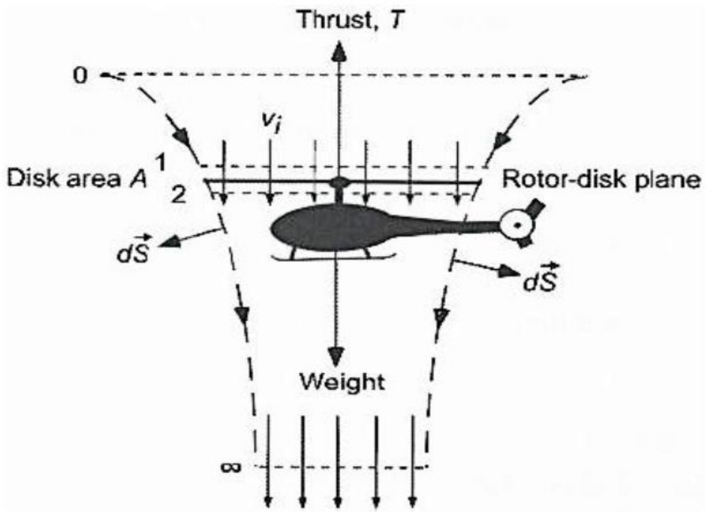

Figure 31 Momentum theory analysis[24]

The finite velocity of the wake decreases as the velocity of the flow increases, (this condition occurs when the flow is continuous. The induced velocity at the plane of the rotor disc is twice that of the velocity at the remote wake $(w = 2v_i)$. Taking the features into consideration the features of the flow passing through the rotor disc and altering the position of the thrust equation, the induced velocity at the rotor plane in hover state is described as [24]:

$$v_h = v_i = \frac{T^{\frac{3}{2}}}{\sqrt{2\rho A}}$$

Equation 3-9

where

(T/A) - disc loading.

According to Leishman [24], the disc loading of the rotors provides increased climb ratio with less power as the rotorcraft disc load varying between 24-48 kg/m^2 [24].

$$\lambda_h = \lambda_i = v_i = \frac{1}{\Omega}\frac{T^{\frac{3}{2}}}{\sqrt{2\rho A}}$$

Equation 3-10

The non-dimensional velocity (λ_h) which is related to the thrust co-efficient of the disk the induced velocity is divided by tip speed of the rotor blades [24]:

Ω - Angular Velocity

R – Rotor radius

Tail Rotor power

The power of the anti-torque system adapts to balance the main rotor torque[65]

$$Q_{tr} = T_{tr} . l_{tr} \qquad \textbf{Equation 3-11}$$

Where

Q_{tr} –tail rotor torque

T_{tr} – tail rotor thrust

l_{tr} – length of the tail rotor

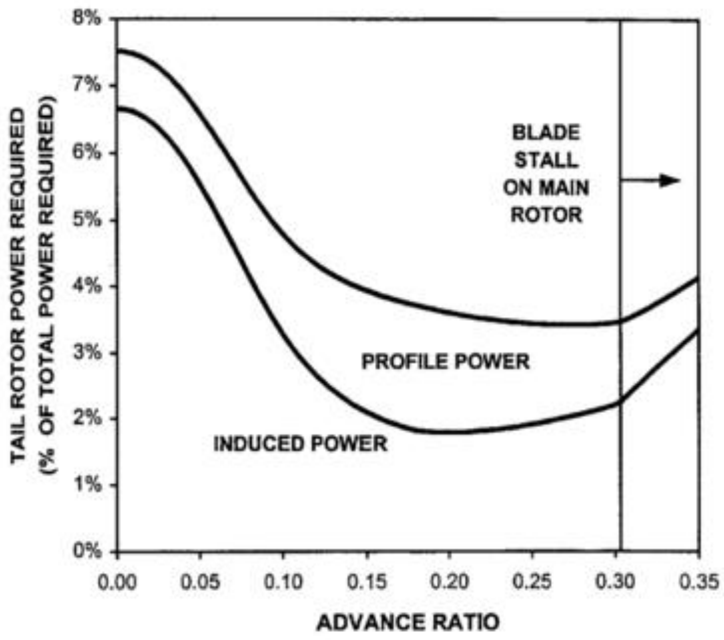

Figure 32 Variation of tail rotor power in level flight[24]

The notable difference in tail rotor power at the forward flight is seen in Figure 32. The power of the tail rotor drops rapidly when the flight is in forward motion, but in the case of the main rotor a sharp increase in the power can be noticed. This observed pattern is due to the induced velocity influenced by the forward flight acceleration of tail rotor blades[24].

Power in Hover

Induced Power in Hover

Induced power is the force required to counteract the gravity in order to obtain required lift the rotorcraft, which is calculated by adopting the momentum theory equations,

$$\boldsymbol{P_i = Tv_i \; \frac{T^{\frac{3}{2}}}{\sqrt{2\rho A}}}$$ **Equation 3-12**

In equation (3-12) the induced power is assumed to be the ideal power as the viscous effects are not considered in this equation. Other losses caused by the blade profile drag and 3D flow at the blade tip will be considered [26].

Total Power in Hover

To estimate the total power required by the tail rotor at hover state the blade tip loss factor (B) varying between 0.95 to 0.98(according to the rotor dimension) is considered[24]. The blade loss occurs as the lift and drag coefficients from the root to the tip of the blade, decreasing till zero at the tip[64].

The total power required by the tail rotor in hover is given by[65]

$$\boldsymbol{P_{tr} = \frac{T^{\frac{3}{2}}}{\sqrt{2\rho A}} \cdot \frac{1}{B} + \frac{1}{8}\sigma C_{d_o} \rho A (\Omega R)^3}$$ **Equation 3-13**

Where

B – no. of Blades

Ω **-** Rotational speed

R – Radius of the blades

Power required by the tail rotor in the Forward flight:

When the rotorcraft moves forward, the tail rotor will have to overcome the air stream similar to the main rotor due to this reason similar method to calculate the main rotor power is adapted to determine the tail rotor power. The compressibility and blade stall are not considered in this equation to analyse the tail rotor power variation. Irrespective of the power differences in the tail rotor is influenced by the main rotor power, due to the inclusion of induced velocity in forward flight condition the change of tail rotor power is not exactly the same as the main rotor[24].

Thus, the tail rotor profile power will be given by:

$$\boldsymbol{P_{tr} = T_{tr} \cdot \gamma_{tr} + \frac{1}{8}\sigma C_{d_o}\rho A(\Omega R)^3(1 + 4.3\mu^2)}$$

Equation 3-14

Where,

$$v_{ih} = \sqrt{\frac{T}{2\rho A}}$$

Equation 3-15

μ – Advance ratio

Power in Climb:

In the hover state of the rotorcraft, it is observed that the momentum and the blade element methods are used to investigate the rotor in vertical flight. Conversely, for very low degrees of descent (depends on the flight conditions), these methods are not applicable to calculate the rotorcraft climb [24].

Axial Climb

Compared to other flight phases, more power is required to overcome the gravity at climb phase of the rotorcraft and it is being influenced by the difference in the take-off weights and altitudes in a given mission, which depends on the variance in rotor's induced velocity at the take-off or landing phase. The velocity at the plane of the rotor becomes $\boldsymbol{V_c + \gamma_i}$ and the finite velocity at the wake is $\boldsymbol{V_c + \omega}$.

Implying that in equation (3-2) the principle of conservation of mass and momentum, the formula for thrust is obtained:

$$\boldsymbol{T} = \dot{m}\boldsymbol{\omega} = \mathbf{2}\boldsymbol{\rho A(V_c + \gamma_i)\,\gamma_i} \qquad \textbf{Equation 3-16}$$

Consecutively, the induced velocity of the rotorcraft during take-off is considered to be:

$$v_i = -\left(\frac{V_c}{2}\right) + \sqrt{\left(\frac{V_c}{2}\right)^2 + \frac{T}{2\rho A}}$$

Equation 3-17

when $\boldsymbol{V_c} \geq \mathbf{0}$the rotorcrafts operates at normal working condition, and at the hover condition ($\boldsymbol{V_c}$ becomes $\mathbf{0}$) the lower limit [24].

Axial Descent

When the flight descents, the conditions are different compared to the axial climb compared to directional changes creating a circular flow pattern at the rotor. Despite the fact, the mass flow rate through the rotor disc is estimated identical to the take-off, except that the operation of the rotor is negative; mainly when the power is obtained from the airflow. As per Prouty [66], ‘this state is known as the windmill brake state’. Thus, the thrust expression is written as:

$$\boldsymbol{T} = -\dot{m}\boldsymbol{\omega} = -2\rho A(\boldsymbol{V_c} + \boldsymbol{\gamma_i})\,\boldsymbol{\gamma_i}$$

Equation 3-18

Total power required in descent

In the conventional rotorcraft, the rotor will produce a torque by the main rotor acts on the fuselage and without any form of anti-torque components, the fuselage will gyrate irrepressibly. The tail rotors are required primarily at the low-speed flight when there is inadequate airflow over the fin to produce a side force that can counteract the torque reaction[65]. Hence:

$$T_{TR} l_{TR} = Q_{MR} = \frac{P_{MR}}{\Omega_{MR}}$$ **Equation 3-19**

The total power required for propelling the tail rotor during the take-off or landing is affected by the induced power of the main rotor

Power required by the tail rotor in the Climb and descent[24]

$$P_{Climb} = P_{Hover} + \frac{\omega \gamma_l}{2}$$ **Equation 3-20**

3.2 Case Study - Sikorsky UH-60A (general Description)

The Sikorsky UH-60A is a conventional (main rotor and tail rotor system) twin-engine medium rotorcraft. The 4-bladed main rotor system made of titanium/fibreglass, controls the lift of the rotorcraft, thrust and lateral control in four directions: forward, aft, right and left. Tail rotor or the anti-torque control designed with variable pitch also balances the torque, if else would turn the fuselage of the helicopter.

The Sikorsky UH-60A rotorcraft is designated under the medium category as its mission gross weight is 16000 lb and maximum gross weight is 20250 lb. The helicopter is propelled by two T700- GE-700 turboshaft engines working parallel at maximum standard sea level, reaching 1150kW each. The engines concurrently provide power to the complete operation of the main rotor and a 20-deg.

tilted tail rotor. The rotorcraft drive train involves of the main transmission, intermediate gearbox and tail rotor gear box with interconnecting shafts.

Figure 33 Sikorsky UH-60A **[67]**

The trim system in Sikorsky UH-60A helicopter provides the inclined power to preserve the cyclic and tail rotor pedal position and the flight path stabilisation is provided by the trim system. The flight path stabilisation is an autopilot operation that boosts the static stability during the pitch, roll, and yaw movements. The stabilator which can vary the angle of incidence of the aerofoil is designed to enhance flying characteristics by arranging in such a way to counteract the collective, airspeed, pitch rate, and lateral acceleration inputs[10].

General Specification		
Empty weight	Approximately 11,154 lbs	
Fuel Capacity	364 gallons	
Fuel weight	2446 lbs	
Rotor Parameters	**Main Rotor**	**Tail Rotor**
Number of Blades	4	4
Diameter	53ft 8in	11ft
Blade Chord	1.73ft	0.81ft
Blade Twist	~18 deg	~18 deg
Blade Area	46.7 ft^2	4.46 ft^2
Solidity Ratio	0.082	0.188
Rotor rotation speed (rad/sec)	27.02	124.54
Tip Speed (ft/sec)	725	685

Table 5 General Specification[68]

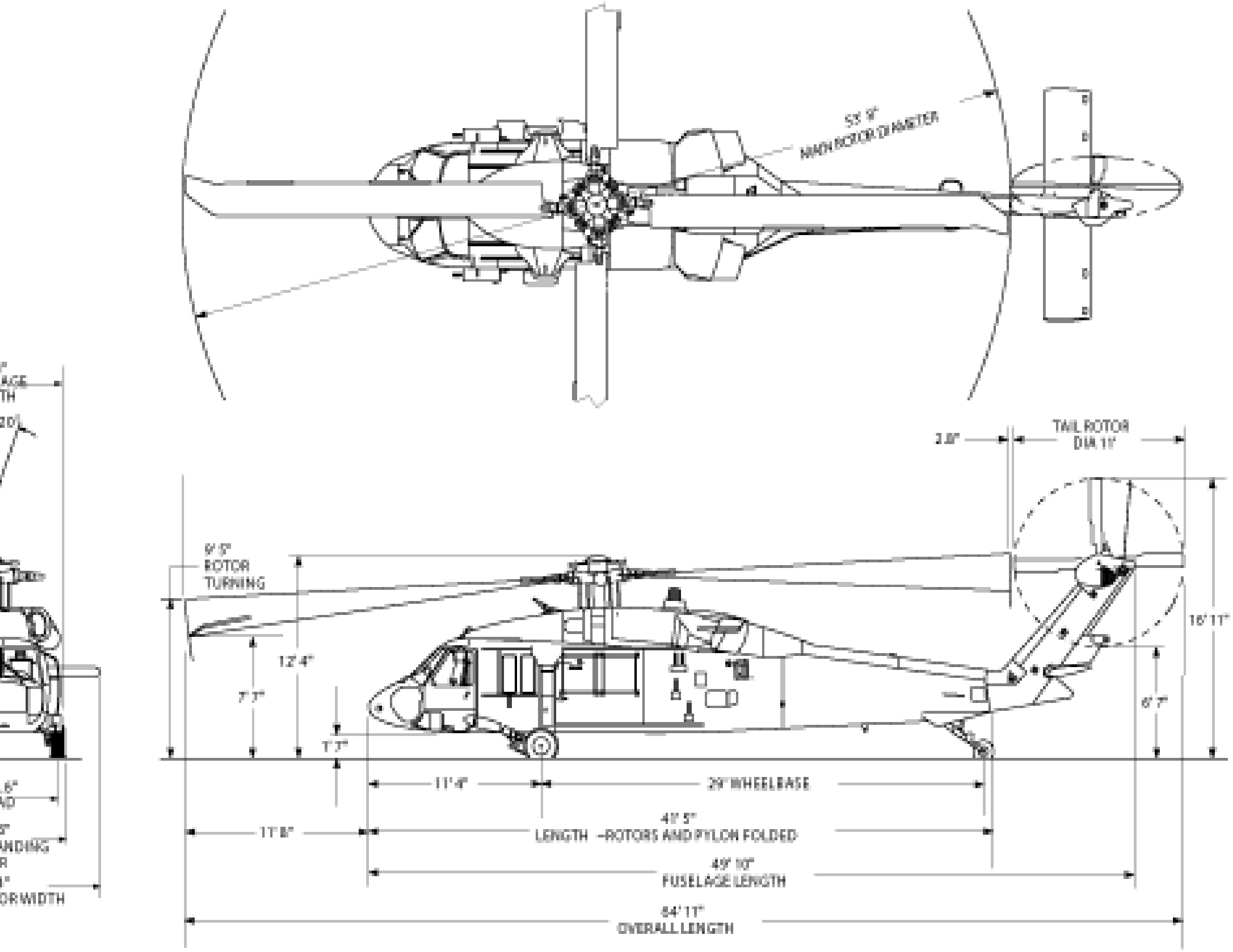

53' 9"
MAIN ROTOR DIAMETER
2.0"
TAIL ROTOR
DIA 11'
9' 5"
ROTOR
TURNING
12' 4"
7' 7"
1' 7"
16' 11"
6' 7"
11' 4"
29' WHEELBASE
11' 8"
41' 5"
LENGTH –ROTORS AND PYLON FOLDED
49' 10"
FUSELAGE LENGTH
64' 11"
OVERALL LENGTH

Figure 34 Sikorsky UH-60A [10]

3.2.1 Sikorsky UH-60A tail rotor

As the Sikorsky, UH-60A tail rotor doesn't have any bearing, the elastic buckle of graphite spars carries the required pitch control motion. The four-bladed tail rotor is formed by bolting two separate paddles with the help of titanium plates. The centrifugal load acts between the spar connection and extends till the tips of two blades and thereby exposing the hub of the tail rotor to immense loads. The main advantage of the Sikorsky UH-60A helicopter is the fibre composites which has unique structural qualities that eliminate the requirement to the pitch bearings to facilitate enough torsional flexibility. This challenging design also provides stabilised aeroelastic rotor throughout the flight mission and attain high rotor figure of merit for equalising the main rotor.

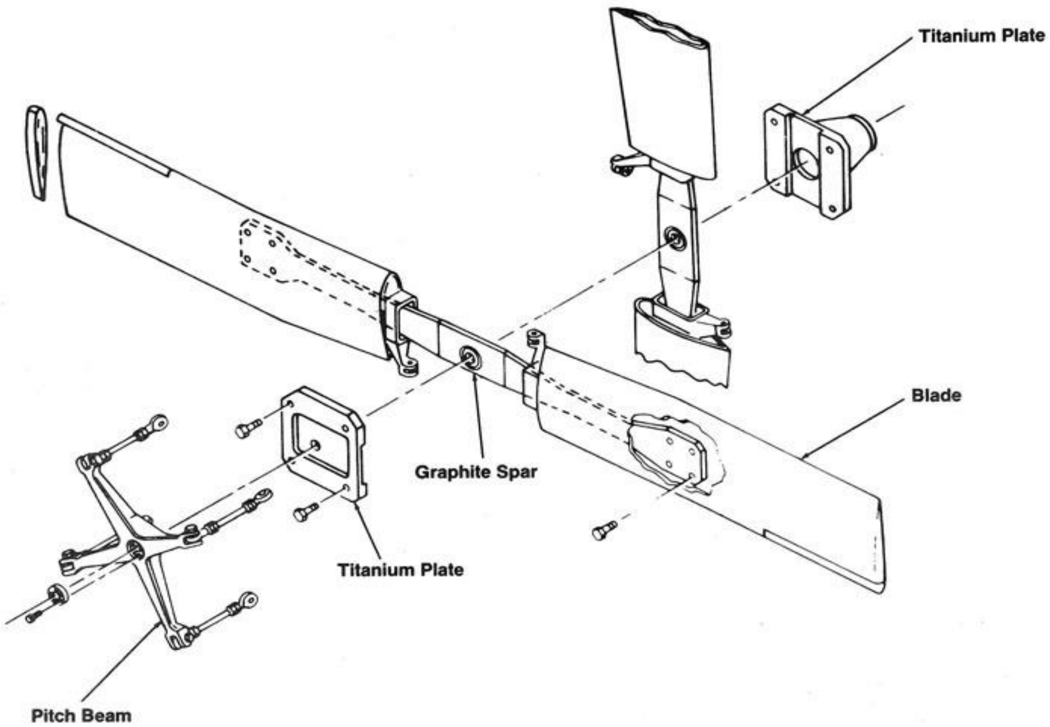

Figure 35 Tail Rotor Construction Detail[69]

The graphite epoxy composite material gives those advantages to the tail rotor spar, which couldn't be achieved with the metals. The graphite fibres act as the perfect tool to optimise the spar's elasticity due to different factors[70] (1) compared to the fibreglass, the graphite has low bending to torsion stiffness ratio and fatigue strain ratio, as it is important to maintain low pitch control loads. (2)

even though the boron fibres were preferred to the higher damage tolerance compared to the graphite laminates, it is not chosen due to non-ready availability and low cost. The graphite composite is handled with scrim cloth for higher damage tolerance.

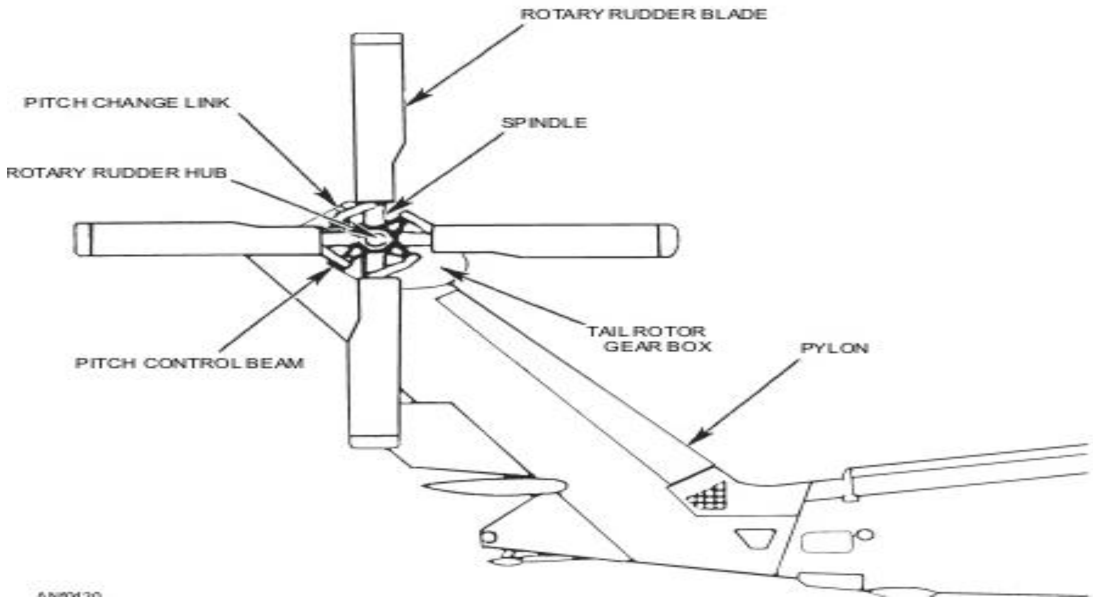

Figure 36 Tail rotor group[71]

The canted tail rotor has two main advantages[70], firstly it increases the total thrust required by the tail rotor to 6.5% compared to that of the typical tail rotors, and increases the overall helicopter thrust by 34%. The lift component is approx. 180kg in the hovering phase of the helicopter. The power required in order to produce lift is only 22 horsepower (hp), this is almost equal to 8kg/hp.

As the power ratio is three times greater than that of the main rotor, as a consequence the main rotor diameter is reduced. Secondly, due to the canted tail rotor - the length of the helicopter fuselage nose is reduced to equalise the centre of gravity of the helicopter. These two reasons make the Sikorsky UH-60A canted tail rotor helicopter more compared to the typical twin-engine medium helicopters.

3.2.2 Sikorsky UH-60A - Drive Train System

The mission of the drive train is to transmit engine power to the rotors and to the accessories mounted on the transmission. The drive train system includes the following major items and is shown in Figure 37[10]:

1. Two engine nose gear boxes

2. Two input shafts

3. APU driveshaft and couplings

4. Couplings and input clutch to the main transmission

5. Main transmission

6. Main rotor drive shaft

7. Tail rotor drive shafts

8. Forward and Aft hanger bearing

9. Intermediate Gearbox

10. Tail rotor gearbox.

Description of the Tail Rotor Drive System

The tail rotor drive system consists of the tail rotor drive shafting, couplings, hanger bearing, damper, anti-flail assemblies, and intermediate and tail rotor gearboxes. There are four tail rotor drive shaft sections. Three tail rotor drive shaft sections lead from the transmission to the intermediate gearbox. The fourth section is installed on the vertical stabilizer between the intermediate and tail rotor gearboxes. Flexible couplings - attached to shaft ends, are capable of accommodating shaft misalignments throughout the power range. The intermediate gearbox (IGB) reduces speed and changes the angle of drive to the tail rotor. The intermediate gearbox is a grease lubricated sealed unit.

Thermistors monitor temperature and an accelerometer measures vibration to provide crewmembers with caution messages. The tail rotor gearbox (TRGB), mounted on the vertical stabilizer, reduces the output speed and changes the angle of drive. The tail rotor output shaft passes through the gearbox mast and all loads are transmitted to the mast. The output shaft transmits only torque to the tail rotor. Lubrication of this gearbox is identical to that of the intermediate gearbox. As with the intermediate gearbox, four Thermistors monitor temperature and an accelerometer measures vibration to provide crewmembers with caution messages[10].

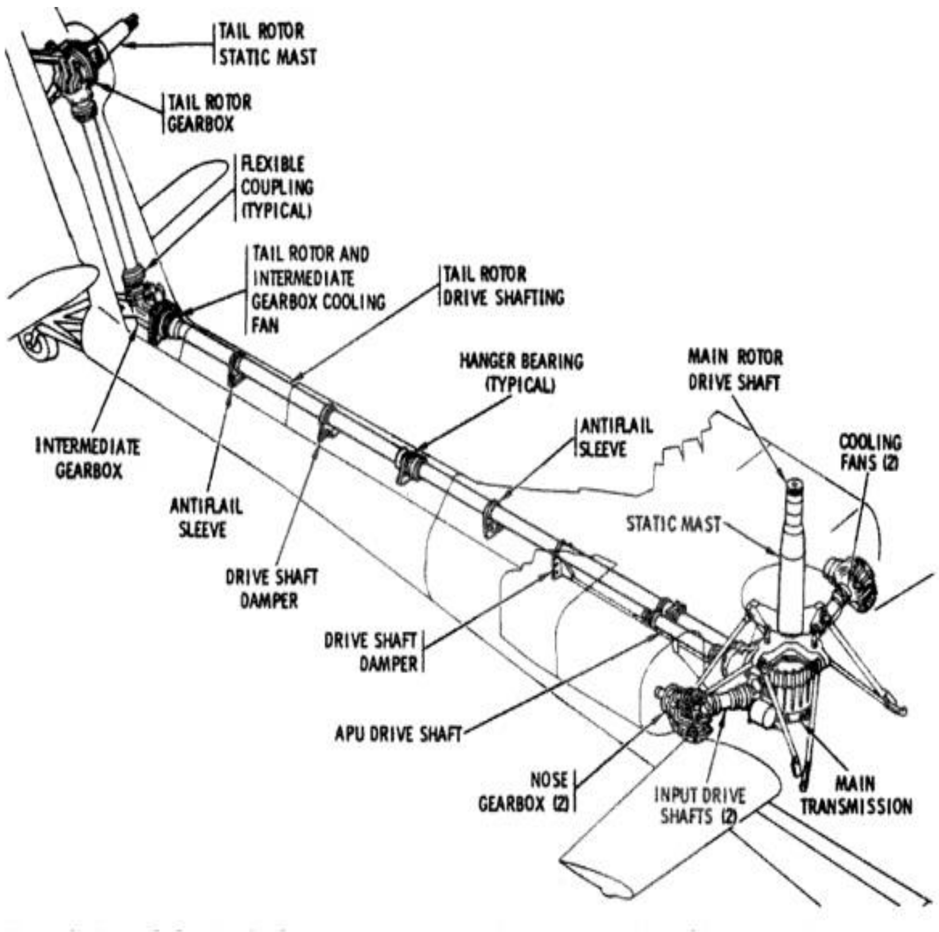

Figure 37 Powertrain UH-60A[10]

Cooling

The intermediate gearbox at the base of the vertical Stabilizer, reduces the rpm and changes the angle of drive. A fan mount (shown in Figure 37) on the gearbox input shaft draws air from an inlet on the vertical stabilizer. The air cools both the tail rotor gearbox and the intermediate gearbox. Four thermistors monitor temperature and an accelerometer measures vibration limits. The intermediate gearbox is a grease-lubricated sealed unit[10].

3.2.3 Power Distribution on Multi-Engine Aircraft

Compared to the single engine helicopters the multi-engine helicopter flies at high altitude, with higher speed and longer distance. Twin engine helicopter such as Sikorsky UH-60A has an advantage of higher redundancy and safer flight. As a consequence, to those qualities, it has more intricate power distribution system. The electrical power requirements of the twin-engine helicopter are satisfied by two generators connected to each of the engines.

In the modern power distribution system of multi-engine aircraft consists numerous buses for power distribution and various control systems and protection tools to ensure the redundancy. The complexity and the reliability of the electrical power distribution increased due to the high demand in electric load, caused due to increased number of electrical equipment in the helicopter[72]. There are two means of ensuring the fidelity of the power distribution (1) availability of more than one source connect to satisfy the required load. (2) Supplying the loads through different buses[18].

The Sikorsky UH-60A contains two starter AC generators utilised to start the engines and generate DC electrical power via TRU. The system can be described as a split-bus power distribution system as the left and right generator bus ruptures the electrical loads that are connected to each of the sub-bus through a diode and current regulator. The generators are operated in parallel and distribute the load correspondingly. The primary load supply provided by the Sikorsky UH-60A is DC via TRU from AC generators, even though small amounts of AC are supplied by two inverters. Figure 37 illustrates the AC power distribution at the top and mid left side. One inverter delivers the AC power and the second works standby. Both inverters produce 26 VAC and 115 VAC. A pilot operated switch is used to choose between the current flowing through the inverters[73].

The ignition exciter gets its input from the low voltage dc supply of the aircraft electrical system. Electrical power for the no.1 engine start system is obtained from the DC essential bus through the ENG START circuit breaker on the pilot's circuit breaker panel[74].

The DC TRU connected to the right and left AC generator operated and supplies the load in parallel, in the case of either one of the DC generators fails. The DC load supply is designed in a way that it is capable of operating independently in case of any of other fails, the battery provides power in case of both the generator failure[18].

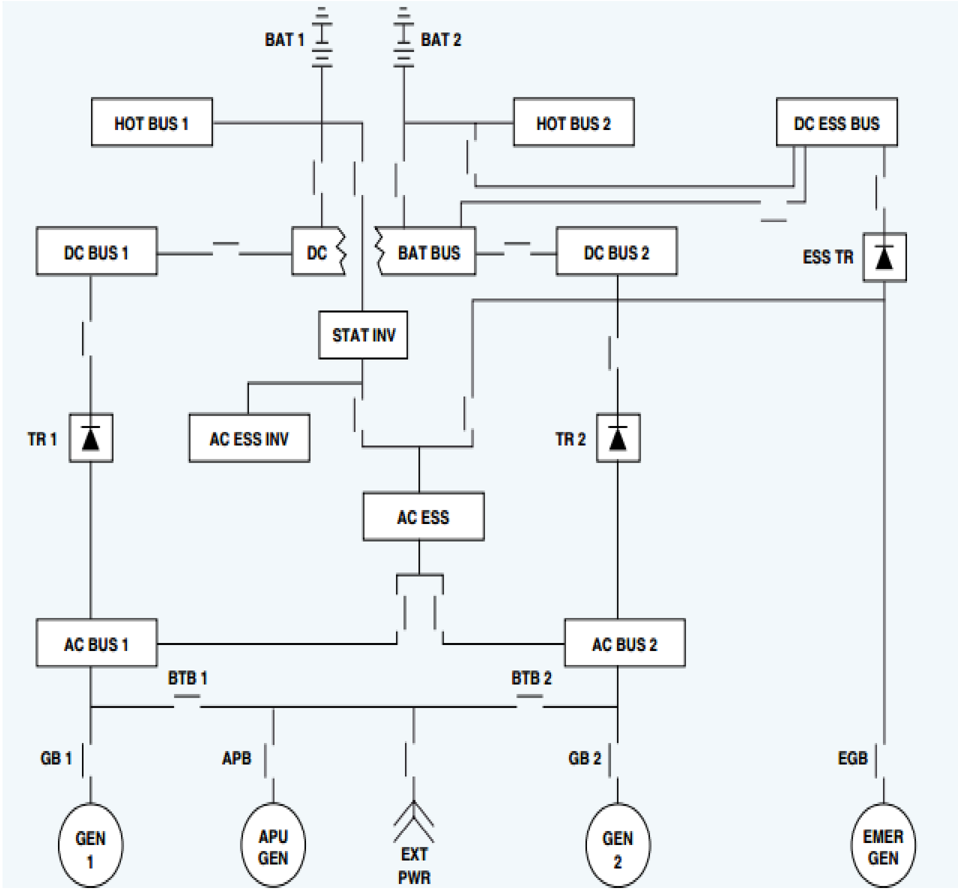

Figure 38 Schematic of split-bus power distribution system[72]

3.3 Power required for the tail rotor drive

To verify the results obtained from the power required for tail rotor model developed as a part of this thesis ‘the baseline performance verification of Sikorsky UH-60A Airloads Program’[75] report is used as a scale.

The inputs used to estimate the power required to drive the tail rotor is obtained from ‘UH–60A Airloads Program’ experiment. (1) the output shaft torque on the engines, (2) the main rotor torque and (3) similar measurements of the tail rotor intermediate drive shaft torque.

The main rotor torque is obtained from the standard strain-gauge bridge installed on the rotor drive shaft. The anti-torque measurements for the tail rotor with cant angle is obtained from the rotor shaft connected to the intermediate gearbox instead of measuring at the tail rotor. So, tail rotor torque was obtained from the gearbox ratios and efficiencies for the intermediate and 90 deg. gearboxes [75]

$$Q_{TR} = Q_{DS}\, R_{IN}\, \eta_{IN} \qquad \textbf{Equation 3-21}$$

Where Q_{TR} - tail rotor torque,

Q_{DS} - intermediate drive shaft torque,

R_{IN} - ratio between the intermediate gear and the tail rotor gear (4.6136)

η_{IN} - integrated efficiencies of the intermediate gear and 90 deg. gearboxes (0.988).

Two capacities of the intermediate drive shaft torque in UH–60A Airloads Program' is acquired from the conventional strain gauge bridges. The values used to calculate the gear ratios and efficiencies of the gearbox are acquired from Nagata et al [68]. Power balance for the rotorcraft is estimated using the torque inputs from the model.

$$SHP_c = \eta_1 SHP_{MR} + \eta_2 SHP_{TR} + \eta_3 SHP_{acc} + \eta_3 SHP_{R/A}$$ **Equation 3-22**

where SHPc - collective output power from both engines,

SHP_{MR} - main rotor power,

SHP_{TR} - tail rotor power,

SHP_{acc} - accessory power required for the normal aircraft electrical systems,

$SHP_{R/A}$ - power required for the NASA-installed RDAS and ADAS data acquisition systems.

The power required for the subsystems to operate in a normal day is approximately 13HP [68]. In the figure below illustrates the efficiency of main rotor and the tail rotor in which the gearbox efficiency is considered and not doesn't include the subsystem power *f*or Cw /σ= 0.08. As acknowledged the main rotor requires more power compared to the tail rotor and engine power is more compared to both the rotor powers.

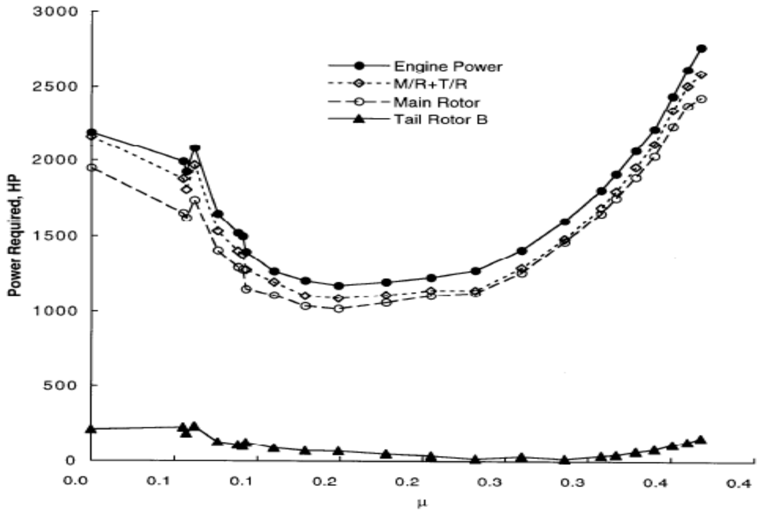

Figure 39 UH–60A power balance, Cw / σ = 0.08[68]**.**

Due to the difference in power over the variance of advance ratios, it is complex to define the regularity of the difference in power.

3.4 PERFORMANCE

3.4.1 General

The inputs obtained are processed using non-dimensional coefficients as follows [68]

Coefficient of Power (C_P):

$$C_P = \frac{SHP(550)}{\rho A(\Omega R)^3}$$ **Equation 3-23**

Coefficient of Power Tail Rotor$C_{P_{TR}}$:

$$C_{P_{TR}} = \frac{SHP_{TR}(550)}{\rho A_{TR}(\Omega R)_{TR}{}^3}$$ **Equation 3-24**

Coefficient of Thrust (C_T):

$$C_T = \frac{GW + Cable\ Tension}{\rho A(\Omega R)^2}$$ **Equation 3-25**

Advance Ratio (μ):

$$\mu = \frac{V_T\,(1.68781)}{\Omega R}$$ **Equation 3-26**

Where:

SHP = Engine output shaft horsepower (total for both engines)

SHP_{TR} = Tail rotor output shaft horsepower

ρ = Ambient air density (lb-sec^2/ft ^{4}) = $\rho_o \frac{\delta}{\theta}$

ρ_o= 0.00 2276892 (lb-sec^2/ft^4)

δ= Pressure ratio =$\frac{P_a}{P_{ao}}$

Pa = Ambient air pressure (in.-Hg)

Pao = 29.92126 in.-Hg

θ = Temperature Ratio = $\frac{OAT+273.15}{288.15}$

OAT = Ambient air temperature (^{o}C)

A = Main rotor disc area = 2262 ft^2

A_{TR} = Tail rotor disc area = 95 ft^2

Ω = Main rotor angular velocity (radians/sec)

Q_{TR} = Tail rotor angular velocity (radians/sec)

R = Main rotor radius = 26.833 ft

R_{TR} = Tail rotor radius = 5.5 ft

GW = Gross weight (lb)

VT = True Airspeed (kt) = $\frac{V_E}{1.68781\sqrt{\frac{\rho}{\rho_o}}}$

V_E = Equivalent airspeed (ft/sec) = $\sqrt{\frac{7(70.7262P_a}{\rho_o}\left[\left[\left(\frac{Q_C}{P_a}\right)+1\right]^{\frac{2}{7}}-1\right]}$

70.7262 = Conversion factor (lb/ft^2-in.-Hg)

Q_c = Dynamic pressure (in.-Hg)

At the normal operating tail rotor speed of 27.07 rad/sec or 257.9 revolutions per minute (rpm) (100%), the following constants may be used to calculate C_P and C_T:

ΩR = 724.685

$(\Omega R)^2$ = 525, 168.15

$(\Omega R)^3$ = 380, 581, 411.2

The output shhp was determined from the engine's output shaft torque and rotational speed by the following equation.

$$SHP_t = \frac{Q(N_P)}{5252.113}$$ **Equation 3-27**

Where:

Q = Engine output shaft torque (ft-lb)

Np = Engine output shaft rotational speed (rpm)

5252.113 = Conversion factor (ft-lb--rev/min-SHP)

The output shp was determined from the tail rotor's output shaft torque and rotational speed by the following equation:

$$SHP_{TR} = \frac{\mathrm{QTR(NP)\ (GTR)\ (\eta\ of\ \ Gearbox)}}{Converstion\ factor} \qquad \textbf{Equation 3-28}$$

Where:

GTR = 15.95825, gear ratio of tail drive shaft to main rotor

η of gearbox = 0.988036, Tail rotor gear box efficiency

Conversion factor = 5252.113 (ft-lb-rev/min-shp)

$$Q_{TR} = Q_{DS}\ R_{IN}\ \eta_{IN} \qquad \textbf{Equation 3-29}$$

And Q_{DS} = 3319 intermediate drive shaft torque (ft-lb)

R_{IN} = 4.6136, Gear ratio between the intermediate drive shaft and tail rotor

$$Q_{TR} = 3319\ \times 4.6136 \times 0.988$$

$$Q_{TR} = 15128.78\ \text{(ft-lb)}$$

$$SHP_{TR} = \frac{15128.78\times\ 15.95825\ \times 0.988036}{5252.113}$$

$$SHP_{TR} = \mathbf{45.4163\ hp}$$

$$SHP_{TR} = \mathbf{33.8669\ kW}$$

The output shp required was assumed to include 33.87 kW for daylight operations of the aircraft electrical system but was corrected for the effects of test instrumentation installation.

4 Modelling - Methods

To create a model of the electrically powered tail rotor, the power required for the Sikorsky UH-60A has to be calculated. Electrical load analysis to find the electrical load of the generator for the entire flight phases is to be conducted and the current electricity generation system has to be up-scaled to compensate the new load.

4.1.1 Mission power requirements

To analyse the power requirements of the helicopter at a different phase of flight the mission profile has to be determined. The flight mission usually has Start at the given origin, take- off/climb, cruise, when the vicinity of destination or visual reference point (VRP) is attained the flight hovers and the landing phase.

Start	The condition during which the rotorcraft engine has been turned on however the vehicle has not lifted off the ground.
Take-off & Climb	The condition when the rotorcraft's take-off and leading to cruise.
Cruise	The condition in which the rotorcraft attains required altitude with a cruising speed at stable altitude

Hover	The condition where the rotorcraft remains airborne at stable altitude without any cruising speed.
Descent/Landing	The condition with the operation of navigational and indication equipment specific to landing approach and following to the landing of the rotorcraft

4.1.2 Modelling power required

Power required in different phases of flight

To calculate the working of the typical tail rotor the calculation has to be provided with working atmosphere such as temperature, density and altitude which are obtained from the Clean Sky TEM project report[11]. The mathematical model of power required calculation is developed in Microsoft Excel Platform.

Assumptions

- The inertia result which is obtained is considered as insignificant.
- The centre of pressure of the fuselage is same as the centre of gravity, as it doesn't have any momentum.
- The flow through the main rotor and tail rotor are considered as uniform steady flow and the density of air to be constant.

4.1.3 Model Description

The MS-Excel based model is based on Gordon Leishman's [24] power required theory for the main rotor and Helicopter Performance written by Donald Layton [65]. The helicopter dimension is taken from the Sikorsky Flight Manual[10] and flight phases are obtained from Clean Sky project report[11] for Twin-engine medium helicopter.

The number of different flight phase is assumed accordingly

0	Prestart
1	Start
2	Take off / climb
3	Cruise
4	Hover
5	Landing

From the theory from this chapter the following formulas will be adapted for the mathematical model for power calculation:

Prestart	0
Start	$P_{tr} = \frac{T^{\frac{3}{2}}}{\sqrt{2\rho A}} \cdot \frac{1}{B}$
Take off / climb Or Landing	$P_{tr} = \frac{W\gamma_l}{2} + \frac{T^{\frac{3}{2}}}{\sqrt{2\rho A}} \cdot \frac{1}{B} + \frac{1}{8}\sigma C_{d_o}\rho A(\Omega R)^3$
Cruise	$P_{tr} = \frac{T^{\frac{3}{2}}}{\sqrt{2\rho A}} \cdot \frac{1}{B} + \frac{1}{8}\sigma C_{d_o}\rho A(\Omega R)^3$
Hover	$P_{tr} = T_{tr}.\gamma_{tr} + \frac{1}{8}\sigma C_{d_o}\rho A(\Omega R)^3(1 + 4.3\mu^2)$

The Equation of hover is considered as the base of this model. At the prestart state, the Thrust and a drag coefficient of the tail rotor are zero making the power requirement null.

The anti-torque is positioned at a stable distance from the rotorcraft's centre of gravity (CG). The torque produced by the tail rotor thrust to counteract the main rotor torque is equal to the product of the thrust and a tail length defined as the distance from the centre of tail rotor thrust to the rotorcraft CG.

$$Q = Tl_T = -Q_M = \frac{P_M * 550}{\Omega_M}$$

Equation 4-1

The suffix M represents to the Main rotor. The thrust required to balance the main rotor torque is a function of the applied torque,

$$T = \frac{550 * P_M / \Omega_M}{l_T} = \frac{Q_M}{l_T}$$

Equation 4-2

where: T = Tail Rotor Thrust

Q = Torque

Ω = angular velocity = 37.07 rad/sec

P_M = = 284hp

l_t = Tail length = 12.6ft

Q_M = 284*550/37.07 = 4214 lbf-ft/s

$$T = \frac{\frac{550 * 284}{37.07}}{12.6}$$

$$T = \frac{4213.65}{12.6}$$

$$T = 334.42\ lbf$$

$$T = 14.09 \frac{kgm^2}{s}$$

In the start phase (1) of the flight the $\boldsymbol{C_{d_o}}$ is taken as zero as the rotorcraft is in ground, which in turn makes the second part of the hover equation zero. The weight of the rotorcraft is assumed to be required thrust.

T_{tr} – $14.09 \frac{kgm^2}{s}$

Rho – Air density (obtained from the ISA model)

A - πr^2 (whereas r = 1.6764m)

B – no. of blades (4)

If the flight at hover state (3) $\boldsymbol{\frac{1}{8}\sigma C_{d_o}\rho A}(\Omega \boldsymbol{R})^{\boldsymbol{3}}$ is added to the first part of the model,whereas

σ - solidity of the tail rotor (0.1875)

Ω - angular velocity of the tail rotor (208.77 m/s)

For the take- off / climb (2) or Landing (3) phase of the flight the formula is the same the results varies due to the altitude differences, which can be calculated by adding Hover formula + $\frac{W\gamma_l}{2}$

W – Mission gross weight of Sikorsky UH-60A (16000 lb) [76]

v_l – vertical velocity (obtained from the Clean Sky project report [11])

Finally, to calculate the Cruise phase (4) of the rotorcraft, the 2nd stage of the model $\frac{1}{8}\sigma C_{d_o}\rho A(\Omega R)^3$ is multiplied with $(1 + 4.3\mu^2)$ and added to the $T_{tr}.\gamma_{tr}$

μ – advance ratio is calculated by $\left(\frac{v_f}{\Omega R}\right)$

v_f- velocity of the flight

γ_{tr} – velocity of tail rotor

4.1.4 Trajectory

The obtained input values for the above model is given by the Clean Sky project report for Twin Engine Medium rotorcraft and the values are altered designated trajectory in the following chapter of this thesis a for passenger mission from London City Airport to Cranfield Airport.

The Trajectory is for the power calculation is done by skydemon software with the available data from the Clean Sky project. Altitudes were established for the assumed trajectory is obtained from Clean Sky project (TE)[11], to provide continuity to the case study done

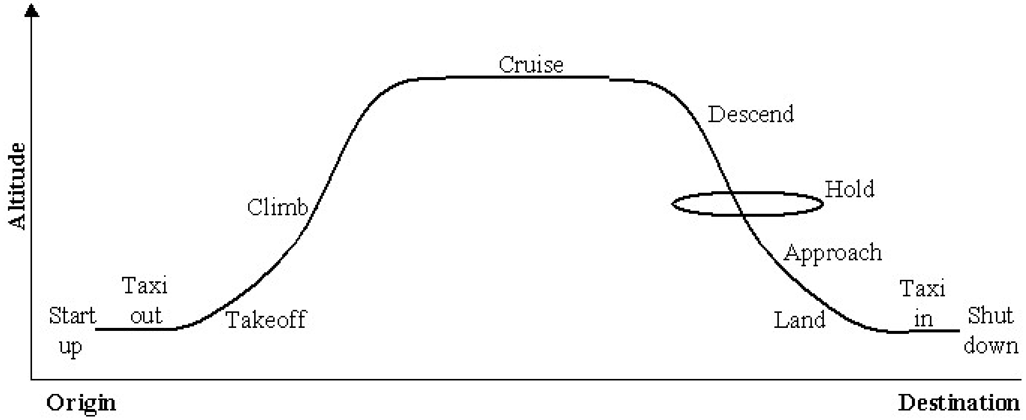

using the current RMEM-TEM model.

Figure 40 Flight Mission Profile[77]

The total duration of the flight mission takes 28 minutes, in which the time for the engine starting and switching off is not considered. The trajectory starts from London City airport and lands at Cranfield airport. The rotorcraft takes a detour, instead of travelling straight. This is because of restricted access to fly through Luton airport.

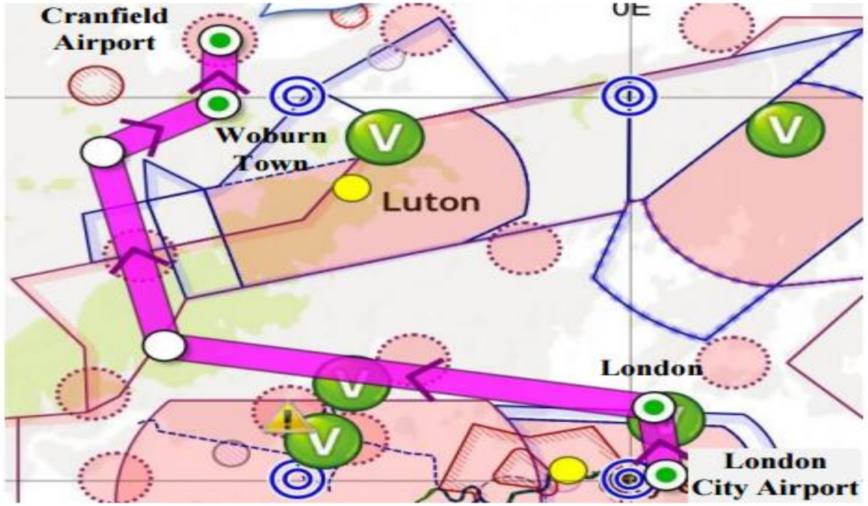

Figure 41 Trajectory from London City Airport to Cranfield Airport

The time estimated for the starting and operational check phase is considered as 5 min; the landing and engine turn off is assumed as 3 min as shown in Figure 42 Flight Plan

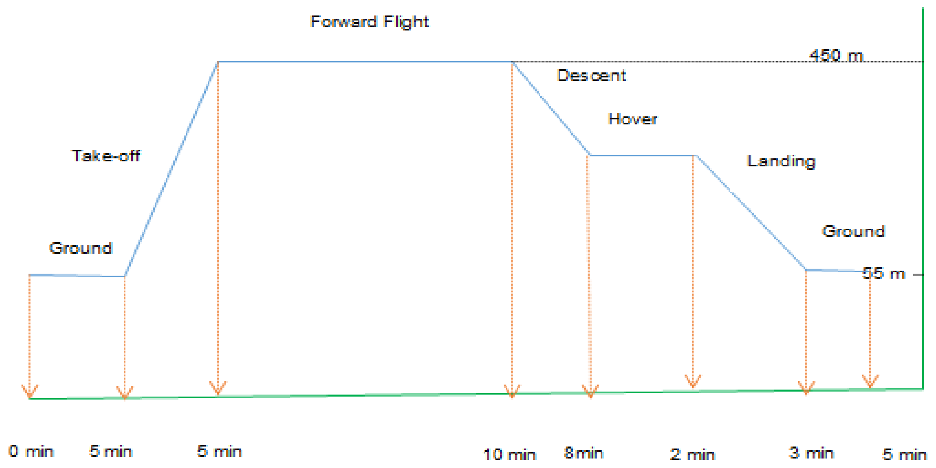

Figure 42 Flight Plan

4.1.5 Modelling Electric Load Analysis

The Electric load analysis model is created for the Sikorsky UH-60A by listing all the electrical equipment used in the different phase of the rotorcraft. The electrical energy usage may differ in accords to the flight state and if the equipment is used continuous or intermittent. In the process of creating Electric load analysis model, the load of the current is estimated by the voltage drop between the bus bar and load. It is important to develop an electrical load model for thesis as it helps to understand the power used at the conventional helicopter.

Furthermore, understand the load required to operate the electrical system in the conventional Sikorsky UH-60A rotorcraft at all phases of flight (start, take-off, cruise, hover and land). Using the results obtain the Electrical tail rotor drive will be designed accordingly. Some of the equipments that are considered for ELA are listed below:

Interior Lights – includes the cockpit dome light, utility lights, instrument panel glare shield, Flight instrument lights etc.

Exterior Lights – Searchlights, Landing lights, Anti-collision lights, Position Lights and Formation Lights.

Flight Instruments such as Pitot- Static System, Attitude Indicator, Turn rate Indicator, Airspeed Indicator, etc.

Environmental control system

Electrical Ice protection system and Windshield heating

Hydraulic and fuel valves, pumps and control valves for auxiliary components.

Calculations

The following calculations is used to calculate the total current, maximum demand and average demand for each of the rotorcraft operating phases (Ground operation and loading, Engine Start, Take-off and Climb, forward flight, Hover and Descent):

- I_{total}(Amps) = No. of equipment in operation x I (per equipment)
- I_{total}(Amps-Min) = No. of equipment in operation x I (per equipments) x Operating time (Min)

- Volt-ampere (VA or kVA) = Voltage x Current
- Maximum Load (Volt-Amps, VA, kVA, kW or Watts) = No. of equipment in operation x I (per equipments) x Operating time (Min) x Supply Voltage (Volts).
- Intermittent Loads - For alternating ultimate demand, root mean square (RMS) values of current should be estimated.
- Continuous Load – If the load flow is continuous, the RMS and the average values will be the same.

Model Development of Electrical Load Analysis

The power requirement for the equipment may differ in accordance with the usage in each flight phase. Hence, in such analysis; an exhaustive list of all equipment requiring electrical power usage on board is tabulated, along with the respective power rating during five different flight segments: Start, Takeoff / Climb, Hover, Cruise, and Landing.

For the Electrical Load Analysis, the operating time for each of the electrical equipment is distinguished as continuous or intermittent. The electrical equipment operational period is relies upon operational time of the rotorcraft [34].

In case if the electrically operated equipments are switched on for the complete mission of the rotorcraft, then it is considered as operating continuously for all flight phases. In other instances, the electrical load is regarded as an intermittent load.

The CAA documentation on Airworthiness Information Leaflet AIL/0914 [34] serves as a guideline for a standard aircraft electrical load and power source analyses. Figure 43 below shows an example of a typical Electrical Load analysis.

	BUS – DC1					NORMAL CONDITIONS					
CIRCUIT/SERVICE	CB	LOAD AT CCT BREAKER	OP TIME	APPROPRIATE CONDITIONS	NOTES	TAXING (NIGHT) 30 MINS		TAKE OFF & LAND (NIGHT) 10 MINS		CRUISE (NIGHT) 60 MINS	
		AMPS	MINS			AMPS	AMP-MINS	AMPS	AMP-MINS	AMPS	AMP-MINS
AIR CONDITIONING											
DUMP DITCH MOTORS	AB1	0.90	0.1	A,B,C	a,b,c	-	-	-	-	-	-
CABIN ALT WARNING	AB2	0.04	CONT	A,B,C	a,b,c	0.04	1.2	0.04	0.4	0.04	2.4
MAN. PRESSURE CONTROL	AB3	0.60	CONT	A,B,C	a,b	-	-	-	-	-	-
COMMUNICATIONS											
ACARS MEMORY	BC1	0.08	CONT	A,B,C	a,c	0.08	2.4	0.08	0.8	0.08	4.8
ELECTRICAL POWER											
BATTERY 1 CHARGE	CD1	3.50	CONT	A,B,C	a,b	3.50	105.0	3.50	35.0	3.50	210.0
**	**	**	**	**	a,c	**	**	**	**	**	**
**	**	**	**	**	a,b,c	**	**	**	**	**	**
**	**	**	**	**	a,b,c	**	**	**	**	**	**
**	**	**	**	**	a,b,c	**	**	**	**	**	**
BATTERY 1 TEMP PROT	CD2	0.04	CONT	A,B,C	a,b	0.04	1.2	0.04	0.4	0.04	2.4
		TOTALS	TOTAL (AMP-MINS)				200		100		300
			MAXIMUM DEMAND (AMPS)			15		24		12	
			AVERAGE DEMAND (AMPS)			6.7		10		5	

Figure 43 Example of an Electrical Load Analysis[34]

As illustrated above, the analysis can be achieved at the detailed design phase, when all the electrical components of the rotorcraft have been decided – hence, the bottom-up approach. Once load summation is conducted, the total electrical power required to be output from the generators is established. In order to establish the shaft power required to drive the generators a suitable efficiency factor is applied[78].

A database is generated by listing all the electrical equipments and the associated nominal power rating for its operation of the selected Sikorsky UH-60A rotorcraft, by means of an Electrical Load Analysis (

Appendix 2) .

4.1.6 Modelling of Electric Tail Rotor

The hybrid rotorcraft concept can reduce emission by combination feasible concepts of both conceptual and electric, merge the high-power density fuel and the high efficient and, reliable of electrical motors. The hybrid design is very different and its practicality is not straightforward. As for the hybrid system components are not readily available equipments, a novel substitute has to be designed to meet the performance, weight, and reliability requirements. The hybrid power production is of three stages: Electric power production, transformation, and transmission.

The main drawback of the Firefly which is an electrically powered helicopter is highly efficient but requires more battery storage to increase the flight timing. In past years, numerous researches are carried out in reducing the weight and the volume of the batteries, to make the electric aircraft more feasible.

In all areas, more novelty is required before the hybrid helicopter can become a reality. In Figure 44 schematic overview of the electrically powered tail rotor can be seen. The focus of this thesis is on the electrically driven tail rotor powered by batteries.

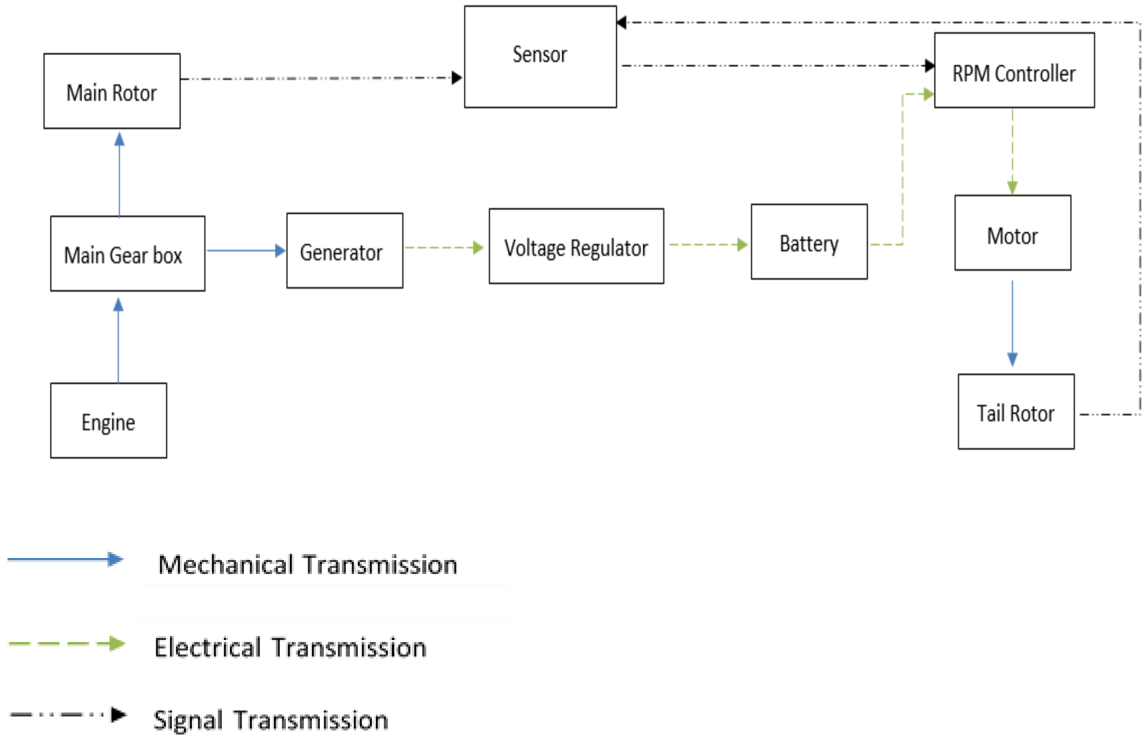

Figure 44 Schematics of Electric power train

Generator

The main source of Alternating current in Sikorsky UH-60A is the AC generator and the sources of Direct current are the TRU and the battery. The DC source relies on the AC generators for supplying the load demand.

The following assumptions are made to design the Electrical Tail rotor drive.

- The Electrical load analysis for the conventional helicopter is done for harsh load requirements and operational conditions such as night time operation at ice condition
- The intermittent load such as the values that is operated by the electrical source is not considered
- The load for the motor is considered to be steady and the inrush power for initiating the motor is not considered.

The voltage from the TRU provides the required current to the motor that drives the Tail rotor. Assuming that the Sikorsky UH-60A model is used for passenger transport rather than for military usage only 75% of the electricity produced by the generators will be consumed. As the power required running the electrical tail rotor is 35kW the generator has to be upscaled.

From the literature review it is noted that the Sikorsky UH-60A uses 30kVA/45kVA, the 45 kVA is used for high power military missions it uses 45 kVA generators. The generator for the case study is assumed to be 45kVA to satisfy the power requirement for the Electrical tail rotor.

Motor

Among all the equipments required to adapt to electrically powered tail rotor the selection motor is considered to be the significant component. The selection of the motor influences the performance of the design (RPM, acceleration, effectiveness) in the electrically powered aircraft.

Furthermore, its impact the selection process of other equipment involved in the design such as the sensors, regulators, batteries, indirectly the battery chargers and the AC/DC converters). There are many types of motors in terms of power, shapes and sizes. Even though it is available in different sizes only two categories: DC brushless (BLDC) motor and AC motor are generally selected to be suitable for electrical vehicle conversion[79].

Comparison of DC and AC Motors for Electric Vehicle Drive

Interestingly, the stators the design of the AC motor and the BLDC motor 3 are almost similar. Both the AC and DC motors have three sets of "distributed windings" which are linked with the stator core that can be differentiated by the rotor design. The major drawback of the DC brushed machines are the brushes that are coupled with the motor's armature that can transfer between high currents to various units of the armature coils[80]. The electrical arcing in the DC brushed motor can cause ignition due to their mechanical wear. Due to this reason, the DC brushed motors are not generally used on electrical vehicles. The DC brush motors are open to mechanical wear and tear leading to high maintenance compared to the Induction motors.

Conversely, an AC induction motor, is generally highly efficient to operate at 240 VAC, so it is used in electric automobiles but require high voltage battery packs and thicker cables which will reduce the efficiency. The BLDC motors generate DC magnetic field using adjustable permanent magnets. The cooling system in the BLDC motors is very effective that helps to attain the peak point of the motor. The BLDC brushless can work at unity power factor, while the AC motor best power factor is approximately 85 percent[79].

Maximum torque of the BLDC motor is expected at low speeds; the magnetic field strength (B) is assumed to be high in that case the inverter and motor currents are retained at their lowest possible values, through the $I^2 R$ losses can be reduced.

The Brushless DC motor will be used in the upscaling process of the electrical generation systems, as they are the optimum choice for the relatively low power suitable for the electrical tail rotor.

So as per DC amps to watts calculation formula

The power P in watts (W) is equal to the current I in amps (A), times the voltage V in volts (V):

$$P (W) = I (A) \times V (V)$$

Required power = 35kW and the power system will supply 270 VDC

$$I = 35 \text{ kW} / 270 \text{ VDC}$$

$$I = 129.63 \text{ amp approx. } 130 \text{ amps}$$

The power required to drive the Electrical tail rotor is 35kW, at such power levels if the bus distribution voltage remains at 28VDC, then the bus current elevates with significant impacts on wiring size, weight and ohmic loss, and therefore the bus voltage is increased to 270V, permitting to the reduction in wiring mass[81].

Battery

The battery is a device made several cells dictated by its usage in the aircraft electrical system. There are two types of batteries primary and secondary; they work under the same principle of exchanging electrons due to electrode materials and electrolyte chemical reaction. In the aircraft electrical system, secondary batteries like Lead-acid or nickel-cadmium is used as the active materials in the cells is converted into other forms, from which it can be reconverted into original form and can be charged again. Unlike the primary batteries where the active materials in the cells are limited to single discharge[35].

The cathode in the li-ion battery is a lithiated metal oxide ($LiCoO2$, $LiMO2$, $LiNiO2$ etc.) and the anode is made of graphitic carbon with a layering structure [82]. When the battery is charged, the lithium atoms in the cathode become ions and migrate through the electrolyte toward the carbon anode where they combine with external electrons and are deposited between the carbon layers as lithium atoms [38].

However presently mass of the Li-ion battery systems are approximately 180 Wh/kg specific energy, next generation Li-S battery chemistries achieving 350Wh/kg have been demonstrated on QinetiQ Zephyr HALE UAV [83]. Further advances in Li-Polymer technologies show potential for achieving 650Wh/kg and beyond (see Figure 45)[84]. Battery technology is trending toward not only significantly higher specific energy's, but also higher specific densities. These higher specific densities reduce the needed volumetric space for batteries in the airframe.

With battery technologies in their current stages of development, lithium-ion batteries are considered the most feasible option for powering the helicopter, as they out- perform the other battery options in the important aspects of energy density and efficiency.

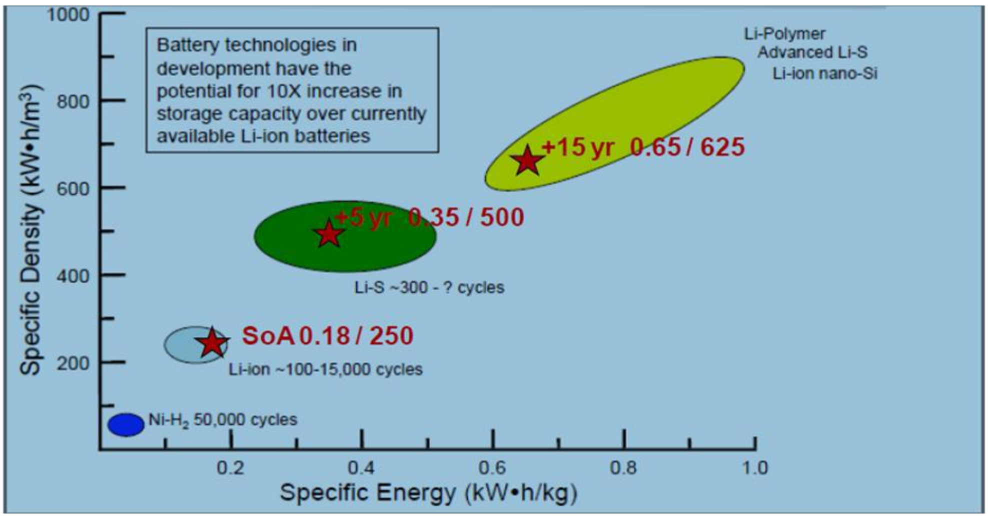

Figure 45 Battery specific energy and density trends[84]

The 270 V Li-ion battery provides back-up power to operate the flight control surfaces during taxi, take off, flight, and landing. Saft’s Li-ion 270 V High Power Batteries and Ni-Cd 28 V Aircraft Maintenance Free Batteries (AMFB) provided essential power to the aircraft. The new Li-ion battery will serve as a technology upgrade and weight reduction solution for the F-35 Lightning II aircraft[85].

According to Chen et al [86], the maximum energy density of these batteries is 200 Wh/kg and the maximum power density is 0.315 kW/kg. Nissan has produced a laminated lithium-ion battery which can increase the power density of a standard type by up to 50% [87]. This could increase the maximum power density of lithium-ion batteries to 0.4725 kW/kg.

Reliability and safety requirements impose a two-failure tolerance on both battery system performance and in preventing catastrophic hazards. Additionally, exposure to high voltage contacts external to the battery is prohibited. The reliability is achieved by providing 3 independent battery modules and 270V buses, each capable of the meeting all vehicle requirements.

Designed with affordability in mind, this versatile aircraft reached maximum power optimisation using two customised batteries from Saft. The 270 V Li-ion battery provides backup power to operate the flight control surfaces during taxi, take off, flight, and landing. Saft’s Li-ion 270 V High Power Batteries and Ni-Cd 28 V Aircraft Maintenance Free Batteries (AMFB) provided essential power to the aircraft. The new Li-ion battery will serve as a technology upgrade and weight reduction solution for the F-35 Lightning II aircraft[85].

This battery can be adapted for the electrical tail rotor and can be charged by the TRU; used in the place of a convertor. The electric motor provides additional power to the conventional drive. The battery unit that is connected to the motor acts as a storage unit and redundant power for the tail rotor. The battery is connected to the constant charged by the electricity from the generator.

RPM Sensor and Controlled

This RPM sensor attached to the main rotor and tail rotor sends a signal to the controller. The controller is a device for regulating the operation of the apparatus to which it is connected. A starter is a controller whose main function is to start and stop a motor. A manual motor starter is a device that will connect or disconnect the motor from the power source, only when someone provides the physical effort to operate it through moving a lever or pushing a button.

The sensor coupled to the main rotor detects the rpm and provides an input signal to the microcontroller that delivers required power for the tail rotor. A battery is connected to the voltage regulator and the RPM regulator for redundancy purposes.

5 Results and discussion

The power required at different phases of flight for the conventional tail rotor drive calculated through the 'Tail Rotor drive power required model' is within the maximum range of output shaft power obtained from the 'the baseline performance verification of Sikorsky UH-60A Airloads Program'[75] report which is mentioned in the Methodology - case study chapter.

The Electrical load analysis for the conventional helicopter is done for electrical load requirements and operational conditions such as night time operation at ice condition.

5.1 Power required of Tail rotor at different Segment of Flight

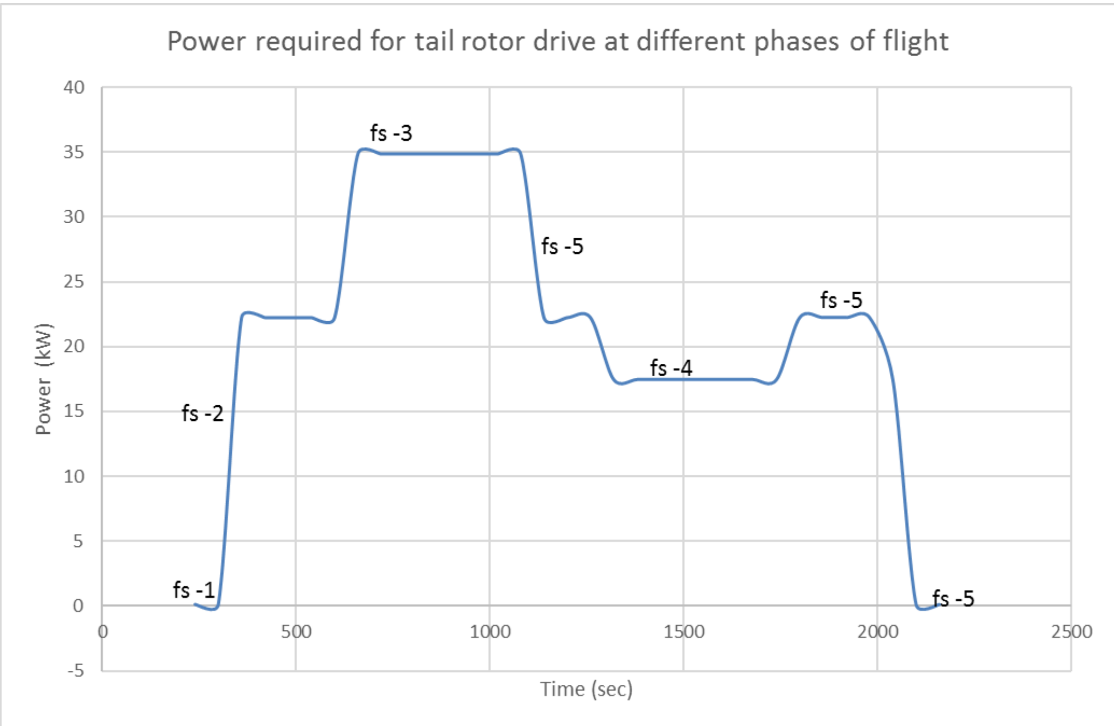

Figure 46 Power requirement of Tail rotor

Flight Segment (fs)	
Fs-1	Take-off
Fs-2	Climb
Fs-3	Cruise
Fs-4	Hover
Fs-5	Decent / Landing

Table 6 Different Flight Segment

The power requirement of the conventional tail rotor follows the pattern of the trajectory. The overall power demands the conventional rotorcraft with the shaft gear system is illustrated in Figure 46. The Excel mathematical model contains the equation to calculate the power required to operate the main rotor. Appendix 1 Model to calculate the power requirement of tail rotorillustrates the complete sub-system 'Tail rotor model' containing different equations that explain the power requirement to drive the tail rotor.

5.2 Electrical Load required

After validation of the Power requirement for tail rotor model at different phases of flight, the Electrical System is analysed with the conventional tail rotor and electrically powered tail rotor using Electrical Load Analysis(Appendix 2 & Appendix 3). The Figure 47 above represents 35kW the increase in Electrical power to propel the tail rotor.

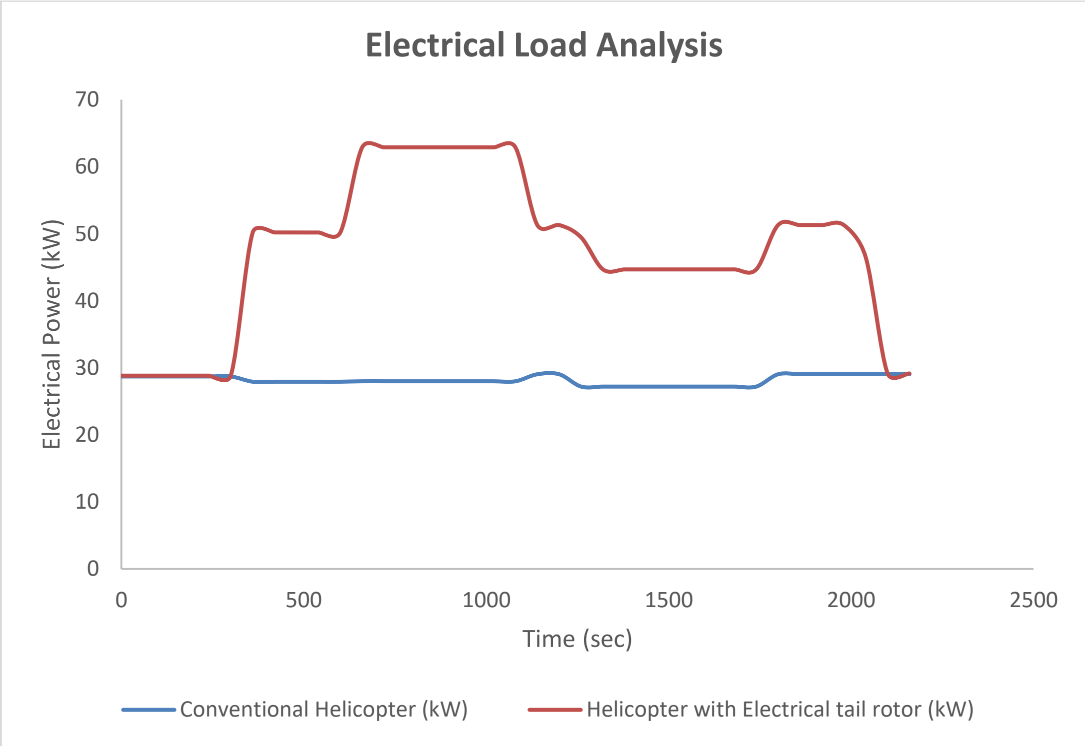

Figure 47 Electrical Load Analysis

5.3 Electrical Tail rotor

The Electrical load distribution similar to B787[38] can be used to power the electrical tail rotor. The load produced by the main generator will be 45 kVA. The hot battery bus noticed on the left side of the diagram illustrates a direct connection to power the battery. This bus also provides power to the cabin lightings, clock, fuel shut-offs, and fuel pumps to which constant power is required. In the case of any system failure, it is designed in such a way that this will be the last bus to fail. When the battery charging is switched off is closed and the battery relay gets activated, battery power is connected to the main battery bus and the isolation bus.

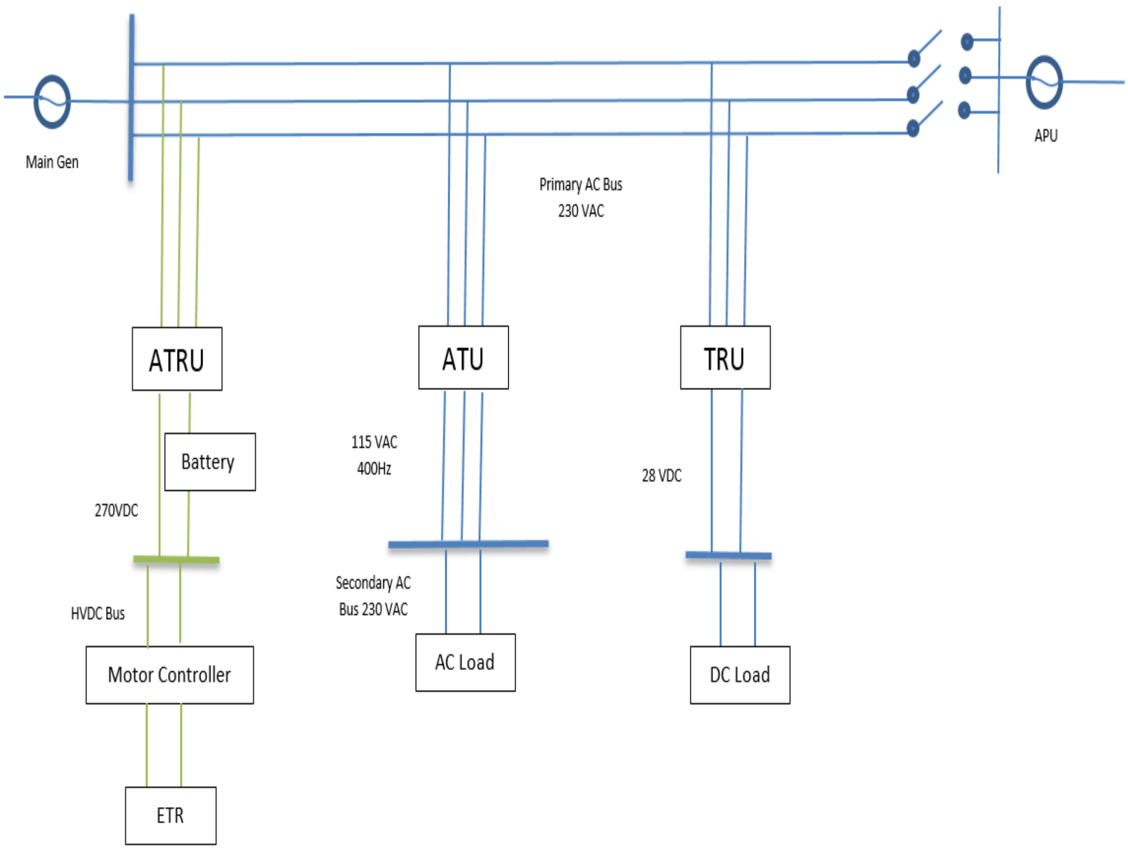

Figure 48 Power distribution for Electrical Tail rotor (ETR)

The main battery bus carries current for engine starts and external power[72]. So, the main battery bus must be large enough to carry the heaviest current loads of the aircraft. It is logical to place this bus as close as practical to the battery and starters and to ensure the bus is well protected from shorts to ground. These features make it be an excellent choice to include the electrical tail rotor to this main bus.

Figure 49 Electrical powered tail rotor

Weight

Weight of the Conventional Tail rotor drive

It is noted from the Weden and Coy's report[22] on Drive Train components in a helicopter the weight of drive train of Sikorsky UH-60A is approximately 1463 lb or 663 kg.

The Tail Rotor Drive System for conventional rotor helicopters contains the shafting, couplings, bearings, supports, and intermediate gearboxes between the tail rotor hub and intermediate rotor gear box.

The weight of tail rotor drive train can be calculated as[88]

$$\boldsymbol{W_{tr} = 300a_{tr}\left[1.1\left(\frac{HP_{tr}}{rotational\ speed_{tr}}\right)\right]^{0.8}}$$ **Equation 5-1**

Where a_{tr} is an adjustment factor (0.9)

HP is the tail rotor power requirement (46.94hp)

Rotational speed of Sikorsky UH-60A tail rotor is 124.54 rad/s

The attained weight of the tail rotor drive is 133.495 lb or approx. 60.55 kg (which almost 10% of the complete drive train system.

Weight of the Electrical Tail rotor drive

Motor

The power required to drive the tail rotor is 35 kW to drive the electrical tail rotor efficiently, a very powerful motor with a power density of 40 kW is selected for redundancy purposes.

The large industrial electric motors database with state-of-the-art DC motors is used as a guide[89], to estimate the weight of the Tesla DC motor (mainly used for automotive purposes), due to its compactness and low weight it is implemented in the Electrical tail rotor design.

$$\boldsymbol{W_{motor}\,(lb) = 1.96\,[P_{motor}]^{0.8}} \qquad \text{Equation 5-2}$$

The weight of the tesla motor used in this design of the electrical tail rotor conversion will weigh up to 37.489lb or 17.005kg.

Cable

The electric cable used in general aviation contains an externally-mounted flexible, multi-conductor cable will weight up to 0.91kg/ft [90].The length of the power transmission from the generators to the tail rotor is 12.6ft. The cable of the electrical tail rotor conversion will weight up to 11.5kg.

Convertor

The primary AC power bus feeds the 270V HVDC through Auto-Transformer Rectifier Unit (ATRU), convert the 230VAC to the 270VDC. The HVDC bus usually used in the only the large motor such as actuation motors and hydraulic pumps[91]. The approximate weight of the ATRU used for to supply the 270VDC motor is 1.6kg[92].

Battery

The batteries using lithium are known to provide the highest specific energy, this can be increased by coupling lithium with sulphur. The Li-S batteries contain very high theoretical specific energy, more than 2,700 Wh/kg, which is 5 times higher than that of lithium-ion (Li-ion) (the same energy stored, the battery is considerably lighter). These batteries can provide 35 kW for 15 min flight time at approximately 12.96 kg, making the Electrical tail rotor feasible with motor-battery powered tail rotor

The conventional tail drive weighs 60.55; the addition of electrical tail rotor drive system and the conversion of main bus bar voltage to +/- 270 VDC will increase the increase the weight by 47.84 kg. The reduction in weight will be 12.71 kg.

Cooling

The Li-ion battery allows twice the energy density per unit volume than Nickel batteries. The Li-ion battery is lighter due to the comparatively low density of lithium metal; so, they are commonly used in cell phone and laptops, the numerous case of possible thermal failure within these batteries as evidenced by the recent battery recalls of Samsung, Sony and Dell battery powered products. In January 2013, Boeing 787 Dreamliners in Japan and Boston had problems with their lithium ion batteries causing a fire on one 787 and damage to another that led to an emergency landing[93].

The thermal failure in Lithium ion battery is caused due to the mechanically and chemically break down that leads to loss of ability to store and deliver charge at high temperature. The polymer or fibre based cell dividers become inherently weaker at higher temperatures, which can induce failure at the cell wall. At high temperature, irreversible chemical reactions may occur which reduce the ability for a battery to maintain charge. Noxious or flammable gases may be produced by these reactions which can present a public safety hazard. The lithium batteries can also suffer from thermal runaway – a condition where the battery becomes unstable and chemical reactions generate rapid and strong heat generation which can cause an explosion or meltdown. The discharge capacity is lowered because at colder temperatures the electrolytic solution has a higher impedance [94].

The heat needs to be extracted in some way from the battery pack to the ambient. The battery compartment can be treated similarly to how thermal designers often treat electronics enclosures. Natural convection cooling or even conduction cooling may be an effective mode of heat transfer if the heat density is low enough and there is adequate space to feature such a design[95]. The motor can be cooled using the existing cooling fan method (as mentioned in Chapter 3.2 Case study) that is used in intermittent gearbox system. Additionally, for more understanding thermal analysis, more detailed designing of helicopter cooling system and its effect on Environmental Control System has to be conducted as further studies.

Reliability

FMEA aims to rank each potential failure mode according to the combined influence of its severity classification and probability of failure based on the best available data. By determining the critical failure mode of an asset, it is possible to target and refine maintenance plans, capital expenditure plans, and investigative activities, to address the potential failure. Risk Priority Number (RPN) is obtained by quantifying the severity (S), probability of occurrence (O) and detectability score (D[96]).

$$\boldsymbol{RPN = Severity * Probability\ of\ Occurrence * detetectablity} \qquad \textbf{Equation 5-3}$$

As shown in Table 7 scale of 1-10 is recommended for evaluating each of the three components. While a scale of one to five may be easier to work with, it does not show fine enough fidelity to separate failure modes and establish a threshold for redesign.

Ranking	**Effect**	**Comment**
1	None	No reason to expect failure to have any effect on Safety, Health, Environment or Mission
2	Very Low	Minor disruption to facility functions. Repair to failure can be accomplished during trouble shooting
3	Low	Minor disruption to facility function. Repair to failure may be **longer** than trouble shooting call but does not delay Mission
4	Low to moderate	Moderate disruption to facility function. Some portion of Mission may need to be reworked or process delayed.
5	Moderate	Moderate disruption to facility function. **100%** of Mission may need to be reworked or process **delayed**.
6	Moderate to high	Moderate disruption to facility function. Some portion of Mission is lost. **Moderate** delay in restoring function
7	High	High disruption of facility function. Some portion of Mission is lost. **Significant** delay in restoring function.
8	Very High	High disruption to facility function. **All** of Mission is lost. Significant delay in restoring function.
9	Hazard	Potential Safety, Health or Environmental issue. Failure will occur **with** Warning
10	Hazard	Potential Safety, Health or Environmental issue. Failure will occur **without** Warning

Table 7 Severity ranking table[96]

Occurrence is the likelihood that a specific mechanism will occur resulting in the failure mode within the design life. The value assign to occurrence is relative based upon the design life for a given component and may vary for the entire system. Detection is a rank of the current method in place to identify that a failure has occurred. A low detection ranking should not be the result of a low occurrence rating. For a properly functioning system to be adequate, the system must be able to detect low-frequency failures.

FMEA description of the Drive Train System

Part Name	Failure Mode	Detection Technique	Failure Effect	S	O	D	RPN
Generator	Fails to transmit required current	GEN OFF indication in the cockpit	Power to the Battery gets cut off	6	3	8	144
Battery	Fails to transmit required current	BATTERY OFF indication in the cockpit	The electrical tail rotor drive shutdown	10	4	1	40
RPM controller	Fails to Transmit Required torque	No stable rotor torque transmission/ will be detected by RPM Sensor	Reduction in tail rotor speed	8	2	2	32
Motor	Fails to Transmit Required torque	RPM Sensor	Motor Shutdown	8	4	3	96
Motor	Temperature increase due overload	Thermistor	Motor Shutdown	8	4	3	96
Motor shaft connected to tail rotor	Fails to Transmit Required torque	No stable rotor torque transmission/ will be detected by RPM Sensor	Loss of tail rotor operation	8	3	4	96

RPM Sensor 1 (Main rotor)	Fails to transmit signals	RPM Sensor / indication in cockpit	Reduction in power transmission to tail rotor	7	3	5	105
RPM Sensor 2 (Tail rotor)	Fails to transmit signals	RPM Sensor / indication in cockpit	Reduction in power transmission to tail rotor	7	3	5	105
DC – TRU	Fails to provide required current	Voltage Regulator	Motor Shut down	9	3	6	162
Cables/Supply	Fails to transmit required current	No stable rotor torque transmission/ will be detected by RPM Sensor	Motor Shutdown	10	1	7	70

Table 8 FMEA for the electrical drivetrain

The electricity from the AC Generator is transmitted to the Motor which rotates the tail rotor. One of the potential failure modes is that there is no transmission or a reduced transmission. The cause of this can be different failure mechanisms. One of these failure mechanisms is the input drive shaft failure. If this occurs, effectively there will be no transmission and the failure effect on the next higher assembly is a loss of control of the rotor speed with resulting in an autorotation and an emergency landing. The detection method is a build in test and if something is wrong the pilot will be informed by a master caution light in the cockpit. The severity classification is that this is a hazard and this failure will occur with a caution light in the cockpit. A severity classification is assigned to each identified failure mode and each item analysed in accordance with the categories in Table 7.

6 Conclusion

A simulation to find the power required to drive the tail rotor is built based on the theories presented in the literature review. The competence of the simulation is tested for a particular mission profile, proving its competencies of generating outputs at the conceptual level for subsequent optimisation. The obtained result closely matches the experimental results of ‘UH-60 program’.

To achieve a close approximation of the power required the following parameters are inputted into the MS-Excel based mathematical model; rotor RPM, altitude, vertical velocity, the thrust of the tail rotor, solidity, angular velocity, cursing speed and so on. The developed model can be altered for any other conventional helicopter drive with the main rotor and a tail rotor or any other mission.

The Electrical load analysis model is created for the Sikorsky UH-60A model helicopter to understand the load required to operate the existing electrical system in the conventional model at all flight phase from engine start-Landing. Using the results obtained the Electrical tail rotor drive with up-scaled electrical sources is designed accordingly. From the case study, it is noted that the Sikorsky UH-60A helicopter operates with 30kVA / 45kVA generators. Due to the increase in load due to the addition of 35 kW motor for Electrical tail rotor drive the 45kVA AC generator is implemented in the design. Due to the change in design requalification of the type is required.

A trajectory for passenger mission from London City airport to Cranfield airport is created using the data from RMEM-TEM report [39]. The mission is estimated for worst weather conditions, the obtained maximum tail rotor power required is estimated as 34.77 kW at take-off phase and the noted minimum at flight operational time is 17.93kW during landing.

An electrically driven anti-torque system is technically feasible with the current advanced technology in electric motor and battery technology. Electrical Tail rotor is designed for the existing model of Sikorsky UH-60A to increase the transmission efficiency as a function of weight and power. The significant advantage of this model is the replacement of tail rotor power transmission system, which is critical cause for tail rotor failure accidents. The Electrical tail rotor architecture is designed to be fail-safe with motor-battery drive, thus redundancy will not be required for the operation of the anti-torque system.

6.1 Further Recommendations

- To increase the utilisation of the developed power requirement model, it is recommended to introduce a multi-disciplinary approach where power conversion analysis integrated within a performance of tail rotor analysis model to obtain more accurate results.
- For a further understanding of the impact, caused due to the Electrical tail rotor drive conversation the structural fatigue and centre of gravity can be analysed.
- The Electrically power tail rotor model can be interfaced into RMEM to estimate the changes in specific fuel consumption and the emission.
- Detailed design analysis of electrically powered tail rotor.
- Detail designing using cad model of the electrically powered tail rotor.

REFERENCES

1. Noor AK., Venneri SL. Future aeronautical and space systems. Reston, VA : American Institute of Aeronautics and Astronautics, 1997.; 1997. Available at: http://search.ebscohost.com/login.aspx?direct=true&db=cat00164a&AN=cran.73561&site=eds-live

2. Clean Sky. Integration of innovative electrical systems (GRC3) | Clean Sky. 2012. Available at: http://www.cleansky.eu/content/page/integration-innovative-electrical-systems-grc3 (Accessed: 9 October 2015)

3. Civil Aviation Authority. Helicopter operations within the London Heathrow and London city control zones. 2016. Available at: http://www.caa.co.uk/Data-and-analysis/Airspace-and-environment/Airspace/London-helicopter-operations/ (Accessed: 1 August 2016)

4. Clean Sky. Aviation - Aviation’s impact:how the sector is taking responsibility. Available at: http://www.cleansky.eu/aviation-0 (Accessed: 27 March 2017)

5. Clean Sky. Aviation & Environment | Clean Sky. 2011. Available at: http://www.cleansky.eu/content/homepage/aviation-environment (Accessed: 4 November 2015)

6. ICAO Environment. Aircraft Engine Emissions. ICAO. 2012. Available at: http://www.icao.int/environmental-protection/pages/aircraft-engine-

emissions.aspx

7. European Commission. 2020 climate & energy package. European Commission. 2016. Available at: http://ec.europa.eu/clima/policies/strategies/2020/index_en.htm

8. Green Rotorcraft. Rotorcraft input for the Technology Evaluator (GRC7). Clean Sky. 2015. Available at: http://www.cleansky.eu/content/page/rotorcraft-input-technology-evaluator-grc7

9. Muetze A., Durkee SR. Conceptual design of an electric helicopter powertrain. 5th IET International Conference on Power Electronics, Machines and Drives (PEMD 2010). 2010; : 353–353. Available at: DOI:10.1049/cp.2010.0047

10. Department of Army. Technical Manual Operator ' S Manual TM1-1520-237-10. Department of Defence. Redstone Arsenal; 2009.

11. Subramanian N., Gonzalez HA., Hashim F. Rotorcraft Mission Energy Management Model Of A Twin Engine Medium Rotorcraft. Cleansky. Miltonkeynes; 2016.

12. Wyatt DD. Aircraft Flight Instruments And Guidance Systems : Principles, Operations And Maintenance [Electronic Resource]. Oxfordshire, England ; New York, New York : Routledge, 2015.; 2015. Available at: http://search.ebscohost.com/login.aspx?direct=true&db=cat00164a&AN=cran.620950&site=eds-live

13. Tooley M., Filippone A., Megson THG., Cook M V., Carpenter PW., Houghton EL., et al. Aerospace Engineering e-Mega Reference. Oxford: Butterworth-Heinemann; 2009. 704 p. Available at: https://books.google.com/books?id=8K6Y8MhqbKgC&pgis=1 (Accessed: 4 August 2015)

14. Munson K. Helicopters and Other Rotorcraft Since 1907. Macmillan; 1969. Available at: https://books.google.co.uk/books?id=V5oUAQAAIAAJ

15. Padfield GD. Helicopter flight dynamics: The theory and application of flying qualities and simulation modeling. 2nd edn. Oxford: Blackwell Publishing; 2007. Available at: http://search.ebscohost.com/login.aspx?direct=true&db=cat00164a&AN=cran.661271&site=eds-live

16. Gazzola J. Helicopter history. helis.com. 1997. Available at: http://www.helis.com/introduction/prin.php (Accessed: 3 August 2015)

17. American Helicopter Society. VS-300 Helicopter (1939). The Americal society of Mechanical Engineers. 1984; (1939).

18. FAA. Helicopter Instructor's Handbook. Oklahoma City: U.S. Department of Transportation; 2012.

19. Department of Army. Fundamentals of Flight. Field Manual-Department of Army. 2007.

20. Wyatt D. Aircraft Flight Instruments and Guidance Systems. Rouledge. Oxon; 2015. Available at:

https://www.dawsonera.com/readonline/9781315858975 (Accessed: 6 August 2015)

21. Wagtendonk WJ. Principles of helicopter flight. Newcastle, WA : Aviation Supplies & Academics, 2006.; 2006. Available at: http://search.ebscohost.com/login.aspx?direct=true&db=cat00164a&AN=cran.517987&site=eds-live

22. Weden GJ., Coy JJ. Summary of Drive-Train Component Technology in Helicopters. NASA. 1984.

23. RJ Helicopter. RJHeli - Technology Compared to Conventional Helicopters. Available at: http://www.rjheli.com/technology.php (Accessed: 28 March 2017)

24. Leishman JG. Principles of helicopter aerodynamics. Cambridge ; New York : Cambridge University Press, 2006.; 2006. Available at: http://search.ebscohost.com/login.aspx?direct=true&db=cat00164a&AN=cran.504189&site=eds-live

25. Broderick M. Helicopter tail rotors – III. Aircraft Maintenance Update. December 2013; Available at: http://amumagazine.com/?p=2442

26. U.S Army Material. Drive system design 7-1. Knovel. 1974.

27. Federal Aviation Administration. Helicopter Components , Sections , and Systems. Helicopter Instructor's Handbook. 2012; : 183.

28. Airbus Helicopters. American Eurocopter - A new and improved Fenestron for the EC145 T2. 2011. Available at:

http://airbushelicoptersinc.com/news_features/2011/3-8-2011_Fenestron.asp (Accessed: 4 April 2017)

29. Scott J. Fenestron Tail Rotor. Aerospaceweb.ord. 2005. Available at: http://www.aerospaceweb.org/question/helicopters/q0212a.shtml (Accessed: 2 June 2016)

30. Filippone A. Flight Performance of Fixed and Rotary Wing Aircraft. Butterworth-Heinemann; 2006. Available at: https://books.google.com/books?id=L9KYFB-wrbgC

31. MOC pages. Electric Backpack Helicopter with Working Coaxial Rotor and Machinegun: A LEGO® creation by Gabor Pauler : MOCpages.com. 2014. Available at: http://www.moc-pages.com/moc.php/392937 (Accessed: 11 August 2016)

32. Griffiths M. Boeing H-47 C. Airliners. 2010. Available at: http://www.airliners.net/photo/UK-Air-Force/Boeing-Chinook-HC3-%28352%29/1740666/L (Accessed: 30 June 2016)

33. David Cenciotti. Air Force's CV-22 Osprey tilt-rotor aircraft accident report is a total distortion of the facts". The Aviationist. 2012. Available at: https://theaviationist.com/2012/09/04/cv-22-osprey-unsafe/ (Accessed: 30 June 2016)

34. Civil Aviation Authority. Safety Regulation Group Ref : Date : March. 2004.

35. Pallett EHJ. Aircraft electrical systems. Harlow : Longman Scientific & Technical, 1987.; 1987. Available at:

http://search.ebscohost.com/login.aspx?direct=true&db=cat00164a&AN=cran.63205&site=eds-live

36. Helfrick AD. Modern aviation electronics. Englewood Cliffs ; London : Prentice-Hall, c1984.; 1984. Available at: http://search.ebscohost.com/login.aspx?direct=true&db=cat00164a&AN=cran.53484&site=eds-live

37. Helfrick AD. Principles of avionics. Leesburg VA : Avionics Communications, 2000.; 2000. Available at: http://search.ebscohost.com/login.aspx?direct=true&db=cat00164a&AN=cran.388002&site=eds-live

38. Abdel-Fadil R., Eid A., Abdel-Salam M. ELECTRICAL DISTRIBUTION POWER SYSTEMS OF MODERN CIVIL AIRCRAFTS. 2013; Available at: https://pdfs.semanticscholar.org/2bf4/12d0231061db3cf3405b194d605441272812.pdf (Accessed: 26 April 2017)

39. Sundberg GR. Advances in Solid State Switchgear Technology for Large Space Power Systems. 19th Intersociety Energy Conversion Engineering Conference: Advanced Energy Systems - Their Role in Our Future. 1984; : 123–132. Available at: http://www.scopus.com/inward/record.url?eid=2-s2.0-0021640972&partnerID=40&md5=e73e2b634039e6b5ba822b5a7f0a2405

40. Moir I., Seabridge AG. Aircraft systems : Mechanical, Electrical, and Avionics Subsystems integration. Chichester, West Sussex, England ;

Hoboken, NJ : Wiley, c2008.; 2008. Available at: http://search.ebscohost.com/login.aspx?direct=true&db=cat00164a&AN=cran.605485&site=eds-live

41. Garrett DF. Aircraft systems and components. Casper,WY : IAP, 1992.; 1992. Available at: http://search.ebscohost.com/login.aspx?direct=true&db=cat00164a&AN=cran.71045&site=eds-live

42. Electrical Engineering Community. DC Generator (back to basics). 2013. Available at: http://engineering.electrical-equipment.org/electrical-distribution/dc-generator-back-to-basics.html (Accessed: 13 October 2015)

43. Chen H., Cong TN., Yang W., Tan C., Li Y., Ding Y. Progress in electrical energy storage system: A critical review. Progress in Natural Science. National Natural Science Foundation of China and Chinese Academy of Sciences; 2009; 19(3): 291–312. Available at: DOI:10.1016/j.pnsc.2008.07.014

44. Karpinski A., Makovetski B., Russell S., Serenyi J., Williams D. Silver–zinc: status of technology and applications. Journal of Power Sources. 1999; 80(1): 53–60. Available at: DOI:10.1016/S0378-7753(99)00164-0

45. Williard N., He W., Hendricks C., Pecht M. Lessons learned from the 787 dreamliner issue on Lithium-Ion Battery reliability. Energies. 2013; 6(9): 4682–4695. Available at: DOI:10.3390/en6094682

46. FAA. Lithium Batteries & Lithium Battery-Powered Devices. 2016; : 1–32.

47. Balakrishnan PG., Ramesh R., Prem Kumar T. Safety mechanisms in lithium-ion batteries. Journal of Power Sources. 2006; 155(2): 401–414. Available at: DOI:10.1016/j.jpowsour.2005.12.002

48. Wang Q., Ping P., Zhao X., Chu G., Sun J., Chen C. Thermal runaway caused fire and explosion of lithium ion battery. Journal of Power Sources. Elsevier B.V.; 2012; 208: 210–224. Available at: DOI:10.1016/j.jpowsour.2012.02.038

49. Federal Aviation Administration. Helicopter Flying Handbook. Skyhorse Publishing Company, Incorporated; 2013. Available at: https://books.google.co.in/books?id=5QVECgAAQBAJ

50. Harris FD., Kasper EF., Iseler LE. U.S. Civil Rotorcraft Accidents, 1963 through 1997. NASA. 2000.

51. Rosero JA., Ortega JA., Aldabas E., Romeral L. Moving towards a more electric aircraft. IEEE Aerospace and Electronic Systems Magazine. 2007; 22(3): 3–9. Available at: DOI:10.1109/MAES.2007.340500

52. Porras HAP. Development of a Tool to Analyse Helicopter Performance Incorporating Novel Systems. Cranfield University. 2013. Available at: DOI:10.1017/CBO9781107415324.004

53. Goulos I. Simulation Framework Development for the Multidisciplinary Optimisation of Rotorcraft. Cranfield University; 2012.

54. Green Rotorcraft. PhoeniX Operational Manual. GRC and Technology Evaluators; 2011. pp. 1–32.

55. Cloyd JS. Status of United States Air Force ' s More Electric Aircraft Initiative. IEEE Systems magazine. 1998; (1943): 17–22.

56. Howse M. All Electric Aircraft. IEEE Power Engineer. 2003; (September): 35–37.

57. Weimer J., Weimer JA. Past, Present & Future of Aircraft Electrical Power Systems. Available at: DOI:10.2514/6.2001-1147

58. Boeing. Take Our Readership Survey. 2007. p. 32.

59. Schilling DR. World's First Manned Electric Powered Helicopter. Industry tap into news. 2013. Available at: http://www.industrytap.com/worlds-first-electric-powered-helicopter/3693 (Accessed: 9 August 2016)

60. Simons CA. Feasibility study of a superconducting helicopter electrical propulsion motor. Delft University of Technology; 2013.

61. Schweickart D., Horwath J., Walko L., Hatfield L., Krompholz H. A Guide to Electrical Insulation Design in Aerospace Vehicles for a Broad Range of Environmental Parameter Space. Ohio; 2010. Available at: http://www.dtic.mil (Accessed: 5 August 2016)

62. Brockschmidt A. Electrical Environments in Aerospace Application. Boeing Information, Space, and Defense Systems. 2014; (2): 81–87. Available at: DOI:10.1007/s13398-014-0173-7.2

63. Christou I., Nelms a., Cotton I., Husband M. Choice of optimal voltage for more electric aircraft wiring systems. IET Electrical Systems in Transportation. 2011; 1(1): 24. Available at: DOI:10.1049/iet-

est.2010.0021

64. Johnson W. Helicopter theory. Princeton: Princeton, N.J : Princeton University Press, c1980.; 1980. Available at: http://search.ebscohost.com/login.aspx?direct=true&db=cat00164a&AN=cran.81696&site=eds-live

65. Layton DM. Helicopter Performance. Massachusetts: Matrix Publishers Inc.,; 1984.

66. Prouty RW. Helicopter performance stability and control. Florida: Malabar, FL : Krieger, 1990.; 1990. Available at: https://search.ebscohost.com/login.aspx?direct=true&db=cat00164a&AN=cran.204405&site=eds-live

67. Anonymous. Sikorsky UH-60M BLACK HAWK vs AgustaWestland NH90 - Helicopters Comparison. Available at: http://helicopters.axlegeeks.com/compare/12-89/Sikorsky-UH-60M-BLACK-HAWK-vs-AgustaWestland-NH90 (Accessed: 18 August 2016)

68. Nagata J l., Piotrowski JL., Young CJ., Lewis MWD., Losier MPW., Lyle CJA. Baseline performance verification of the 12th year production UH-60A black hawk helicopter. ST. LOUIS,; 1988.

69. Devine V. Sikorsky Archives | R-4 Coast Guard. Igor I Sikorsky. 2012. Available at: http://www.sikorskyarchives.com/S-76.php (Accessed: 9 May 2016)

70. Leoni RD. Black hawk : the story of a world class helicopter.

Reston,Virginia: AIAA; 2007. Available at: http://search.ebscohost.com/login.aspx?direct=true&db=cat00164a&AN=cran.525057&site=eds-live

71. Keypoint. Chapter 4. Navy Aviation. 2008; : 1–26. Available at: DOI:10.1007/978-0-387-77282-0

72. FAA. Aviation Maintenance Technician Handbook - Airframe Volume 1. Mepcount Media, LLC; 2012. Available at: https://books.google.co.uk/books?id=2LDqAgAAQBAJ

73. Rucker F. UH-60A Electrical System. United States Army Aviation Warfighting Center. 2008.

74. U.S. Army Aviation and Troop Command. General Information, Equipment Description and Theory of Operation for S-70i Helicopters. St.Louis; 2010.

75. NASA. UH–60A Airloads Program Occasional Note 1999–04 Discrepancies in the Measurement of Aircraft and Rotor Power. Washington; 1989.

76. Nasa. UH-60A Mathematical Model. Nasa Contractor Report. 1981.

77. Amanda Sigworth., Dávila J., McNeil T., Nicolalde J., Scheve D., Funk K. Mission Analysis. 2000. Available at: http://flightdeck.ie.orst.edu/ElectronicChecklist/HTML/mission.html (Accessed: 1 August 2016)

78. Hashim F., Judt D., Lawson C., Goulos I., Pardo AC., Pachidis V. Clean Sky RMEM Model of a Twin-Engine Heavy Rotorcraft. 2015.

79. Gerhold RR. Comparison of DC Brushed Motors vs. AC Induction Motors for Electric Vehicle Drive. heaa.org/wp-content/uploads/library/DC_vs_AC_motors.pdf. 2010. Available at: DOI:10.1017/CBO9781107415324.004

80. Rippel W. Induction Versus DC Brushless Motors. Tesla. 2007. Available at: https://www.tesla.com/en_GB/blog/induction-versus-dc-brushless-motors (Accessed: 21 July 2016)

81. Green Rotorcraft. Multi-source Regenerative Systems Power Conversion. 2015. Available at: http://www.cleansky.eu/sites/default/files/documents/grc_3_-_regenesys.pdf (Accessed: 28 April 2017)

82. SAFT. BATTERY. 2016. Available at: http://www.saftbatteries.com/solutions/products/battery-search

83. Business Wire. UAV Flight Time Increased By 80% Using SION Power's New High Energy Battery System. Business wire. 2006; Available at: http://www.businesswire.com/news/home/20061205005871/en/UAV-Flight-Time-Increased-80-SION-Powers (Accessed: 15 February 2016)

84. Dudley M. Promising electric aircraft drive systems. EAA electric aircraft world symposium. 2010; : 1–23.

85. Saft. Saft batteries power first flight for the F-35 Lightning II Joint Strike Fighter. 2006;

86. Chen H., Cong TN., Yang W., Tan C., Li Y., Ding Y. Progress in electrical

energy storage system: A critical review. Progress in Natural Science. 2009; 19(3): 291–312. Available at: DOI:10.1016/j.pnsc.2008.07.014

87. Masson PJ., Brown G V., Soban DS., Luongo C a. HTS machines as enabling technology for all-electric airborne vehicles. Superconductor Science and Technology. 2007; 20(8): 748–756. Available at: DOI:10.1088/0953-2048/20/8/005

88. Crabtree JA. Weight estimation for helicopter design analysis. THE SOCIETY OF AERONAUTICAL WEIGHT ENGINEERS. 1958; Available at: http://www.sawe.org/files/0177.PDF

89. Sinsay JD., Alonso JJ., Kontinos DA., Melton JE., Grabbe S. Air Vehicle Design and Technology Considerations for an Electric VTOL Metro-Regional Public Transportation System. American Institute of Aeronautics and Astronautics. 2012; (September): 1–16. Available at: DOI:doi:10.2514/6.2012-5404

90. MCM Engineering. 2 7 0 VDC Ground power cable. Burlingame;

91. Brombach J., Schr T., Schulz D. Optimizing the Weight of an Aircraft Power Supply System through a +/-270 VDC Main Voltage. Electrical Review. 2012; (1): 47–50.

92. Excelitas Technologies. Auto-Transformer Rectifier Unit (ATRU) Converter. ohio; 2014. Available at: http://www.excelitas.com/Downloads/DTS_ATRU_750.pdf

93. Peter Cohan. Boeing, Dell Technologies, Samsung, Tesla And Burning

Lithium Ion Batteries. Forbes. 2016. Available at: https://www.forbes.com/sites/petercohan/2016/09/12/boeing-dell-technologies-samsung-tesla-and-burning-lithium-ion-batteries/#5172b4e45ad5 (Accessed: 25 April 2017)

94. Battery University Group. Lithium-ion Safety Concerns. 2010. Available at: http://batteryuniversity.com/learn/archive/lithium_ion_safety_concerns (Accessed: 25 April 2017)

95. O J. Lithium Ion Battery Overheating Seen in Boeing 787: Why and Solutions. Cooling Zone. 2013. Available at: http://www.coolingzone.com/index.php?read=508 (Accessed: 25 April 2017)

96. Lazzaroni M., Cristaldi L., Peretto L., Rinaldi P., Catelani M. Reliability engineering: basic concepts and applications in ICT. Springer. 2011.

APPENDICES

Appendix 1 Model to calculate the power requirement of tail rotor

V_air(m/se	Brick_Type	fs	Abs_Altitude(m)	Rho	Temp(K)	Thrust(kgm/s^2)	vt(m/s)	R(m)	A(m^2)	sigma	cd0	B	omega	W	kW
0.0001	Start	1	55	1.225	287.79	14.09	680.165	3.35	35.23865	0.188	0	4	208.77	122.8568	0.122857
0.00001	Start	1	55	1.225	287.79	14.09	680.165	3.35	35.23865	0.188	0	4	208.77	122.8568	0.122857
0.00001	Start	1	55	1.225	287.79	14.09	680.165	3.35	35.23865	0.188	0	4	208.77	122.8568	0.122857
0.00001	Start	1	55	1.225	287.79	14.09	680.165	3.35	35.23865	0.188	0	4	208.77	122.8568	0.122857
0.00001	Start	1	55	1.225	287.79	14.09	680.165	3.35	35.23865	0.188	0	4	208.77	122.8568	0.122857
0.00001	Start	1	55	1.225	287.79	14.09	680.165	3.35	35.23865	0.188	0	4	208.77	122.8568	0.122857
40.31129	Take off	2	130	1.225	287.305	14.09	679.59	3.35	35.23865	0.188	0.0001	4	208.77	22261.86	22.26186
40.31129	Take off	2	165	1.225	287.0775	14.09	679.32	3.35	35.23865	0.188	0.0001	4	208.77	22259.96	22.25996
40.31129	Take off	2	250	1.225	286.525	14.09	678.666	3.35	35.23865	0.188	0.0001	4	208.77	22255.35	22.25535
40.31129	Take off	2	310	1.225	286.135	14.09	678.204	3.35	35.23865	0.188	0.0001	4	208.77	22252.1	22.2521
40.31129	Take off	2	370	1.225	285.745	14.09	677.742	3.35	35.23865	0.188	0.0001	4	208.77	22248.84	22.24884
60	Cruise	3	450	1.225	285.225	14.09	677.125	3.35	35.23865	0.188	0.0001	4	208.77	34889.81	34.88981
60	Cruise	3	450	1.225	285.225	14.09	677.125	3.35	35.23865	0.188	0.0001	4	208.77	34889.81	34.88981
60	Cruise	3	450	1.225	285.225	14.09	677.125	3.35	35.23865	0.188	0.0001	4	208.77	34889.81	34.88981
60	Cruise	3	450	1.225	285.225	14.09	677.125	3.35	35.23865	0.188	0.0001	4	208.77	34889.81	34.88981
60	Cruise	3	450	1.225	285.225	14.09	677.125	3.35	35.23865	0.188	0.0001	4	208.77	34889.81	34.88981
60	Cruise	3	450	1.225	285.225	14.09	677.125	3.35	35.23865	0.188	0.0001	4	208.77	34889.81	34.88981
60	Cruise	3	450	1.225	285.225	14.09	677.125	3.35	35.23865	0.188	0.0001	4	208.77	34889.81	34.88981
60	Cruise	3	450	1.225	285.225	14.09	677.125	3.35	35.23865	0.188	0.0001	4	208.77	34889.81	34.88981
60	Decent	5	310	1.225	286.135	14.09	678.204	3.35	35.23865	0.188	0.0001	4	208.77	22252.1	22.2521
60	Decent	5	270	1.225	286.395	14.09	678.512	3.35	35.23865	0.188	0.0001	4	208.77	22254.27	22.25427
40.31	Hover	4	250	1.225	286.525	14.09	678.666	3.35	35.23865	0.188	0.0001	4	208.77	22255.35	22.25535
40.31	Hover	4	250	1.225	286.525	14.09	678.666	3.35	35.23865	0.188	0.0001	4	208.77	17474.15	17.47415
40.31	Hover	4	250	1.225	286.525	14.09	678.666	3.35	35.23865	0.188	0.0001	4	208.77	17474.15	17.47415
40.31	Hover	4	250	1.225	286.525	14.09	678.666	3.35	35.23865	0.188	0.0001	4	208.77	17474.15	17.47415
40.31	Hover	4	250	1.225	286.525	14.09	678.666	3.35	35.23865	0.188	0.0001	4	208.77	17474.15	17.47415
40.31	Hover	4	250	1.225	286.525	14.09	678.666	3.35	35.23865	0.188	0.0001	4	208.77	17474.15	17.47415
40.31	Hover	4	250	1.225	286.525	14.09	678.666	3.35	35.23865	0.188	0.0001	4	208.77	17474.15	17.47415
40.31	Hover	4	250	1.225	286.525	14.09	678.666	3.35	35.23865	0.188	0.0001	4	208.77	17474.15	17.47415
40.31	Hover	4	250	1.225	286.525	14.09	678.666	3.35	35.23865	0.188	0.0001	4	208.77	17474.15	17.47415
40.31	Decent	5	220	1.225	286.72	14.09	678.897	3.35	35.23865	0.188	0.0001	4	208.77	22256.98	22.25698
40.31	Decent	5	190	1.225	286.915	14.09	679.128	3.35	35.23865	0.188	0.0001	4	208.77	22258.61	22.25861
40.31	Decent	5	175	1.225	287.012	14.09	679.24	3.35	35.23865	0.188	0.0001	4	208.77	22259.4	22.2594
0.00001	Landing	5	160	1.225	287.11	14.09	679.358	3.35	35.23865	0.188	0.0001	4	208.77	22260.23	22.26023
0.00001	Landing	5	100	1.225	287.5	14.09	679.82	3.35	35.23865	0.188	0.0001	4	208.77	17474.15	17.47415
0.00001	Landing	5	55	1.225	287.79	14.09	680.165	3.35	35.23865	0.188	0	4	208.77	122.8568	0.122857
0.00001	Landing	5	55	1.225	288.08	14.09	680.51	3.35	35.23865	0.188	0	4	208.77	122.8568	0.122857

Appendix 2 Electrical Load Analysis

Sikorsky UH-60A Electrical System Specifications:	Rating (W)	AC Voltage	DC Voltage
2 x 45kVA 115 V AC generators	48000	115	28.00
24 V 110 Ah battery	720		24.00

Equipment	Quan.	N Power (W)	Current (A)	Total current (A)	Usage: Cont	Usage: Inter	Normal Conditions: Pre-Start Day Cont	Pre-Start Day Int	Pre-Start Night Cont	Pre-Start Night Int	Take-Off/Climb Day Cont	Take-Off/Climb Day Int	Take-Off/Climb Night Cont	Take-Off/Climb Night Int	Hover Day Cont	Hover Day Int	Hover Night Cont	Hover Night Int	Cruise Day Cont	Cruise Day Int	Cruise Night Cont	Cruise Night Int	Landing Day Cont	Landing Day Int	Landing Night Cont	Landing Night Int
INDICATING/RECORDING SYSTEMS																										
Integrated Standby Instrument System (ISIS) for airspeed, altimeter and gyro-horizon back-up display	2	172.5	0.75	1.50	✔		172.5		172.5		172.5		172.5		172.5		172.5		172.5		172.5		172.5		172.5	
6" x 8" LCD displays	2	844.1	3.67	7.34	✔		844.1		844.1		844.1		844.1		844.1		844.1		844.1		844.1		844.1		844.1	
Dual tachometers	2	18.4	0.08	0.16	✔		18.4		18.4		18.4		18.4		18.4		18.4		18.4		18.4		18.4		18.4	
Cockpit Voice Recorder	2	57.5	0.25	0.50	✔		57.5		57.5		57.5		57.5		57.5		57.5		57.5		57.5		57.5		57.5	
LIGHTS																										
External Lighting System																										
Instrument Light System	2	115	0.5	1.00	✔		115		115		115		115		115		115		115		115		115		115	
Position lights LED	3	86.25	0.25	0.75	✔		86.25		86.25		86.25		86.25		86.25		86.25		86.25		86.25		86.25		86.25	
Navigation Lights - Daylight Operations	3	759	2.2	6.60	✔		759		759		759		759		759		759		759		759		759		759	
Navigation Lights - Night Operations	3	759	2.2	6.60	✔																				759	
Anti-collsion light	1	402.5	3.5	3.50		✔		402.5		402.5		402.5		402.5		402.5		402.5		402.5		402.5		402.5		402.5
Landing relay	1	6.9	0.06	0.06	✔																		6.9		6.9	
Landing Lights	2	600	10	20.00		✔		0		0		0		0		0		0		0			600		600	
Cockpit Lighting System																										
Cockpit Dome Light	2	46	0.2	0.40	✔				46				46				46				46				46	
Green pedestal system	2	128.8	0.56	1.12	✔		128.8		128.8		128.8		128.8		128.8		128.8		128.8		128.8		128.8		128.8	
Overhead panel integrated lighting	2	29.9	0.13	0.26		✔		29.9		29.9		29.9		29.9		29.9		29.9		29.9		29.9	29.9		29.9	
White general lighting	2	128.8	0.56	1.12		✔		128.8		128.8		128.8		128.8		128.8		128.8		128.8		128.8	128.8		128.8	

White extension light	2	128.8	0.56	1.12		✔	128.8	128.8	128.8	128.8	128.8	128.8	128.8	128.8	128.8	128.8
White map lights	2	46	0.2	0.40		✔	46	46	46	46	46	46	46	46	46	46
Cabin Lighting System																
Cabin Lighting System (2 lighting strips, "Emergency Exit", "No Smoking", and "Fasten Seat Bealts" signs)	2	4.6	0.02	0.04		✔	4.6	4.6	4.6	4.6	4.6	4.6	4.6	4.6	4.6	4.6
Passenger Notice System (Fasten Seat Belt - No Smoking)	1	2.3	0.02	0.02	✔		2.3	2.3	2.3	2.3	2.3	2.3	2.3	2.3	2.3	2.3
Storm Lighting	2	4.6	0.02	0.04		✔	4.6	4.6	4.6	4.6	4.6	4.6	4.6	4.6	4.6	4.6
Cabin Emergency Lights	3	17.25	0.05	0.15		✔	17.25	17.25	17.25	17.25	17.25	17.25	17.25	17.25	17.25	17.25
NAVIGATION																
Airspeed Indicators - Public Transport Operations	2	6.9	0.03	0.06	✔		6.9	6.9	6.9	6.9	6.9	6.9	6.9	6.9	6.9	6.9
Altimeters - Public Transport (Day) Operations	2	195.5	0.85	1.70	✔		195.5	195.5	195.5	195.5	195.5	195.5	195.5	195.5	195.5	195.5
Altimeters - Public Transport (Night) Operations	2	195.5	0.85	1.70	✔		195.5	195.5		195.5		195.5		195.5		195.5
Altitude Indicators - Day VFR	2	69	0.3	0.60	✔		69	69	69	69	69	69	69	69	69	69
Altitude Indicators - IFR or Night Operations	2	69	0.3	0.60	✔		69	69	69	69	69	69	69	69	69	69
Gyroscopic Direction Indicator (c)	1	7	0.25	0.25	✔		7	7	7	7	7	7	7	7	7	7
Gyroscopic Direction Indicator (I)	1	16.8	0.6	0.60		✔	16.8	16.8	16.8	16.8	16.8	16.8	16.8	16.8	16.8	16.8
Slip and Skid Indicator	4	138	0.3	1.20	✔		138	138	138	138	138	138	138	138	138	138
Outside Air Temperature Indicator	2	29.9	0.13	0.26	✔		29.9	29.9	29.9	29.9	29.9	29.9	29.9	29.9	29.9	29.9
Traffic Alert and Collision Avoidance System (TCAS) (if installed)	2	575	2.5	5.00	✔		575	575	575	575	575	575	575	575	575	575
WARNING LIGHT SYSTEM																
Warning LT panel(I)	2	322	1.4	2.80		✔	322	322	322	322	322	322	322	322	322	322
Warning LT panel©	2	64.4	0.28	0.56	✔		64.4	64.4	64.4	64.4	64.4	64.4	64.4	64.4	64.4	64.4
FUEL SYSTEM							0	0								
Fuel circuit control and monitoring panel with 2 fuel content displays	2	943	4.1	8.20	✔		943	943	943	943	943	943	943	943	943	943
Fuel Quantity Gauges	2	82.8	0.36	0.72	✔		82.8	82.8	82.8	82.8	82.8	82.8	82.8	82.8	82.8	82.8
Fore and Aft Tank Gauges	2	82.8	0.36	0.72	✔		82.8	82.8	82.8	82.8	82.8	82.8	82.8	82.8	82.8	82.8
Centre Tank Gauge (if centre tank installed)	2	82.8	0.36	0.72	✔		82.8	82.8	82.8	82.8	82.8	82.8	82.8	82.8	82.8	82.8
ENGINE FUEL AND CONTROL																
Low Fuel Pressure Indicator Lights	4	36.8	0.08	0.32		✔	36.8	36.8	36.8	36.8	36.8	36.8	36.8	36.8	36.8	36.8
Fuel Pressure Gauges	2	18.4	0.08	0.16	✔		18.4	18.4	18.4	18.4	18.4	18.4	18.4	18.4	18.4	18.4
No.1 FWR Pump 1 to 3	6	467.04	2.78	16.68	✔		467.04	467.04	467.04		467		467		467	

No.1 AFT Pump 1 to 3	6	467.04	2.78	16.68	✔		467.04	467.04	467.04		467		467		467	
Engine Torquemeter	2	11.5	0.05	0.10	✔		11.5	11.5	11.5	11.5	11.5	11.5	11.5	11.5	11.5	11.5
Engine Hour Meter	2	3.45	0.015	0.03	✔		3.45	3.45	3.45	3.45	3.45	3.45	3.45	3.45	3.45	3.45
Engine Monitoring Unit	2	41.4	0.18	0.36	✔		41.4	41.4	41.4	41.4	41.4	41.4	41.4	41.4	41.4	41.4
Engine FADEC	2	1150	5	10.00		✔	1150	1150	1150	1150	1150	1150	1150	1150	1150	1150
Engine Igniter	2	172.5	0.75	1.50		✔			172.5	172.5						
Torque Sensor	2	82.8	0.36	0.72			82.8	82.8	82.8	82.8	82.8	82.8	82.8	82.8	82.8	82.8
Fuel Sensor	2	82.8	0.36	0.72			82.8	82.8	82.8	82.8	82.8	82.8	82.8	82.8	82.8	82.8
Oil sensor	2	82.8	0.36	0.72			82.8	82.8	82.8	82.8	82.8	82.8	82.8	82.8	82.8	82.8
Fire sensor	2	82.8	0.36	0.72			82.8	82.8	82.8	82.8	82.8	82.8	82.8	82.8	82.8	82.8
PTIT	2	82.8	0.36	0.72			82.8	82.8	82.8	82.8	82.8	82.8	82.8	82.8	82.8	82.8
Engine Temperature recoder	2	82.8	0.36	0.72			82.8	82.8	82.8	82.8	82.8	82.8	82.8	82.8	82.8	82.8
AFCS sensor	2	82.8	0.36	0.72			82.8	82.8	82.8	82.8	82.8	82.8	82.8	82.8	82.8	82.8
AC Rectifier	20	1794	0.78	15.60			1794	1794	1794	1794	1794	1794	1794	1794	1794	1794
VGI	4	165.6	0.36	1.44			165.6	165.6	165.6	165.6	165.6	165.6	165.6	165.6	165.6	165.6
HYDRAULICS																
Primary sensor	1	41.4	0.36	0.36			41.4	41.4	41.4	41.4	41.4	41.4	41.4	41.4	41.4	41.4
Auxillary sensor	1	41.4	0.36	0.36			41.4	41.4	41.4	41.4	41.4	41.4	41.4	41.4	41.4	41.4
XMFRS	7	289.8	0.36	2.52			289.8	289.8	289.8	289.8	289.8	289.8	289.8	289.8	289.8	289.8
DC Essential BUS																
Rectifier	2	280	5	10.00			280	280	280	280	280	280	280	280	280	280
Fuel Transfer pump	2	280	5	10.00					280	280	280	280	280	280	280	280
VGI	10	1400	5	50.00			1400	1400	1400	1400	1400	1400	1400	1400	1400	1400
Tail take off	1	140	5	5.00			140	140	140	140						
Tail take off	1	690	6	6.00			690	690	690	690						
Landing Lights	1	280	10	10.00											280	280
Cargo Sling	1	280	10	10.00							280	280			280	280

Radio power	2	1400	25	50.00				1400	1400	1400	1400	1400	1400	1400	1400	1400	1400
Inverter Power	1	980	35	35.00				980	980	980	980	980	980	980	980	980	980
Overtemp Alternator	1	140	5	5.00				140	140	140	140	140	140	140	140	140	140
Windshield Wash	1	140	5	5.00				140	140	140	140	140	140	140	140	140	140
VHF Radio	2	560	10	20.00				560	560	560	560	560	560	560	560	560	560
ADF	1	140	5	5.00				140	140	140	140	140	140	140	140	140	140
PA Test	1	140	5	5.00				140	140	140	140	140	140	140	140	140	140
ADF	1	575	5	5.00				575	575	575	575	575	575	575	575	575	575
PA Test	1	575	5	5.00				575	575	575	575	575	575	575	575	575	575
Weather Radar	1	575	5	5.00				575	575	575	575	575	575	575	575	575	575
ENGINE OIL				0.00													
Pressure Warning Lights	2	18.4	0.08	0.16		✔		18.4	18.4	18.4	18.4	18.4	18.4	18.4	18.4	18.4	18.4
Engine Oil Pressure Gauges	2	18.4	0.08	0.16		✔		18.4	18.4	18.4	18.4	18.4	18.4	18.4	18.4	18.4	18.4
Engine Oil Pressure Captions	2	82.8	0.36	0.72	✔			82.8	82.8	82.8	82.8	82.8	82.8	82.8	82.8	82.8	82.8
ENVIRONMENTAL CONTROL SYSTEM																	
Air Conditioning																	
Compressor	1	345	3	3.00	✔			345	345	345	345	345	345	345	345	345	345
Evaporator blower	1	1380	12	12.00	✔			1380	1380	1380	1380	1380	1380	1380	1380	1380	1380
Condenser fan	2	920	4	8.00	✔			920	920	920	920	920	920	920	920	920	920
A/C power relay	1	6.9	0.06	0.06	✔			6.9	6.9	6.9	6.9	6.9	6.9	6.9	6.9	6.9	6.9
Blower relay	1	6.9	0.06	0.06	✔			6.9	6.9	6.9	6.9	6.9	6.9	6.9	6.9	6.9	6.9
Time delay relay	1	6.9	0.06	0.06	✔			6.9	6.9	6.9	6.9	6.9	6.9	6.9	6.9	6.9	6.9
Ventilation	1	201.25	1.75	1.75				201.25	201.25	201.25	201.25	201.3	201.3	201.3	201.3	201.3	201.3
ICE & RAIN PROTECTION SYSTEM										0	0	0	0	0	0	0	
Pitot Heating System	6	2760	4	24.00	✔			2760	2760	2760	2760	2760	2760	2760	2760	2760	2760
Enigne	4	3920	35.00	140.00				3920	3920	3920	3920	3920	3920	3920	3920	3920	3920
COMMUNICATIONS SYSTEM										0	0	0	0	0	0	0	0
HF(receiving signal)	2	56	1	2.00	✔			56	56	56	56	56	56	56	56	56	56
HF(sending signal)	2	392	7.00	14.00		✔		392	392	392	392	392	392	392	392	392	392

Intercom system	2	1.68	0.03	0.06	✔		1.68		1.68		1.68		1.68		1.68		1.68		1.68		1.68		1.68		1.68	
Advanced Cabin Audio System	2	1.12	0.02	0.04	✔		1.12		1.12		1.12		1.12		1.12		1.12		1.12		1.12		1.12		1.12	
Bose Headset©	5	3.5	0.025	0.13	✔		3.5		3.5		3.5		3.5		3.5		3.5		3.5		3.5		3.5		3.5	
Bose Headset(I)	5	70	0.5	2.50		✔	70		70		70		70		70		70		70		70		70		70	
Blind encoder	2	33.6	0.6	1.20	✔		33.6		33.6		33.6		33.6		33.6		33.6		33.6		33.6		33.6		33.6	
DOORS											0		0		0		0		0		0					
Door Warning Light System	1	9.2	0.08	0.08		✔	9.2		9.2		9.2		9.2			9.2		9.2		9.2		9.2		9.2		9.2
Electrical Power system																										
Voltage Regulator	2	16.8	0.3	0.60	✔		16.8		16.8		16.8		16.8		16.8		16.8		16.8		16.8		16.8		16.8	
Battery Relay	2	33.6	0.6	1.20	✔		33.6		33.6		33.6		33.6		33.6		33.6		33.6		33.6		33.6		33.6	
External Relay	2	28	0.5	1.00	✔		28		28		28		28		28		28		28		28		28		28	
Starter Relay	2	28	0.5	1.00	✔		28		28		28		28		28		28		28		28		28		28	
Line control Relay	2	28	0.5	1.00	✔		28		28		28		28		28		28		28		28		28		28	
Aux Power plug	2	112	2	4.00	✔		112		112		112		112		112		112		112		112		112		112	
Battery Charging	2	280	5	10.00	✔		280		280		280		280		280		280		280		280		280		280	
TOTALS (A)		**32133.58**		**610.50**			**27640**	**2069**	**27686**	**2069**	**27490**	**2477**	**26601**	**2672**	**26758**	**2486**	**25870**	**2681**	**26478**	**2486**	**25590**	**2681**	**27964**	**2166**	**27835**	**2362**
Totals (% Rating)		66.9					56.7	4.2	56.8	4.2	56.4	5.1	54.6	5.5	54.9	5.1	53.1	5.5	54.3	5.1	52.5	5.5	57.4	4.4	57.1	4.8

Appendix 3 Electrical Load Analysis at different phases of flight

Time(sec)	Conventional Helicopter (kW)	Helicopter with Electrical tail rotor (kW)
0	28.720755	28.84361179
60	28.720755	28.84361179
120	28.720755	28.84361179
180	28.720755	28.84361179
240	28.720755	28.84361179
300	28.720755	28.84361179
360	27.937525	50.19938909
420	27.937525	50.19748694
480	27.937525	50.19287951
540	27.937525	50.18962472
600	27.937525	50.18636993
660	28.000755	62.89056254
720	28.000755	62.89056254
780	28.000755	62.89056254
840	28.000755	62.89056254
900	28.000755	62.89056254
960	28.000755	62.89056254
1020	28.000755	62.89056254

1080	28.000755	62.89056254
1140	29.047505	51.29960472
1200	29.047505	51.30177458
1260	27.210425	49.46577951
1320	27.210425	44.68457754
1380	27.210425	44.68457754
1440	27.210425	44.68457754
1500	27.210425	44.68457754
1560	27.210425	44.68457754
1620	27.210425	44.68457754
1680	27.210425	44.68457754
1740	27.210425	44.68457754
1800	29.047505	51.3044869
1860	29.047505	51.3061143
1920	29.047505	51.30690334
1980	29.047505	51.30773465
2040	29.047505	46.52165754
2100	29.047505	29.17036179
2160	29.047505	29.17036179